(2)

AD-A202 235 OCUMENTATION PAGE

Form Approved
OMB No. 0704-0188

1b. RESTRICTIVE MARKINGS

2a. SECURITY CLASSIFICATION AUTHORITY

2b. DECLASSIFICATION / DOWNGRADING SCHEDULE

3. DISTRIBUTION / AVAILABILITY OF REPORT

Approved for public release;
Distribution is unlimited

4. PERFORMING ORGANIZATION REPORT NUMBER(S)

5. MONITORING ORGANIZATION REPORT NUMBER(S)

AFOSR-TR- 88-1234

6a. NAME OF PERFORMING ORGANIZATION

University of Tennessee

6b. OFFICE SYMBOL (If applicable)

7a. NAME OF MONITORING ORGANIZATION

AFOSR/NC

6c. ADDRESS (City, State, and ZIP Code)

Department of Chemistry
Knoxville, TN 37996-1600

7b. ADDRESS (City, State, and ZIP Code)

Building 410
Bolling AFB, DC 20332-6448

8a. NAME OF FUNDING / SPONSORING ORGANIZATION

AFOSR

8b. OFFICE SYMBOL (If applicable)

NC

9. PROCUREMENT INSTRUMENT IDENTIFICATION NUMBER

AFOSR-85-0321

8c. ADDRESS (City, State, and ZIP Code)

Building 410
Bolling AFB, DC 23032-6448

10. SOURCE OF FUNDING NUMBERS

PROGRAM ELEMENT NO.	PROJECT NO.	TASK NO.	WORK UNIT ACCESSION NO.
61102F	2303	A1	

11. TITLE (Include Security Classification)

Electrochemical and Spectroscopic Investigation of Molten Chloroaluminates and Related Solvents

12. PERSONAL AUTHOR(S)

Gleb Mamantov

13a. TYPE OF REPORT	13b. TIME COVERED	14. DATE OF REPORT (Year, Month, Day)	15. PAGE COUNT
Final	FROM 9/15/85 TO 9/14/88	November 7, 1988	73

16. SUPPLEMENTARY NOTATION

17. COSATI CODES			18. SUBJECT TERMS (Continue on reverse if necessary and identify by block number)
FIELD	GROUP	SUB-GROUP	

19. ABSTRACT (Continue on reverse if necessary and identify by block number)

See Back

20. DISTRIBUTION / AVAILABILITY OF ABSTRACT

☐ UNCLASSIFIED/UNLIMITED ☐ SAME AS RPT. ☐ DTIC USERS

21. ABSTRACT SECURITY CLASSIFICATION

UNCLASSIFIED

22a. NAME OF RESPONSIBLE INDIVIDUAL	22b. TELEPHONE (Include Area Code)	22c. OFFICE SYMBOL
Dr. John S. Wilkes	(719) 472-2655	NC

DD Form 1473, JUN 86 Previous editions are obsolete. SECURITY CLASSIFICATION OF THIS PAGE

UNCLASSIFIED

19. In the reduction of $(W6Cl8)^{4+}$ in acidic alkali chloroaluminates, ESCA studies point to the formation of W(I) although the chemical nature of this unusual oxidation state remains unknown. A satisfactory X-ray powder diffraction pattern of the reduction product of W(II) could not be obtained. The magnetic susceptibility of the reduction product is much higher than for WCl5.
Raman spectroscopic studies of fluoride-containing chloroaluminate melts have led to the characterization of new species $AlCl3F^-$, $AlCl2F2^-$ and $AlCl3F^-$. It was discovered that these fluoride containing high temperature melts can be handled in quartz provided that the molar ratio of fluorine to aluminum does not exceed four.
Further examinations of CO2 dissolved in AlCl3-NaCl (52-48 Mole% and NaCl saturated melt) indicates that the previously observed reduction waves at platinum electrodes involve H^+ and possibly OH^-; CO2 itself appears to be electrochemically inactive in this medium. The main reduction wave increases with the pressure of HCl and is quite dependent on the electrode material.

FINAL TECHNICAL REPORT

AFOSR Grant 85-0321

Department of Chemistry
University of Tennessee, Knoxville

Gleb Mamantov
Principal Investigator

November 7, 1988

The following is a summary of research accomplishments and progress made during the period September 15, 1985 through September 14, 1988 under AFOSR Grant #85-0321.

Cont'd pg. 2

A. List of Publications Resulting from this Grant

P. A. Flowers and G. Mamantov, "Infrared Spectroscopic Determination of Oxide in Molten Chloroaluminates", Anal. Chem., 59, 1062 (1987).

S. D. Williams, J. P. Schoebrechts, J. C. Selkirk, and G. Mamantov, "A New Room Temperature Molten Salt Solvent System: Organic Cation Tetrachloroborates", J. Am. Chem. Soc., 109, 2218 (1987).

G. Mamantov, "A Brief Introduction to Electrochemistry in Molten Salts and Chloroaluminate Melts", in Molten Salt Chemistry: An Introduction and Selected Applications, G. Mamantov and R. Marassi, eds., Reidel Publishing Company, 1987, pp. 259-270.

J.-P. Schoebrechts, P. A. Flowers, and G. Mamantov, "An Electrochemical Approach for the Determination of Oxide Impurities in Acidic Alkali Chloroaluminates", in Proceedings of the Joint International Symposium on Molten Salts, G. Mamantov, M. Blander, C. L. Hussey, C. B. Mamantov, M. L. Saboungi, and J. S. Wilkes, eds., The Electrochemical Society, Pennington, NJ, 1987, pp. 437-444.

B. Gilbert, S. D. Williams, and G. Mamantov, "Raman Spectroscopy of Fluoride-Containing Chloroaluminate Melts", Inorg. Chem., 27, 2359 (1988).

J.-P. Schoebrechts, P. A. Flowers, G. W. Hance, and G. Mamantov, "Electrochemical and Spectroscopic Studies of Tungsten Hexachloride in an Acidic Sodium Chloroaluminate Melt", J. Electrochem. Soc., 135, 3057 (1988).

P. A. Flowers and G. Mamantov, "Thin-Layer Transmittance Cell for Infrared Spectroelectrochemistry", Anal. Chem., in press.

T. R. Blackburn and G. Mamantov, "Voltammetry of Ag(I) in Solid $NaAlCl_4$", J. Electrochem. Soc., in press.

P. A. Flowers and G. Mamantov, "Infrared Spectroscopic and Spectroelectrochemical Investigation of Chloranil in Molten Sodium Chloroaluminates" submitted to J. Electrochem. Soc.

B. Development of Spectroelectrochemical and Other Methodology for Alkali Chloroaluminates

1. **UV-visible absorption spectroelectrochemistry;** Our earlier studies in this area (1) were conducted with a Tektronix vidicon spectrometer located at the Oak Ridge National Laboratory. This instrument became obsolete and parts for it were no longer available; therefore, a new experimental facility was established at the University of Tennessee. This facility utilizes a Tracor-Northern rapid scan spectrometer equipped with a diode array detector and a Spex spectrograph, with all components positioned on a Newport optical table. This spectrometer facility is presently being used for spectroelectrochemical studies of selected refractory metal solutes in acidic ($AlCl_3$-rich) sodium chloroaluminate molten salts, some of which are described below.

2. **Infrared spectroscopy and spectroelectrochemistry;** Infrared spectroscopy has been proven useful for determining dissolved oxide at the millimolar level in both basic and acidic alkali chloroaluminates (Appendix I). This work was performed using a modified version of a cell design (2) which employed a diamond window and permitted sampling of the melt by emittance and external reflectance techniques. A silicon-windowed transmittance cell was subsequently developed and characterized using tetracyanoquinodimethane in acetonitrile as a model system (Appendix II). This cell has been employed in several spectroscopic and spectroelectrochemical studies in molten sodium

chloroaluminates, i. e., Lewis acid complexation of chloranil (Appendix III), the reaction of tungsten hexachloride with melt oxide (Appendix IV), and the solution chemistry of iridium carbonyl complexes known to be active Fischer-Tropsch catalysts (described below). These studies represent the first successful in situ infrared spectroelectrochemical studies performed in molten salt media.

3. **Raman spectroscopy and spectroelectrochemistry.** Two spectrometer/detector combinations for use with molten salt solutions have been evaluated (Appendix V). Characterization of a Raman spectroelectrochemical cell was performed on each of these systems employing aqueous ferricyanide in 0.5 M KCl as a model system. Application of this spectroelectrochemical methodology to a molten salt system was demonstrated by studying the oxidation of I_2 in an acidic sodium chloroaluminate melt (3). Present efforts are directed at studies of refractory metal species, e. g., tungsten, in chloroaluminate melts.

4. **Studies with ultramicroelectrodes.** Ultramicroelectrodes have several interesting applications in electrochemistry (4); their extension to studies in molten salts is being investigated (5).

We have recently been successful in using an ultramicroelectrode to perform cyclic voltammetry in a frozen chloroaluminate solution (Appendix VI). A 25 μm diameter tungsten button electrode was employed to obtain cyclic voltammograms of the AgCl/Ag couple in a slightly basic sodium chloroaluminate both above and below the melting point.

Diffusion constants for Ag^+ in the frozen chloroaluminate solvent were calculated from the voltammetric data and found to be roughly two orders of magnitude smaller than those measured in liquid $NaAlCl_4$ (6). Present work in this area includes epoxy-free fabrication of ultramicroelectrodes from 8 μm carbon fibers for use in molten salt media.

C. Electrochemical and Other Studies of Selected Redox Systems -

1. Tungsten species in sodium chloroaluminate melts: Our laboratory began the study of this very complex redox system some time ago (7). Recent work has shown that the highest oxidation state of tungsten, W(VI), exists in acidic $AlCl_3$-NaCl melts as either WCl_6 or $WOCl_4$, depending upon the level of oxide impurities in the melt. Based on this behavior we have developed an electrochemical method for determining oxide in acidic ($AlCl_3$-rich) alkali chloroaluminates. These results were presented at the Joint International Symposium on Molten Salts, the Electrochemical Society meeting, Honolulu, October 1987 and will be published in the Journal of the Electrochemical Society (Appendix IV).

UV-visible spectroscopic and spectroelectrochemical studies of several tungsten chloride species in acidic sodium chloroaluminate melts have been performed; these results were presented at the Electrochemical Society meeting in Atlanta, 1988 (Appendix VII). Although the higher valence species (i. e., WCl_6, $WOCl_4$, and WCl_5) may be characterized in this manner, UV-visible spectroscopic studies of

the lower oxidation states have not been very illuminating.

X-ray photoelectron spectroscopy (XPS or ESCA) has been employed to examine the reduction of W(II), believed to exist as $W_6Cl_8^{4+}$, in acidic chloroaluminates. Earlier ESCA results suggested the formation of W(I) upon reduction of W(II), although the chemical nature of this unusual oxidation state remains unknown (8). It is interesting that the magnetic susceptibility of this reduction product is higher than that of WCl_5, which has one unpaired electron. The magnetic susceptibility of W_6Cl_{12} is zero. A paper summarizing our results on the tungsten system in acidic melts is in preparation.

2. **Electrochemical studies of CO_2 and HCl in molten alkali chloroaluminates.** Early work in this laboratory indicated that carbon dioxide is reduced at platinum electrodes in alkali chloroaluminate melts. An extensive reinvestigation has shown that previously observed reduction waves at platinum involve H^+ and possibly OH^-. Carbon dioxide itself appears to be electrochemically inactive in this medium. The major reduction wave increases with HCl pressure and is quite dependent on the electrode material. Further electrochemical studies, e. g., double potential step chronocoulometry, of this system are in progress.

3. **Chemistry of iridium carbonyls in sodium chloroaluminates.** The iridium carbonyl species $Ir_4(CO)_{12}$ and $IrCl(CO)_3$ have previously been shown to serve as Fischer-Tropsch catalysts in acidic sodium chloroaluminates (9-11). Discrepancies between product distributions

observed by different research groups, in addition to fundamental interest, have prompted our group to examine these systems in an attempt to identify the catalytically active species. Earlier work in our laboratory showed $Ir_4(CO)_{12}$ to be unstable in the melt and indicated that this cluster species decomposes to yield a mononuclear complex (12). Subsequent infrared spectroscopic studies of melt solutions under various atmospheres (N_2, $CO:H_2$, $CO:D_2$) have provided evidence which suggests formation of an iridium hydridocarbonyl complex under catalytic conditions (13). The existence of such a species has recently been confirmed by a proton NMR investigation; further studies of this system are in progress.

D. Molten Salt Batteries

1. Examination of Na^+ conducting glasses: We have investigated the potential utility of sodium ion conducting glasses as separators for use in molten salt batteries of the type $Na/Na^+(glass)/S(IV)$ in $AlCl_3$-NaCl melts. Several Na^+ conducting glasses have been prepared by Dr. I. Bloom of Argonne National Laboratory. One of these, the so-called "T-glass", has been shown to be compatible with sodium chloroaluminate melts. We have employed very thin membranes of this T-glass (2 mm^2 area) sealed to the end of an α-alumina tube in miniaturized cells based on the Na/S(IV) system previously studied by our group (14). Although these cells could be charged to 3.90 V (compared to 4.2 V for larger cells with β"-alumina separators), their discharge behavior was very poor, exhibiting low capacities and

voltages.

2. Studies of cobalt electrodes in basic $AlCl_3$-NaCl melts. Cells based on the reaction

$$2Na_{(l)} + MCl_{2(s)} \longleftrightarrow 2NaCl_{(s)} + M_{(s)}$$

(where M = Fe, Ni, Co, Cu, ...) using β"-alumina and $AlCl_3$-$NaCl_{sat}$ melts as electrolytes have recently been described in the literature (15) and show some promise. We have studied the electrochemical behavior of cobalt electrodes in these melts in order to gain an understanding of the charge/discharge processes. Galvanostatic charging (oxidation) of the cobalt electrode involves two plateaus which apparently correspond to electrolysis in a locally basic melt (lower plateau) and an acidic melt (higher plateau). In the basic region, the oxidation product may be quantitatively reduced, indicating that it is largely insoluble and remains associated with the electrode. Spectroelectrochemistry in the visible region reveals the presence of some dissolved cobalt as $CoCl_4^{2-}$. A manuscript dealing with this work is being prepared for publication.

3. Studies with $FeCl_3$-NaCl melts. The use of melts of the type $FeCl_3$-NaCl has been briefly studied. Use of the Fe(III)/Fe(II) couple in such melts could possibly yield higher energy densities than those achieved in batteries based on $AlCl_3$-NaCl melts. A test cell using molten $FeCl_3$-NaCl in contact with a β"-alumina separator performed very poorly; the internal resistance rose rapidly and the separator failed structurally after only four days of operation at 200 °C. The Fe(III)

clearly reacts with the β"-alumina, particularly along grain boundaries. The incompatibility of Fe(III) and β"-alumina suggests that it will be impractical to construct cells in which these two materials are in contact.

E. New Molten Salt Solvents

1. **Fluoride-containing chloroaluminate melts;** Raman spectroscopic studies of fluoride-containing chloroaluminate melts have led to the characterization of the new species $AlCl_3F^-$, $AlCl_2F_2^-$, and $AlClF_3^-$ (Appendix VIII). During the course of this work, it was discovered that these fluoride-containing high temperature melts could be handled in quartz provided that the molar ratio of fluorine to aluminum does not exceed four. These higher temperature chlorofluoroaluminate molten salts may prove to be useful solvents for the electrodeposition of certain refractory metals (e. g., W, Nb, Ta) that may not be recovered from chloroaluminate media. Continued effort in this area will involve electrochemical studies of these refractory solutes as a function of fluoride concentration.

2. **Room temperature organic tetrachloroborates;** A new molten salt system comprised of boron trichloride and N-butylpyridinium chloride (BPC) or 1-methyl-3-ethylimidazolium chloride (MEIC) has been developed and characterized (Appendix IX). These melts exhibit subambient melting points and are different from other chloroaluminate systems in that $AlCl_3$-rich compositions show no evidence of the $Al_2Cl_7^-$ ion.

Although it was initially hoped that elemental boron could be electrodeposited from these melts, it appears that the limiting cathodic process is reduction of the organic cation.

3. **Calcium halide melts.** Preliminary voltammetric studies of nickel fluoride in molten $CaCl_2$-CaF_2 (81.5-18.5 mol%) have been performed with the aim of identifying a suitable redox couple for use in a reference electrode for this melt system. Calcium halide based melts are presently being used in pyrochemical plutonium recovery operations at the Los Alamos National Laboratory (16); an increased knowledge of the fundamental chemical and physical properties of these melts and pertinent solutes would facilitate the development of such operations. Results of these preliminary investigations indicate that reduction of the NiF_2 to metallic Ni is a reversible, diffusion-controlled process at platinum and gold working electrodes. The data also suggested that alloy formation (Ni/Pt and Ni/Au) may be involved in the redox scheme.

REFERENCES

1. V. E. Norvell and G. Mamantov, "Spectroelectrochemistry", in Molten Salt Techniques, Vol. 1, D. G. Lovering and R. J. Gale, eds., Plenum Press, 1983, pp. 151-176.

2. J. Hvistendahl, P. Klaeboe, E. Rytter, and H. A. Oye, Inorg. Chem., 23, 706 (1984).

3. K. Tanemoto, G. Mamantov, R. Marassi, and G. M. Begun, J. Inorg. Nucl. Chem., 43, 1779 (1981).

4. S. Pons and M. Fleischmann, Anal. Chem., 59, 1391A (1987).

5. R. Carlin and R. A. Osteryoung, paper presented at the U. S. Army Workshop on Capacitors and Batteries for Pulse Power Applications, Asbury Park, NJ, November 1987.

6. L. G. Boxall, H. L. Jones, and R. A. Osteryoung, J. Electrochem. Soc., 121, 212 (1974).

7. D. L. Brotherton, Ph. D. Dissertation, University of Tennessee, Knoxville, 1974.

8. A. G. Cavinato, G. Mamantov, and X. B. Cox III, J. Electrochem. Soc., 132, 1136 (1985).

9. G. C. Demitras and E. L. Muetterties, J. Am. Chem. Soc., 99, 2796 (1977).

10. H. Wang, H. W. Choi, and E. L. Muetterties, Inorg. Chem., 20, 2661 (1981).

11. J. P. Collman, J. I. Brauman, G. Tustin, and G. S. Wann III, J. Am. Chem. Soc., 105, 3913 (1983).

12. B. L. Harward, Ph. D. Dissertation, University of Tennessee, Knoxville, 1985.

13. P. A. Flowers, Ph. D. Dissertation, University of Tennessee, Knoxville, 1988.

14. G. Mamantov and J. Hvistendahl, J. Electroanal. Chem., 168, 451 (1984).

15. J. L. Sudworth, Chemistry and Industry, 77 (1988).

16. L. J. Mullins, D. C. Christensen, and B. R. Babcock, Los Alamos National Laboratory Report LA-9154-MS (January 1982).

Reprinted from Analytical Chemistry, 1987, 59, 1062.

Infrared Spectroscopic Determination of Oxide in Molten Chloroaluminates

Sir: Oxide impurities in molten chloroaluminates (*1*) are difficult to avoid and may have pronounced effects on the behavior of other solute species of interest (*2–4*). The determination of oxide in these media thus represents an analytical problem of considerable importance. Several methods for quantifying oxide in chloroaluminate melts have been reported (*5–7*), all of which employ electroanalytical techniques. Recently, Laher et al. have described a voltammetric method employing Ta(V) as the probe solute that may be used to determine small amounts of dissolved oxide in $AlCl_3$–NaCl melts saturated with NaCl (*8*).

Infrared emission spectra of several binary chloroaluminate systems have been obtained by Hvistendahl et al. (*9*) using a diamond-windowed cell. Bands observed at 680 and 801 cm^{-1} in the spectra of $AlCl_3$–$NaCl_{sat}$ melts were initially assigned to combination modes of the tetrachloroaluminate ion (*9*), but work in our group showed that the intensities of these bands increase with increasing oxide concentration (*10*). This observation was confirmed by Rytter (*11*), who suggested that the bands were instead attributable to solvated AlOCl. In this paper, infrared spectroscopy is examined as a means of determining oxide in molten chloroaluminates.

By use of Hvistendahl's cell design, infrared emission spectra of several $AlCl_3$–$NaCl_{sat}$ samples were obtained and band intensities at 680 and 801 cm^{-1} were correlated to oxide concentration. As a further demonstration of the utility of the IR spectroscopic method, a standard addition experiment was performed by using external reflectance sampling, a cell of new design, and a 65/35 mol % $AlCl_3$–NaCl melt.

EXPERIMENTAL SECTION

Procedures for the purification of starting materials and preparation of melts have been described previously (*12*).

The spectroscopic cells were loaded in a nitrogen-purged drybox (Vacuum Atmospheres, HE 493 Dri-Train) before being transferred to a Digilab FTS-20E Fourier transform infrared spectrometer. Heavy insulation heating tape (Thermolyne) was used to heat the cells to 200 °C and an Omega Model 199 monitor equipped with a chromel–alumel thermocouple was employed to measure temperature. Scans were collected at an instrumental resolution of 8 cm^{-1} with the spectrometer's optical bench under dynamic vacuum.

The oxide levels of the NaCl-saturated melts were determined by the voltammetric method (*8*) prior to analysis via IR emittance sampling as described by Hvistendahl et al. (*9*). Two alternative methods of calculating the emittance of a sample, i.e., by using either an artificial blackbody or a thick sample as reference, are described in ref 9. The former method was employed to calculate the emittance spectra in this work. The artificial blackbody consisted of a stainless steel cylinder whose interior had been coated with carbon black. The source of oxide in these melt samples was AlOCl (*10*).

Infrared spectra of the 65/35 mol % melt were obtained by using external reflectance sampling and the cell shown in Figure 1. This cell is essentially an enlarged version of Hvistendahl's design (*9*) with the exception of an additional glass section that is sealed to the top of the melt-containing nickel cup via a Viton O-ring. The glass section adds an element of versatility to the cell, allowing for experiments involving in situ additions of solutes (e.g., the standard addition experiment described here) as well as making spectroelectrochemical investigations possible. The spectrometer's infrared beam was directed into the cell through the diamond window by a gold-surfaced mirror. After passing through a thin layer of the sample, the beam was reflected from the polished end of a gold piston back through the sample and out of the cell. A second gold-surfaced mirror directed the beam to the spectrometer's TGS detector. After this cell was mounted in the spectrometer sample chamber and a reference spectrum was acquired, quantitative additions of oxide were made by injecting appropriate amounts of distilled water into small glass boats and adding the boats to the cell through an "Ace-thred" port. The glass boats were employed to ensure accurate delivery of the water to the melt.

Table I. Variation of Emittance with Voltammetrically Determined Oxide Concentration[a]

oxide concn, mM	−log (1 − *e*) 680 cm^{-1}	−log (1 − *e*) 801 cm^{-1}
5	0.009	0.016
30	0.021	0.038
144	0.053	0.119
318	0.118	0.281

[a] Linear regression: (680 cm^{-1}) $y = 0.0003x + 0.0078$, $r = 0.9981$; (800 cm^{-1}) $y = 0.0008x + 0.0086$, $r = 0.9981$.

RESULTS AND DISCUSSION

An approximate equation relating emittance to concentration may be easily derived from basic physical relations. Kirchhoff's theorem is stated in the following way (*13, 14*):

$$L/a = L_{bb} \quad (1)$$

where L is the sample luminance, a is the sample absorptance, and L_{bb} is the blackbody luminance. Emittance is defined as the ratio of a sample's luminance to that of a perfect blackbody (*14, 15*), i.e.

$$e = L/L_{bb} \quad (2)$$

When eq 1 and 2 are compared, it is seen that a sample's emittance and absorptance are equal.

The total light flux falling on a sample is divided into reflected, absorbed, and transmitted components (*15*):

$$r + a + t = 1 \text{ or } r + e + t = 1 \quad (3)$$

where r is the reflectance, a is the absorptance, t is the transmittance, e is the emittance. If the sample's reflectance is neglected ($t \gg r$ for weak bands), the following relation between emittance and transmittance is obtained:

$$e = 1 - t = 1 - 10^{-kbc} \quad (4)$$

where k is the absorptivity, b is the sample thickness, and c is the sample concentration. This equation is the same as that reported by Griffiths and deHaseth (*16*) for gaseous samples and condensed samples on metallic supports.

Emittance spectra for NaCl-saturated melts of low and intermediate oxide concentrations are shown in Figure 2. The ν_3 of the tetrachloroaluminate ion is observed at ca. 470 cm^{-1} and is free of splitting and distortion, indicating that the sample layer is sufficiently thin (*9*). Clearly seen in the melt spectrum of higher oxide content are bands at 801 and 680 cm^{-1}.

Equation 4 and emittance spectra for several NaCl-saturated melts were employed to obtain the data presented in Table I. In order to account for any variations in sample thickness, the measured emittances were normalized with respect to the intensity of the ν_3 vibration of $AlCl_4^-$. Plots of −log (1 − *e*) at 680 and 800 cm^{-1} vs. oxide concentration were linear ($r = 0.998$) and exhibited a small positive y intercept (see regression equations in Table I). The observed linearity supports the reassignment of these modes to solvated oxide.

0003-2700/87/0359-1062$01.50/0

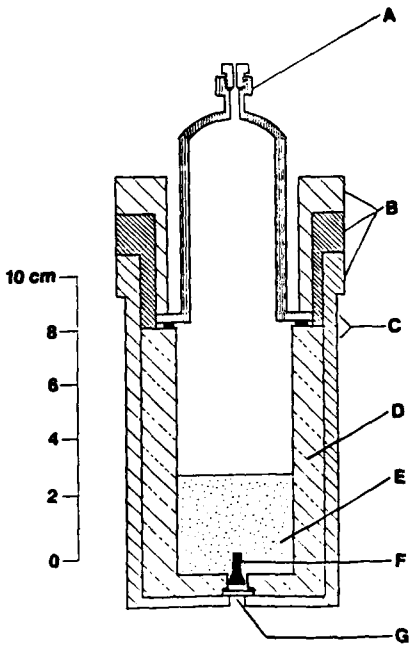

Figure 1. Sample cell used in standard addition experiments (bolts connecting stainless steel pieces have been omitted for sake of clarity): (A) glass section with Ace-thred port; (B) stainless steel clamping pieces; (C) glass–Viton–nickel seal; (D) nickel cup; (E) sample; (F) reflecting piston; (G) diamond window (with gold O-ring). The sample thickness between the diamond and piston is greatly exaggerated.

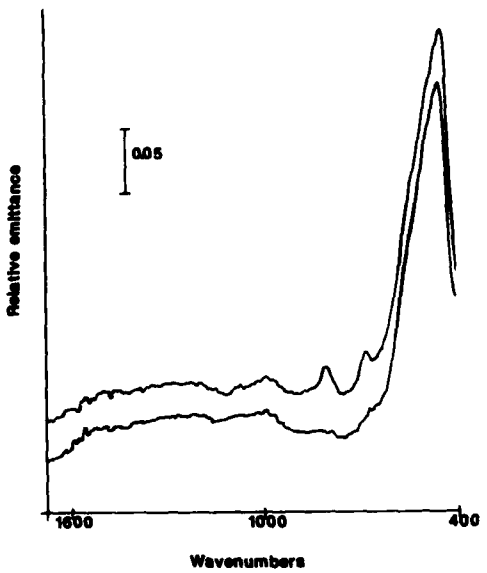

Figure 2. Infrared emittance spectra of $AlCl_3$–$NaCl_{sat}$ melts at 200 °C. $[O^{2-}]$ = 2.09 mM (bottom) and 30.16 mM (top).

Water reacts with molten chloroaluminates to produce HCl and an oxychloride species as shown below for a NaCl-saturated melt (*10*).

$$NaAlCl_4 + H_2O \rightleftharpoons 2HCl + \text{"}NaAlOCl_2\text{"}$$

Possible structures for the aluminum oxychloro complexes have been recently proposed by Rytter (*11*) and Berg and Ostvold (*17*).

Quantitative addition of water to the 65/35 melt resulted in the growth of bands at 691 and 791 cm^{-1} (Figure 3). These bands were also observed by Hvistendahl et al. who assigned them to overtone and combination modes of the $Al_2Cl_7^-$ ion (*9*). Plots of absorbance at 691 and 791 cm^{-1} vs. added oxide

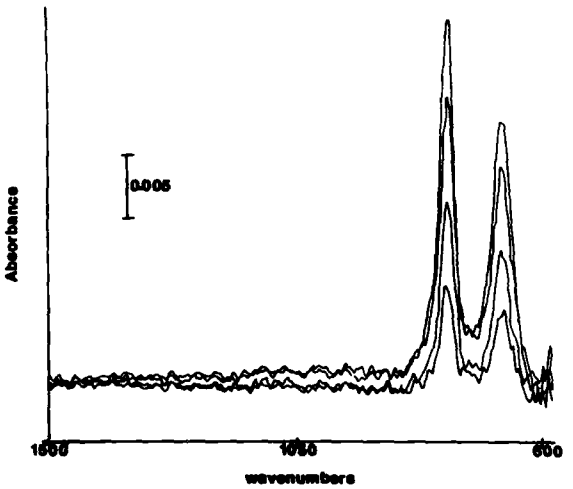

Figure 3. Difference spectra showing the growth of oxide bands at 691 and 791 cm^{-1} after additions of 14, 24, 38, and 48 mM of water (65/35 mol % $AlCl_3$–NaCl, external reflectance sampling, 200 °C).

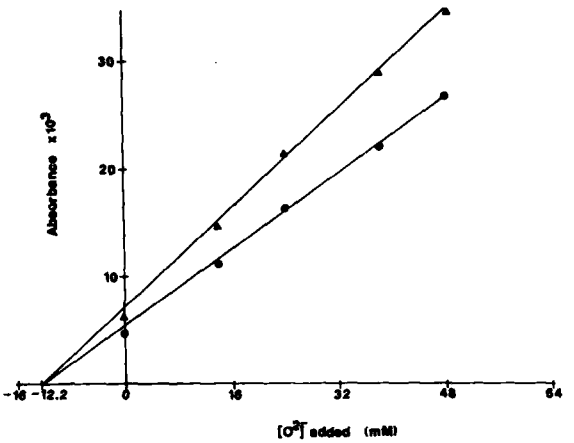

Figure 4. Plots of absorbance vs. added oxide concentration for the spectra in Figure 3 (● 691 cm^{-1} band, ▲ 791 cm^{-1} band).

concentration are shown in Figure 4. Extrapolation of the plots to zero absorbance yields a value of 12.2 mM for the initial oxide concentration, a typical value for samples prepared via the cited procedures.

The similarity of the spectral change produced by addition of either AlOCl, as in the emittance experiments, or H_2O, as in the external reflectance experiment, indicates that the same species is generated in both cases. The slight frequency shifts observed are probably due to the presence of different solvating ions, i.e., $AlCl_4^-$ in the NaCl-saturated melts and $Al_2Cl_7^-$ in the 65/35 melt.

These results demonstrate that infrared spectroscopy is an effective method for determining dissolved oxide in chloroaluminate melts. Though experimentally more difficult than the complementary Raman spectroscopic technique, infrared spectroscopy is the preferred method for reasons of sensitivity (*11*). Unlike the reported electroanalytical techniques, this spectroscopic method should be applicable to virtually any solvent system that is compatible with cell materials. Additional advantages include shorter analysis times and reduced procedural complexity.

Registry No. $AlCl_3$, 7446-70-0; NaCl, 7647-14-5.

LITERATURE CITED

(1) Mamantov, G.; Osteryoung, R. A. In *Characterization of Solutes in Nonaqueous Solvents*; Mamantov, G., Ed.; Plenum: New York, 1978; pp 223–249.

12

(2) Ting, G. Ph.D. Dissertation, University of Tennessee, 1973.
(3) Linga, H.; Stojek, Z.; Osteryoung, R. A. *J. Am. Chem. Soc.* **1981**, *103*, 3754.
(4) Scheffler, J. B.; Hussey, C. L.; Seddon, K. R.; Kear, C. M.; Armitage, P. D. *Inorg. Chem.* **1983**, *22*, 2099.
(5) Tremillon, B.; Bermond, A.; Molina, R. *J. Electroanal. Chem. Interfacial Electrochem.* **1976**, *74*, 53.
(6) Berg, R. W.; Hjuler, H. A.; Bjerrum, N. J. *Inorg. Chem.* **1984**, *23*, 557.
(7) Stojek, Z.; Linga, H.; Osteryoung, R. A. *J. Electroanal. Chem. Interfacial Electrochem.* **1981**, *119*, 365.
(8) Laher, T. M.; McCurry, L. E.; Mamantov, G. *Anal. Chem.* **1985**, *57*, 500.
(9) Hvistendahl, J.; Klaeboe, P.; Rytter, E.; Oye, H. A. *Inorg. Chem.* **1984**, *23*, 706.
(10) Mamantov, C. B.; Laher, T. M.; Walton, R. P.; Mamantov, G., In *Light Metals 1985*; Bohner, H. O., Ed.; The Metallurgical Society of AIME: 1985; pp 519–528.
(11) Rytter, E. *Extended Abstract*; Fall Meeting of the Electrochemical Society, Las Vegas, NV, 1985; No. 485.
(12) Marassi, R.; Chambers, J. Q.; Mamantov, G. *J. Electroanal. Chem. Interfacial Electrochem.* **1976**, *69*, 345.
(13) Levich, B. G. *Theoretical Physics*; North-Holland: Amsterdam, Holland, 1971; Vol. 2, pp 357–358.
(14) Hvistendahl, J.; Rytter, E.; Oye, H. A. *Appl. Spectrosc.* **1983**, *37*, 182.
(15) Harrison, T. R. *Radiation Pyrometry and Its Underlying Principles of Radiant Heat Transfer*; Wiley: New York, 1960; pp 28–38.
(16) Griffiths, P. R.; de Haseth, J. A. *Fourier Transform Infrared Spectroscopy*; Wiley: New York, 1986; p 202.
(17) Berg, R. W.; Ostvold, T. *Acta Chem. Scand., Ser. A*, in press.

Paul A. Flowers
Gleb Mamantov*

Department of Chemistry
University of Tennessee
Knoxville, Tennessee 37996-1600

RECEIVED for review July 7, 1986. Accepted December 15, 1986.

THIN-LAYER TRANSMITTANCE CELL FOR INFRARED SPECTROELECTROCHEMISTRY

Paul A. Flowers and Gleb Mamantov*
Department of Chemistry, University of Tennessee
Knoxville, Tennessee 37996-1600

Abstract

A silicon-windowed thin-layer transmittance cell for infrared spectroelectrochemistry is described and characterized using the system tetracyanoquinodimethane (TCNQ) in acetonitrile. The cell is constructed by sealing the silicon windows directly to a Pyrex glass body containing threaded glass ports, resulting in an inert, vacuum-tight vessel suitable for use with a wide variety of solvents. The cell geometry allows close placement of the reference and counter electrodes, hence minimizing ohmic potential drop and permitting reasonably accurate control of the working electrode voltage. Modifications to the described cell, designed for use in molten chloroaluminate solvents, are proposed which would permit variation of the path length and operating temperature.

THIN-LAYER TRANSMITTANCE CELL FOR INFRARED SPECTROELECTROCHEMISTRY

Paul A. Flowers and Gleb Mamantov*
Department of Chemistry, University of Tennessee
Knoxville, Tennessee 37996-1600

Since their introduction in the mid-sixties (1), spectroelectrochemical (SEC) techniques have been developed for use in virtually every region of the electromagnetic spectrum, from gamma rays (Moessbauer SEC) to radio waves (NMR SEC) (2,3). Spectroelectrochemical studies in the infrared region, however, have been somewhat limited relative to other regions, e. g., the UV-VIS, for reasons of general insensitivity (4). The advent of FTIR spectroscopy and the development of potential and polarization modulation techniques (5) have served to overcome these limitations to a great extent. The structural specificity afforded by infrared spectroscopy provides motivation for the continued pursuit of IR SEC methodology.

In situ IR SEC studies to date have employed transmittance, attenuated total reflectance (ATR), external reflectance (ER), and photothermal (PT) sampling methods. In recent years the external reflectance approach has received the most attention, having been applied to studies of adsorption, electrocatalysis, corrosion, and other surface phenomena (5-7). Because of this contemporary emphasis on surface sensitive analyses, most of the effort directed towards new cell designs has been focused on ER sampling geometries (8-10). Works involving transmittance studies of solution species have generally employed cells of the same basic "sandwich" design first utilized in the infrared region by Heineman et al. (11). Despite their proven utility, there are several drawbacks associated with these types of cells.

For example, many designs require the use of adhesive materials which may be dissolved by common organic solvents, mechanical spacers which are subject to deformation and subsequent path length errors, and o-ring arrangements which are susceptible to leakage.

Work in our laboratory has for several years been concerned with the development and application of spectroelectrochemical methods suitable for use with molten alkali chloroaluminate solvents. The extremely corrosive and hygroscopic nature of these solvents imposes special experimental constraints, e. g., the use of inert cell materials and constant isolation of the solutions from the atmosphere (12). Infrared analyses in these media are particulary difficult, primarily because of a lack of suitable window materials; diamond and silicon have been used most frequently (13).

This paper describes the design and characteristics of a versatile silicon-windowed thin-layer transmittance cell for infrared spectroelectrochemical studies. The silicon windows are directly sealed into a Pyrex glass body, avoiding the use of adhesives and o-ring materials which may be subject to dissolution in the sample. Threaded glass connectors serve both as electrode ports and a stopcock assembly, resulting in a vacuum-tight vessel which facilitates solution degassing as well as anaerobic operation. The cell geometry permits close placement of the reference and counter electrodes to the working electrode and thus minimizes ohmic potential drop. The performance of the cell is characterized using the system tetracyanoquinodimethane (TCNQ) in acetonitrile.

EXPERIMENTAL SECTION

Reagents. Acetonitrile (Aldrich, gold label), tetracyanoquinodimethane or TCNQ (Aldrich, 98%), and tetraethylammonium perchlorate or TEAP (Eastman Chemicals, reagent grade) were used as received from the manufacturer.

Cell Construction. An illustration of the spectroelectrochemical cell is given in Figure 1. The cell was constructed by torch-sealing two 10 mm dia. X 2 mm silicon windows (Spectra-Tech, Inc.) into separate Pyrex tubes. A purge of nitrogen (MG Scientific Gases, 99.997%) was maintained within the tubes during the sealing process to minimize oxidation of the window faces. Once sealed, the windows were cut and ground on a glass saw to ca. 1 mm thickness in order to reduce their contribution to background absorbance. The exposed silicon faces were polished with successively finer grades of alumina powder (Buehler Ltd.) to a mirror-like finish. The tubes were then mounted face to face in a lathe, positioned ca. 0.5 mm apart, and sealed into a larger Pyrex tube; upon cooling, contraction of the glass resulted in a path length of 0.35 mm as determined by measurement with calipers. Finally, threaded glass connectors (Ace Glass) were attached above and to the sides of the resultant "cuvette" to allow for insertion of electrodes and a Teflon stopcock. A 10 mm X 13 mm platinum screen (Aesar, 80-mesh) welded to a Pt lead at the end of a sealed Pyrex tube was employed as the optically transparent (working) electrode (OTE). Platinum foil isolated in a fritted Pyrex tube (Ace Glass, 4-8 μm porosity) was used as the auxiliary electrode, and a potassium chloride-saturated calomel electrode (SCE) served as reference.

Instrumentation. Spectra were acquired using a Digilab FTS-20E Fourier transform infrared spectrometer (Bio-Rad, Digilab Division) configured for standard mid-infrared analysis. This configuration included a high temperature ceramic source, germanium/KBr beamsplitter, and deuterated triglycine sulfate detector. Electrochemical measurements were performed using a Princeton Applied Research (PAR) Model 174A Polarographic Analyzer in conjunction with a PAR Model 175 Universal Programmer. Open circuit potentials were determined with a Keithley Model 179 TRMS digital multimeter. Voltammograms were recorded on a Houston Omnigraphic Model 2000 X-Y recorder.

Procedure. A 5 mM solution of TCNQ in 0.1 M TEAP/acetonitrile was prepared, loaded in the SEC cell, and thoroughly degassed by bubbling nitrogen prior to beginning the experiment. The auxiliary electrode chamber was filled with the pure electrolyte solution.

Potential difference spectra were calculated by subtracting absorbance spectra of the sample solution obtained with the OTE at different applied potentials. These spectra exhibit bands pointing upward and downward due to species produced and consumed, respectively, as the working electrode potential is changed. The larger the difference in potential of the subtracted spectra, therefore, the more intense are these positive and negative features, assuming a simple electrode process. An attractive aspect of this mode of data presentation is that only those features due to electroactive species are observed; absorptions due to the solvent, cell windows, and atmospheric water and carbon dioxide are effectively eliminated. The potential of the OTE was stepped through the voltammetric features by small increments, collecting spectra 1 minute after each

potential step (see "Results and Discussion") and subtracting from these spectra the appropriate reference spectrum. Typically 50 scans were coadded at 8 cm^{-1} nominal resolution (i. e., before apodization), resulting in an acquisition time of ca. 1 min. per spectrum.

RESULTS AND DISCUSSION

The reduction of TCNQ in aprotic solvents proceeds via two quasireversible one-electron steps (14), i. e.,

$$TCNQ + e^- \rightleftharpoons TCNQ^{\cdot -} \quad (1)$$

$$TCNQ^{\cdot -} + e^- \rightleftharpoons TCNQ^{2-} \quad (2)$$

The radical anion and dianion are both chemically stable and have previously been characterized by Raman (14,15) and, more recently, infrared (16) spectroelectrochemical methods.

A cyclic voltammogram (CV) for a 5 mM solution of TCNQ in 0.1 M TEAP/acetonitrile obtained in the SEC cell is shown in Figure 2. Two cathodic waves corresponding to stepwise reduction of neutral TCNQ to the dianion are seen at peak potentials of +0.170 V and -0.375 V (vs. SCE). The corresponding anodic features are observed upon scan reversal at peak potentials of -0.255 V and +0.305 V. These rather large peak separations, 135 and 120 mV for the first and second couples, respectively, are probably indicative of an ohmic potential drop across the OTE due to the high resistance of the thin solution layer (5). Peak current ratios, $i_{p,c}/i_{p,a}$, are near unity (> 0.95) for both pairs of features, indicating that the

potential step (see "Results and Discussion") and subtracting from these spectra the appropriate reference spectrum. Typically 50 scans were coadded at 8 cm^{-1} nominal resolution (i. e., before apodization), resulting in an acquisition time of ca. 1 min. per spectrum.

RESULTS AND DISCUSSION

The reduction of TCNQ in aprotic solvents proceeds via two quasireversible one-electron steps (14), i. e.,

$$TCNQ + e^- \rightleftharpoons TCNQ^{\cdot -} \quad (1)$$

$$TCNQ^{\cdot -} + e^- \rightleftharpoons TCNQ^{2-} \quad (2)$$

The radical anion and dianion are both chemically stable and have previously been characterized by Raman (14,15) and, more recently, infrared (16) spectroelectrochemical methods.

A cyclic voltammogram (CV) for a 5 mM solution of TCNQ in 0.1 M TEAP/acetonitrile obtained in the SEC cell is shown in Figure 2. Two cathodic waves corresponding to stepwise reduction of neutral TCNQ to the dianion are seen at peak potentials of +0.170 V and -0.375 V (vs. SCE). The corresponding anodic features are observed upon scan reversal at peak potentials of -0.255 V and +0.305 V. These rather large peak separations, 135 and 120 mV for the first and second couples, respectively, are probably indicative of an ohmic potential drop across the OTE due to the high resistance of the thin solution layer (5). Peak current ratios, $i_{p,c}/i_{p,a}$, are near unity (> 0.95) for both pairs of features, indicating that the

redox products are stable on the electrochemical time scale. The voltammogram exhibits an "edge effect", a result of the thin layer being exposed to the bulk about its entire perimeter. The fact that it was possible to obtain a voltammogram of this quality at the OTE in the thin layer, however, shows that reasonably accurate control of the working electrode potential has been obtained (17).

Potential difference spectra (referenced to the open circuit potential, +0.5 V) produced upon stepping the OTE through the first reduction wave are shown in the upper half of Figure 3. The negative feature at 2224 cm^{-1} corresponds to coincident ν_{19} and ν_{33} C-N stretching vibrations of neutral TCNQ (18). As the working electrode voltage is made more negative, this band disappears and two features appear at 2186 and 2156 cm^{-1} due to the same vibrational modes of the radical anion, $TCNQ^{\cdot -}$. Potential difference spectra for the second reduction wave (referenced to -0.15 V) are shown in the lower half of Figure 3. Reduction of $TCNQ^{\cdot -}$ results in the disappearance of the 2186 and 2156 cm^{-1} bands and the appearance of bands at 2153 and 2107 cm^{-1} due to the dianion, $TCNQ^{2-}$. These spectral results are in good agreement with literature data (16).

For a simple reversible couple, the equilibrium ratio of the concentrations of oxidized to reduced forms at the electrode (C_O/C_R) is determined by the applied potential, E, according to the Nernst equation,

$$E = E^{O'} + RT/nF \ln (C_O/C_R) \qquad (3)$$

where $E^{O'}$ is the formal potential, R is the molar gas constant, T is the temperature, n is the number of electrons involved in the reaction, and F is

the Faraday constant. A plot of E versus ln (C_o/C_r) yields a straight line whose slope and y-intercept give n and $E^{o'}$, respectively. In a thin-layer spectroelectrochemical experiment, the ratio C_o/C_r may be defined in terms of the observed absorbances as follows (19):

$$C_o/C_r = A_o/(A_{oi}-A_o) = (A_{ri}-A_r)/A_r \quad (4)$$

where A_x (x = r or o) is the absorbance of species x at any given potential and A_{xi} is the absorbance of species x at a potential where it is the only form of the redox couple present. Using values for C_o/C_r derived from the spectra in Figure 3, Nernst plots for the first and second reductions of TCNQ were generated. Both plots were linear (correlation coefficient of 0.999) and gave n values close to the theoretical value of one (0.96 and 0.93 for the first and second reductions, respectively). Formal reduction potentials of +0.218 V for TCNQ/TCNQ$\cdot^-$ and -0.355 V for TCNQ$\cdot^-$/$TCNQ^{2-}$ were determined from these plots, in fair agreement with the values derived from the average of peak potentials (+0.238 and -0.315 V) and literature data (+0.202 and -0.332 V) (9).

An absorbance-time curve was generated by monitoring the absorbance at 2186 cm^{-1} after stepping the working electrode potential from +0.5 V (only TCNQ present) to -0.1 V (only TCNQ$\cdot^-$ present). This curve is presented in Figure 4 and shows that complete electrolysis of the thin layer is achieved in less than one minute.

In summary, the following points may be noted concerning this SEC cell design:

(1) The long path length, relative to ER and ATR sampling, permits high

quality spectra to be obtained rapidly (typical scan times of a minute or so) and at electrochemically favorable concentrations (i. e., a few millimolar). Under the experimental conditions employed, the strongest band of the radical anion at 2186 cm^{-1} exhibited a signal-to-noise ratio of approximately 150. One may then estimate the lowest detectable concentration of this species, based on $S/N \geq 2$, to be on the order of 0.1 mM.

(2) Close placement of the reference and auxiliary electrodes allows for reasonably accurate control of the working electrode voltage by minimizing ohmic potential drop.

(3) Although edge effects are observed, exhaustive electrolysis of the optically sampled region may be achieved in less than one minute.

(4) For use with solvents less aggressive than alkali chloroaluminates, this cell design could be modified to allow variation of the path length. Incorporating threaded glass connectors at the ends of the cell body through which the window-containing tubes could be inserted (instead of being permanently sealed) should enable one to adjust the spacing between the windows, producing whatever path length is desired. This modification would also permit polishing of the silicon faces exposed to the sample should they become marred during use.

(5) An additional modification which could be useful for applications to aqueous or organic solvent systems would involve the addition of a water jacket around the cylindrical cell body. This could be easily accomplished and would allow one to control the working temperature of the solution being studied by use of a circulating water bath.

The cell described herein has been used in several spectroscopic and

spectroelectrochemical investigations in molten sodium chloroaluminates (20) and has shown no evidence of leakage or other mechanical failure. Descriptions of some of these studies are presently being prepared for publication.

LITERATURE CITED

1. Kuwana, T.; Darlington, R. K.; Leedy, D. W. Anal. Chem. 1964, 36, 2023.
2. Bard, A. J.; Faulkner, L. R. "Electrochemical Methods: Fundamentals and Applications"; Wiley: New York, 1980; Chapter 14.
3. Heineman, W. R. J. Chem. Ed. 1983, 60, 305.
4. Robinson, J. In "Electrochemistry"; A Specialist Report; The Royal Society of Chemistry: London, 1984; Vol. 9, Chapter 3.
5. Foley, J. K.; Pons, S. Anal. Chem. 1985, 57, 945A.
6. Korzeniewski, C; Pons, S.; Prog. Analyt. Spec. 1987, 10, 1.
7. Ashley, K.; Pons, S. Chem. Rev. 1988, 88, 673.
8. Seki, H.; Kunimatsu, K.; Golden, W. G. Appl. Spec. 1985, 39, 437.
9. Roe, K. K.; Sass, J. K.; Bethune, D. S.; Luntz, A. C. J. Electroanal. Chem. 1987, 216, 293.
10. Hinman, A. S.; Pavelich, B. J. Can. J. Chem. 1987, 65, 919.
11. Heineman, W. R.; Burnett, J. N.; Murray, R. W. Anal. Chem. 1968, 40, 1974.
12. Norvell, V. E.; Mamantov, G. In "Molten Salt Techniques"; Lovering, D. G.; Gale, R. J., Eds.; Plenum Press: New York, 1983; Vol. 1, Chap. 7.

13. Gilbert, B. in "Molten Salt Chemistry: An Introduction and Selected Applications"; Mamantov, G.; Marassi, R., Eds.; D. Reidel Publishing Company: Boston, 1987; p. 201.

14. Jeanmaire, D. L.; Van Duyne, R. P. J. Am. Chem. Soc. 1976, 98, 4029.

15. Van Duyne, R. P.; Suchanski, M. R.; Lakovita, J. M.; Siedle, A. R.; Parks, K. D.; Cotton, T. M. J. Am. Chem. Soc. 1979, 101, 2832.

16. Khoo, S. B.; Foley, J. F.; Korzeniewski, C.; Pons, S.; Marcott, C. J. Electroanal. Chem. 1987, 233, 223.

17. Bard, A. J.; Faulkner, L. R. "Electrochemical Methods: Fundamentals and Applications"; Wiley: New York, 1980; p. 569.

18. Khatkale, M. S.; Devlin, J. P. J. Chem. Phys. 1979, 70, 1851.

19. DeAngelis, T. P.; Heineman, W. R. J. Chem. Ed. 1976, 53, 594.

20. Flowers, P. A., Dissertation, University of Tennessee, Knoxville, 1988.

CREDIT

The authors wish to gratefully acknowledge financial support from the Air Force Office of Scientific Research. They would also like to thank L. H. Norman for the construction of the cell and useful discussions.

FIGURE CAPTIONS

Figure 1. Side (1) and end (2) views of the transmittance cell used for infrared spectroscopic and SEC experiments: (A) port for OTE; (B) ports for reference and auxiliary electrodes; (C) silicon windows; (D) Teflon stopcock assembly; (E) light path. The reference and auxiliary ports have been omitted from the side view (1) and the stopcock assembly from the end view (2) for sake of clarity.

Figure 2. Cyclic voltammogram for 5 mM TCNQ in 0.1 M TEAP/acetonitrile obtained in the thin layer cell: Pt mesh working, Pt foil auxiliary, SCE reference, 5mV/s.

Figure 3. Potential difference spectra for TCNQ reduction. Upper spectra (referenced to +0.5 V): E = 0.295, 0.255, 0.210, and 0.130 V; lower spectra (referenced to -0.15 V): E = -0.250, -0.315, -0.350, -0.400, -0.450 V.

Figure 4. Absorbance at 2186 cm^{-1} versus time for generation of $TCNQ^{\cdot -}$ (OTE potential stepped from +0.5 to -0.1).

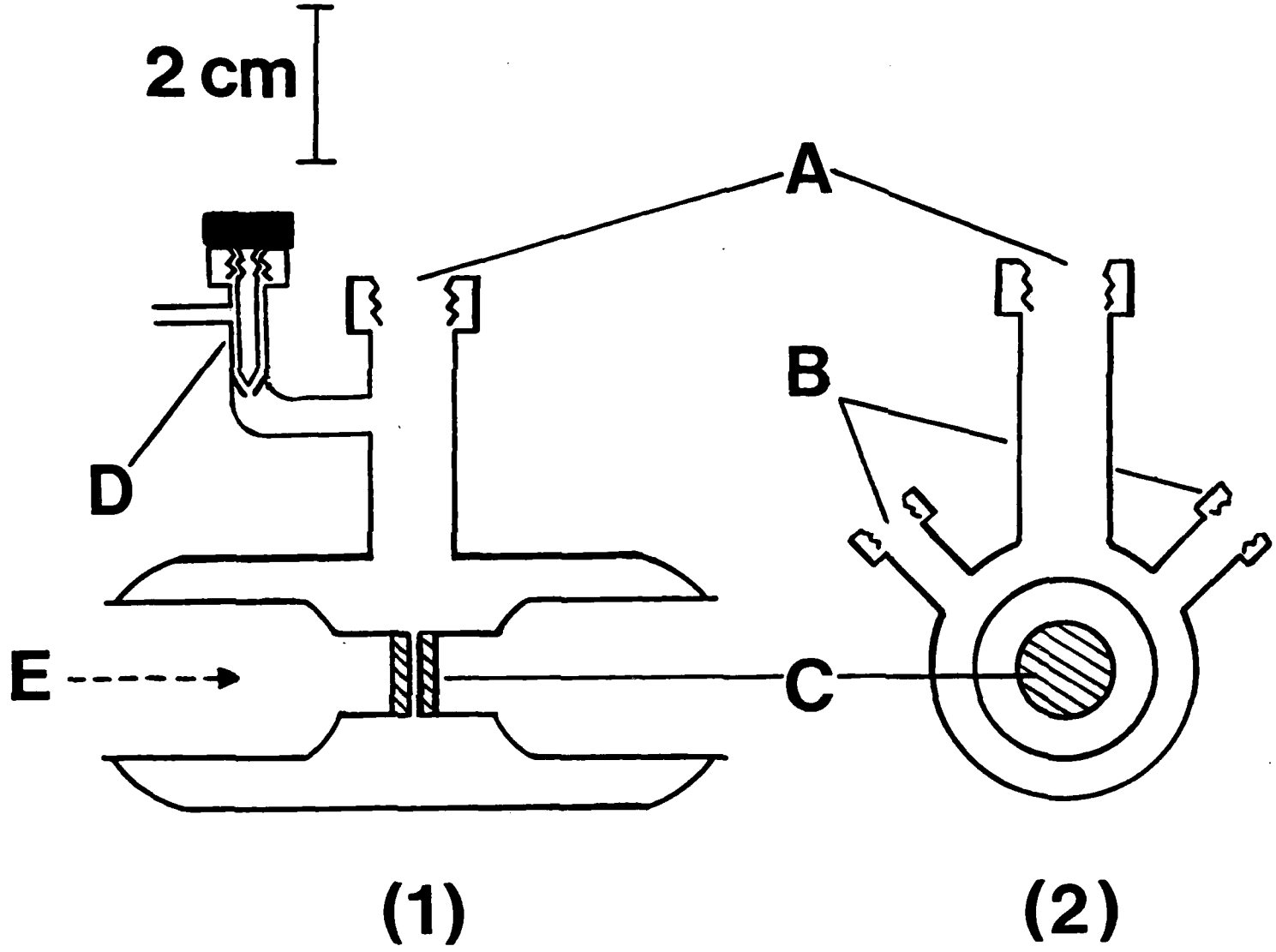
2 cm
A
B
C
D
E
(1)
(2)

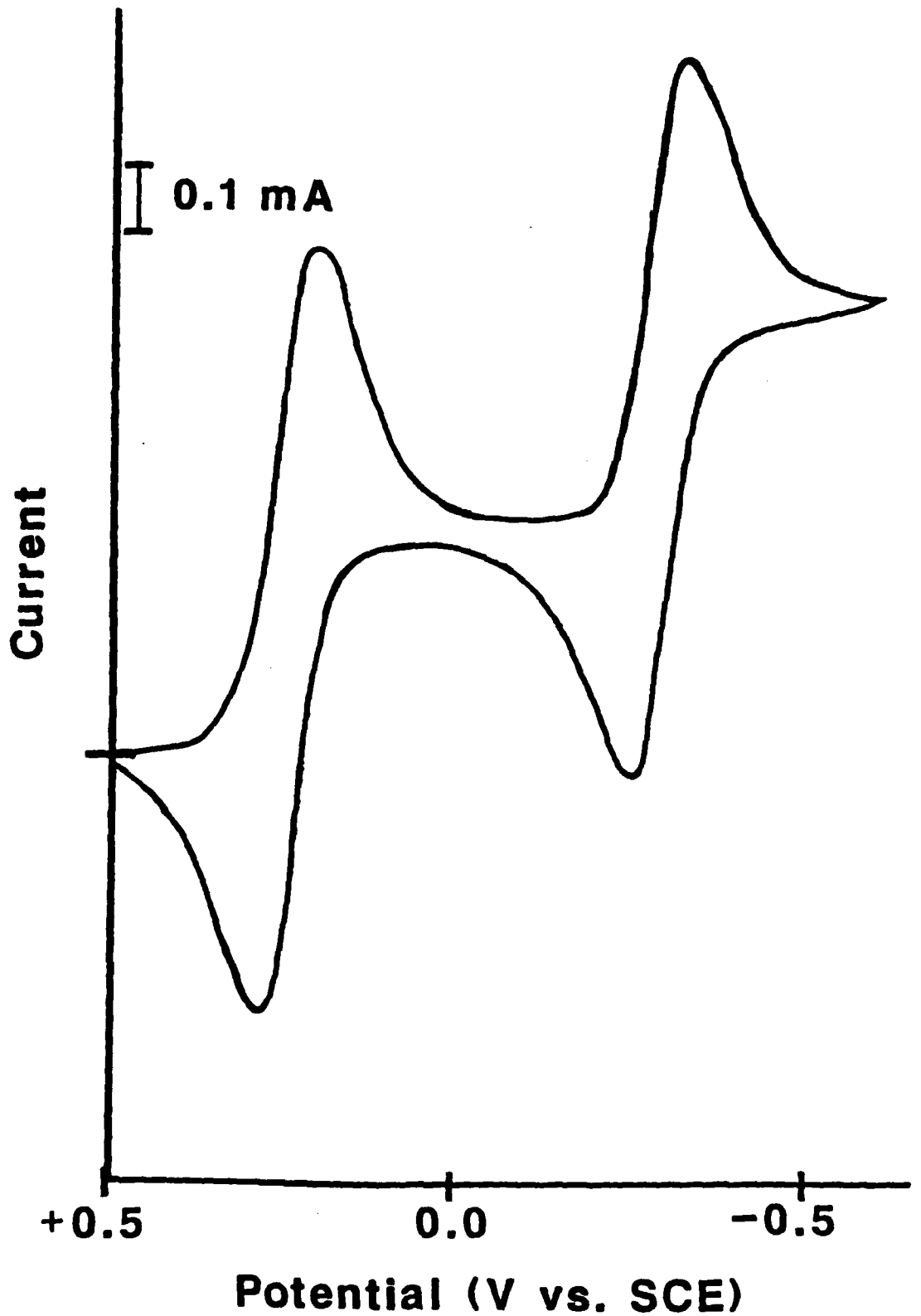
0.1 mA
Current
+0.5
0.0
−0.5
Potential (V vs. SCE)

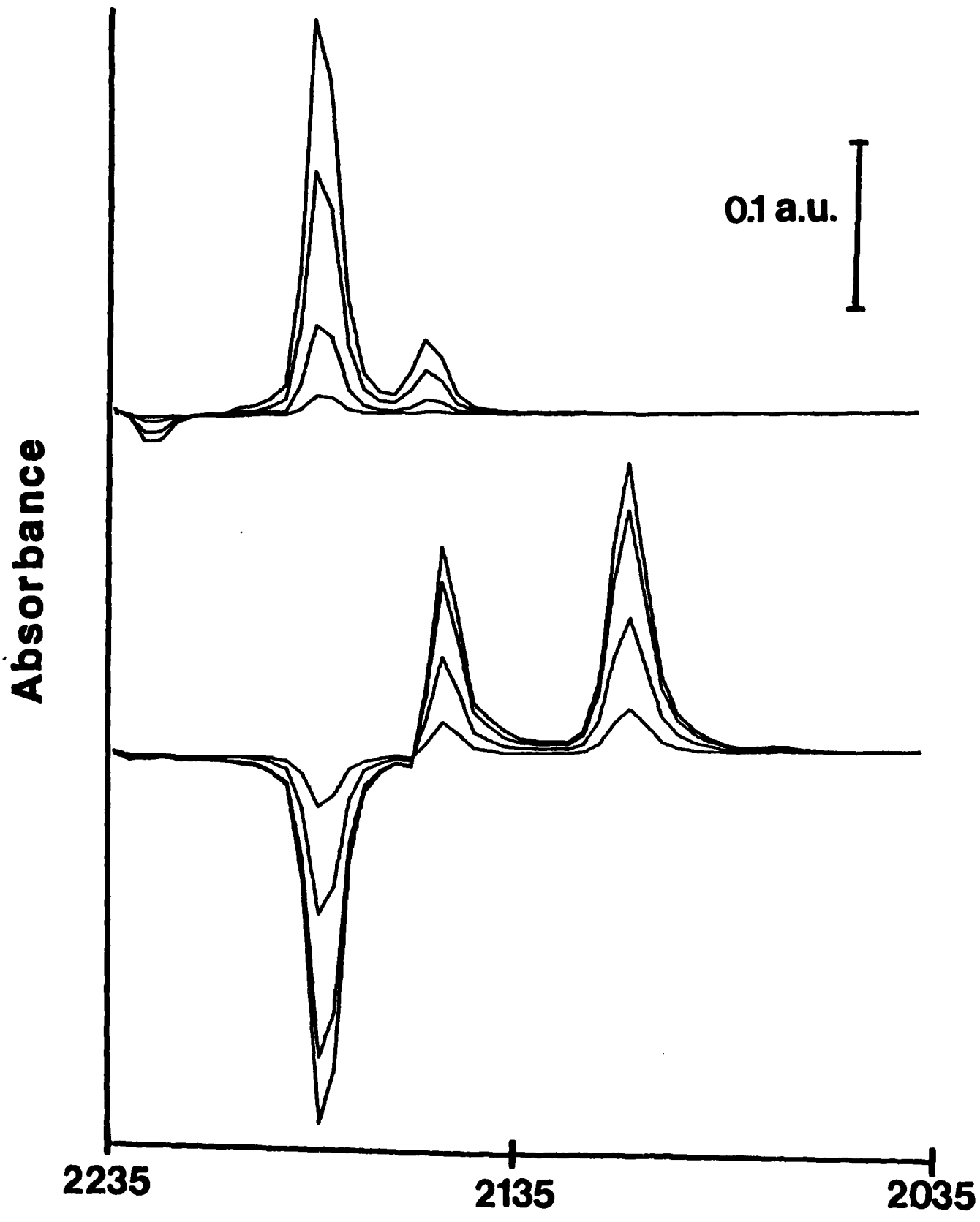
0.1 a.u.
Absorbance
2235
2135
2035
Wavenumbers (cm⁻¹)

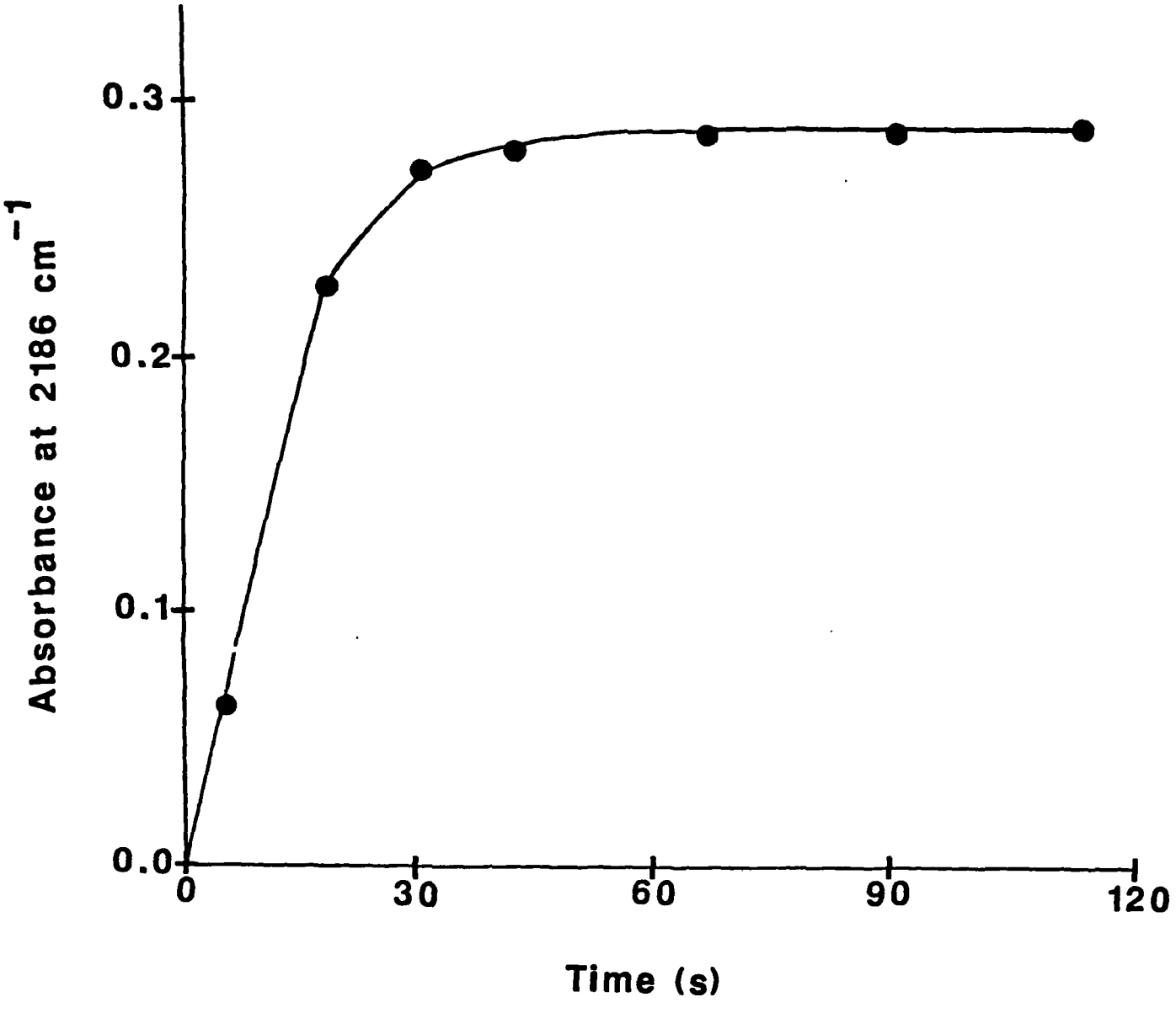
0.3
0.2
0.1
0.0
Absorbance at 2186 cm^{-1}
0
30
60
90
120
Time (s)

APPENDIX III Submitted to
J. Electrochem. Soc.

INFRARED SPECTROSCOPIC AND SPECTROELECTROCHEMICAL INVESTIGATION OF CHLORANIL IN MOLTEN SODIUM CHLOROALUMINATES

Paul A. Flowers and Gleb Mamantov*

Department of Chemistry, University of Tennessee
Knoxville, Tennessee 37996-1600

ABSTRACT

The infrared spectroscopic and spectroelectrochemical properties of tetrachloro-p-benzoquinone (chloranil or Q) in molten aluminum chloride-sodium chloride mixtures have been examined. Spectroscopic results suggest that in acidic melts (> 50 mol% $AlCl_3$) chloranil exists as a Lewis acid adduct with $AlCl_3$ (or $Al_2Cl_7^-$) coordinated at one of the carbonyl oxygens and at the carbon-carbon double bonds. No evidence for adduct formation was observed in basic melts (< 50 mol% $AlCl_3$). Spectroelectrochemical data indicate that chloranil is reduced in an overall two-electron process in basic melts, in agreement with previously reported electrochemical results. In acidic melts, however, the data suggest stepwise one-electron reductions to produce the radical anion and dianion. The presence of two closely spaced one-electron reduction steps is confirmed by differential pulse voltammetry.

Molten chloroaluminates, produced by fusing mixtures of $AlCl_3$ and other chloride salts, have long been recognized as unusual and interesting media for the study of inorganic solutes (1-3). More recently, chloroaluminate melts have been employed as solvents for investigations of organic species (4-6). The behavior of these solutes is frequently dependent upon the Lewis acidity of the melt, which may be adjusted by varying the molar ratios of the component salts (7).

The solution chemistry of quinones in molten chloroaluminate solvents has received a considerable amount of attention (8-12). In particular, there has been interest in tetrachloro-p-benzoquinone (chloranil or Q) because of its potential utility as a cathode material for high energy molten salt batteries (8,10,13). Bartak and Osteryoung examined the electrochemical behavior of chloranil in $AlCl_3$-NaCl melts (8) and found that the reduction proceeds via the ECEC mechanism shown below:

$$Q + e^- \rightleftharpoons Q^{\cdot -} \quad (1)$$

$$Q^{\cdot -} + A \longrightarrow QA^{\cdot -} \quad (2)$$

$$QA^{\cdot -} + e^- \rightleftharpoons QA^{2-} \quad (3)$$

$$QA^{2-} + A \longrightarrow QA_2^{2-} \quad (4)$$

where A represents a Lewis acidic solvent species, either $AlCl_3$ or $Al_2Cl_7^-$. The adduct formation reaction (equation 2) is rapid and the complexed radical anion $QA^{\cdot -}$ is reduced at potentials consistent with Q reduction (equation 1), hence only one cathodic wave corresponding to

an overall two-electron reduction is observed. At very fast scan rates, reaction 2 may be "outrun" and two waves corresponding to stepwise one-electron reductions of Q to Q^{2-} are observed.

A similar redox behavior was observed for chloranil in $AlCl_3$-butylpyridinium chloride (BPC) melts (10) with slight differences owing to the greater Lewis acidity of the sodium chloroaluminate solvent. Based on infrared results, the authors concluded that, in the acidic $AlCl_3$-BPC melts, Q is complexed by $AlCl_3$ at one of the carbonyl oxygens and at the ring chlorines (10).

Walters has reported the only attempt thus far at examining the infrared spectroelectrochemical behavior of chloranil (or any other solute) in molten sodium chloroaluminates (14). A cell employing a silicon internal reflectance element was used to obtain infrared spectra of chloranil and its reduction products in an acidic $AlCl_3$-NaCl melt (63 mol% $AlCl_3$). Bands were observed at 1697, 1630, 1578, and 1529 cm^{-1} for the neutral chloranil species. Electrolyzing the solution at negative potentials with a platinum foil electrode placed near the silicon crystal resulted in a decrease in the intensity of these bands and the appearance of a feature at 1495 cm^{-1}. Unfortunately, these spectra were of somewhat poor quality, a result of the low transmittance of the cell (2.7% maximum) and its relatively short path length. As a result, fairly concentrated solutions, i. e., 130 mM, were required to achieve acceptable signal-to-noise ratios. In addition, the long path length of the infrared beam through the silicon crystal resulted in total absorption below ca. 1450 cm^{-1}.

While infrared spectra of aluminum chloride-organic chloride melts

(e. g., the $AlCl_3$-BPC system) may be obtained using fairly conventional cell materials (9,10,12), the more corrosive aluminum chloride-alkali chloride mixtures and their concomitant higher working temperatures pose a more difficult experimental situation as evidenced by the work of Walters described above (14). The most successful cell design to date for use with alkali chloroaluminates has been that first introduced by Hvistendahl et al. (15). This cell basically consists of a nickel container to which a diamond window is sealed via a gold gasket; a polished nickel piston within the cell allows for sampling of a thin layer of melt by either emittance or external reflectance techniques. Our laboratory subsequently constructed a modified version of this cell (16) with the aim of performing spectroelectrochemical studies. Unfortunately, many of the solutes intended for analysis (including chloranil) were found to be reduced by the nickel cell body. A transmittance cell employing silicon windows sealed directly to a glass body was subsequently constructed and shown to be useful for infrared studies in molten sodium chloroaluminates (17). The spectroelectrochemical characteristics of this cell have been described (18).

This paper presents the results of infrared studies of chloranil in molten sodium chloroaluminates. The transmittance cell described above is employed to examine the spectroscopic and spectroelectrochemical behavior of chloranil in basic (49.8 mol% $AlCl_3$) and acidic (63 mol% $AlCl_3$) melts.

Experimental

Chemicals.--Aluminum chloride (Fluka Chemical Corp., puriss. grade) was purified by an extraction/distillation procedure similar to one previously reported (19). Sodium chloride (Mallinckrodt Inc., reagent grade) was dried under vacuum at 450 °C for at least four days prior to use. Melts of the desired composition were prepared by placing the appropriate quantities of component salts in a Pyrex tube, evacuating and sealing the tube, and fusing the mixture in a rocking furnace at 200 °C for ca. 24 h. Tetrachloro-p-benzoquinone (Fluka Chemical Corp., > 99%) was used as received.

Infrared Cell.--An illustration of the infrared cell is given in Figure 1. The cell was constructed by torch-sealing two 10 mm dia. X 2 mm silicon windows (Spectra-Tech, Inc.) into separate Pyrex tubes. A purge of nitrogen (MG Scientific Gases, 99.997%) was maintained within the tubes during the sealing process to minimize oxidation of the window faces. Once sealed, the windows were cut and ground on a glass saw to ca. 1 mm thickness in order to reduce their contribution to background absorbance. The exposed silicon faces were polished with successively finer grades of alumina powder (Buehler Ltd.) to a mirror-like finish. The tubes were then mounted face to face in a lathe, positioned ca. 0.5 mm apart, and sealed into a larger Pyrex tube; upon cooling, contraction of the glass resulted in a path length of 0.35 mm as determined by measurement with calipers. Finally, threaded glass connectors (Ace Glass) were attached above and to the sides of the resultant "cuvette" to allow for insertion of electrodes and a Teflon

stopcock. A 10 mm X 13 mm platinum screen (Aesar, 80-mesh) welded to a Pt lead at the end of a sealed Pyrex tube was employed as the optically transparent working electrode (OTE). A coiled aluminum wire was used as the auxiliary electrode, and an aluminum wire immersed in $AlCl_3$-NaCl (63 mol% $AlCl_3$) served as the reference electrode. Both the reference and auxiliary electrodes were isolated from the bulk of the melt in fritted glass tubes (Ace Glass, 4-8 μm porosity).

Instrumentation.--Spectra were acquired using a Digilab FTS-20E Fourier transform infrared spectrometer configured for standard mid-infrared analysis. Electrochemical experiments were performed using a Princeton Applied Research (PAR) Model 174A Polarographic Analyzer in conjunction with a PAR Model 175 Universal Programmer. Voltammograms were recorded with a Houston Omnigraphic 2000 XY recorder. A Keithley Model 177 Microvoltmeter was employed to measure open circuit potentials.

Procedure.--Potential difference spectra were calculated by subtracting absorbance spectra of the sample solution obtained with the OTE at different applied potentials. These spectra exhibit bands pointing upward and downward due to species produced and consumed, respectively, as the working electrode potential is changed. An attractive aspect of this mode of data presentation is that only those features due to electroactive species are observed; absorptions due to the solvent, cell windows, and atmospheric water and carbon dioxide are effectively eliminated. The potential of the OTE was stepped through the voltammetric features by small increments, collecting spectra one minute after each potential step and subtracting from these spectra the

appropriate reference spectrum. Typically 50 scans were coadded at 8 cm^{-1} nominal resolution, resulting in an acquisition time of ca. one minute per spectrum.

Results and Discussion

Adduct Formation.--Solutions of chloranil in NaCl-saturated melts are amber and become violet when the melt is made acidic by addition of $AlCl_3$. This color change is reversible, as the amber color returns when the solution is re-saturated with NaCl, and is apparently a result of adduct formation between the chloranil and Lewis acidic solvent species (i. e., $Al_2Cl_7^-$ or $AlCl_3$). Similar color changes were observed by Cheek and Osteryoung (10) for chloranil in $AlCl_3$/BPC melts. Infrared spectra of basic $AlCl_3$/BPC solutions were obtained which showed bands at 1692 cm^{-1} (C-O stretching) and 1570 cm^{-1} (C-C stretching). Acidic solutions also exhibited the 1692 cm^{-1} feature, though diminished in intensity relative to the basic solution spectrum, and a new band at 1545 cm^{-1}. The authors attributed this new band to a complexed carbonyl stretch and, based on the persistence of the 1692 cm^{-1} band, concluded that one carbonyl group remained uncomplexed. Based on the absence of the 1570 cm^{-1} feature from the acidic solution spectrum, in addition to electrochemical results, the authors suggested that further complexation at the chlorine atom lone pairs had occurred.

Infrared spectra of ca. 8 mM solutions of chloranil in $AlCl_3$-NaCl melts of composition ranging from 63 mol% $AlCl_3$ to NaCl-saturated (ca. 49.8 mol% $AlCl_3$) are shown in Figure 2. These spectra were obtained by

beginning with a frozen 63/37 $AlCl_3$-NaCl solution to which an excess of NaCl had been added. Spectra were acquired immediately after melting (composition ca. 63/37) and at regular intervals thereafter over a 24 h period as the solution gradually became saturated with NaCl. The acidic solution spectrum exhibited bands at 1698, 1630, 1530, 1130, and 749 cm^{-1}; as the melt became basic, these features disappeared and new bands grew in at 1690, 1555, 1119, and 745 cm^{-1}. The transition between these two sets of spectral features was smooth and continuous, indicating a simple conversion of one species to another. These data are presented in Table I.

The presence of $AlCl_3$ and $Al_2Cl_7^-$ in the acidic melt results in the formation of Lewis acid adducts between these species and neutral chloranil. This adduct formation involves charge transfer from the chloranil molecule to the acidic solvent species and, consequently, produces shifts in the infrared frequencies of vibrations involving affected bonds. Complexation of one carbonyl oxygen causes a decrease in the C-O stretching frequency of that carbonyl group (from 1690 to 1630 cm^{-1}) and a slight increase in the C-O stretching frequency of the carbonyl group which remains uncomplexed (from 1690 to 1698 cm^{-1}). The former shift is a result of the reduced carbon-oxygen bond order which accompanies the transfer of electron density from the complexed carbonyl oxygen to the Lewis acid entity; the now electron deficient oxygen atom withdraws charge from the C-O double bond, hence lowering its bond order and decreasing the C-O stretching frequency. Likewise, this complexation results in a slight increase of the uncomplexed carbonyl stretching frequency as the now electron deficient pi system

withdraws a small amount of charge from the uncomplexed oxygen atom, hence increasing the carbon-oxygen bond order (20). The C-C double bond stretching mode exhibits a significant negative shift upon complexation, from 1555 to 1530 cm^{-1}, and the C-Cl stretching modes exhibit small positive frequency shifts, from 745 to 749 cm^{-1} and from 1119 to 1130 cm^{-1}. This is apparently not a result of complexation at the chlorine atoms, as the carbon-halogen stretching modes of such adducts typically display negative frequency shifts (21). The directions and the relative magnitudes of these shifts suggest that the chloranil molecule in the acidic melt is further complexed at the carbon-carbon double bonds.

Spectroelectrochemistry in Basic Melts.--A cyclic voltammogram of a 9 mM solution of chloranil (Q) in an $AlCl_3$-$NaCl_{sat}$ melt (49.8 mol% $AlCl_3$) obtained in the spectroelectrochemical cell is shown in Figure 3. A small oxidation wave is seen upon the initial anodic scan, indicating that a slight chemical reduction of the chloranil has occurred. This supports previous findings which suggest that Q undergoes a partial reduction in the sodium chloroaluminate melt, possibly a result of chloride oxidation (8,13). Although no such anodic feature was observed by Bartak and Osteryoung (8) in 50/50 $AlCl_3$-NaCl, the higher levels of Cl^- in the NaCl-saturated melt used here may be responsible for a more extensive reduction of the chloranil. Scanning cathodically yielded a single wave at +1.345 V due to the overall two-electron reduction of Q to the complexed dianion. Upon scan reversal, a wave corresponding to oxidation of the dianion

was observed at +1.535 V. The ratio of cathodic to anodic peak currents is greater than the theoretical value of one; this may be a result of the proximity of the anodic feature to the electrochemical limit of the solvent, making an accurate measurement of the current difficult.

Potential difference spectra (referenced to +1.60 V) for the reduction of chloranil in the basic melt are shown in Figure 4. Strong bands corresponding to the reduction product are observed at 1435 and 949 cm^{-1} with weaker features at 1373, 1215, and 1180 cm^{-1}. These spectral features are compared to literature data in Table II. A Nernst plot generated using C_o/C_r ratios calculated from the 1690 cm^{-1} band is shown in Figure 5 and yields an n-value of 1.74 (in fair agreement with the theoretical value of 2) and an $E^{o'}$ of 1.42 V (close to the value derived from the average of the cathodic and anodic peak potentials, 1.44 V).

Spectroelectrochemistry in Acidic Melts.--A cyclic voltammogram of an 8 mM solution of chloranil in 63/37 $AlCl_3$-NaCl obtained in the spectroelectrochemical cell is shown in Figure 6. Cathodic and anodic waves are observed at +1.625 and +1.815 V, respectively, exhibiting the expected positive shift relative to the voltammetric features of the basic solution (8). Again, the proximity of the anodic wave to the solvent limit prevented an accurate measurement of the peak current ratio.

Potential difference spectra (referenced to +1.90 V) for the reduction of Q in this melt exhibited two different sets of product

features as shown in Figure 7. For the first few potential increments bands were observed to grow in at 1486, 1180, and 980 cm^{-1} (upper half of Figure 7). At more negative potentials, these features began to shrink and new bands appeared at 1391 and 880 cm^{-1} (lower half of Figure 7). Two separate Nernst plots generated using C_o/C_r ratios calculated from a neutral chloranil band (1630 cm^{-1}) and a band of the latter reduction product (1391 cm^{-1}) are shown in Figure 8. These data indicate that the chloranil is reduced via a one-electron step (n = 1.09) at a standard potential of +1.751 V. The species represented by the 1391, 880, and 707 cm^{-1} bands is likewise produced by a one-electron reduction step (n = 1.12), but at a standard reduction potential of +1.673 V. Although two separate waves are not readily discernable in the cyclic voltammogram at scan rates between 5 and 500 mV/s, a differential pulse voltammogram (DPV) of an identical solution exhibited two reduction features at +1.740 and +1.675 V (Figure 9). The location and separation of these DPV peaks are in good agreement with the Nernst plot data.

These results suggest that chloranil is reduced via two consecutive, closely spaced one-electron steps in the 63/37 melt. In less acidic media (i. e., near the equimolar composition), one-electron reduction of Q results in a rapid complexation of the resultant radical anion to produce a species that is reducible at the same potential as that for the reduction of the neutral. At normal scan rates, therefore, an overall two-electron reduction is observed (8). Perhaps the higher levels of $AlCl_3$ (or $Al_2Cl_7^-$) present in the 63/37 melt result in a complexed chloranil molecule whose one electron reduction

potential is shifted sufficiently positive to permit resolution of this step from the subsequent reduction of the radical anion to the dianion. The first set of product bands observed in the potential difference spectra (upper half of Figure 7) must then correspond to the complexed radical anion of chloranil and the latter set (lower half of Figure 7) to the complexed dianion. These spectral features are compared to literature data in Table II.

It should be noted that the chloranil radical anion is reportedly stable in the acidic HF/SbF_5 system (22). The existence of $Q^{\cdot -}$ has also been suggested as an alternative interpretation of electrochemical results obtained by Cheek and Osteryoung in acidic $AlCl_3$-BPC (10).

Acknowledgement

The authors wish to gratefully acknowledge financial support from the Air Force Office of Scientific Research.

REFERENCES

1. T. C. F. Munday and J. D. Corbett, *Inorg. Chem.*, 5, 1263 (1966).

2. N. J. Bjerrum, C. R. Boston, and G. P. Smith, *Inorg. Chem.*, 6, 1162 (1967).

3. G. Torsi, K. W. Fung, G. M. Begun, and G. Mamantov, *Inorg. Chem.*, 10, 2285 (1971).

4. H. L. Jones and R. A. Osteryoung, in "Advances in Molten Salt Chemistry", Vol. 3, J. Braunstein, G. Mamantov, and G. P. Smith, Editors, Plenum Press, New York (1975), pp. 121-176.

5. G. P. Smith and R. M. Pagni, in "Molten Salt Chemistry: An Introduction and Selected Applications", G. Mamantov and R. Marassi, Editors, D. Reidel Publishing Company, Boston (1987), pp. 383-404.

6. R. M. Pagni, in "Advances in Molten Salt Chemistry", Vol. 6, G. Mamantov, C. B. Mamantov, and J. Braunstein, Editors, Elsevier Scientific Publishing Company, Amsterdam (1987), pp. 211-346.

7. G. Mamantov and R. A. Osteryoung, in "Characterization of Solutes in Nonaqueous Solvents", G. Mamantov, Editor, Plenum Press, New York (1978), Chapter 11, pp. 223-249.

8. D. E. Bartak and R. A. Osteryoung, *J. Electroanal. Chem.*, 74, 69 (1976).

9. G. Cheek and R. A. Osteryoung, *J. Electrochem. Soc.*, 129, 2488 (1982).

10. G. Cheek and R. A. Osteryoung, *J. Electrochem. Soc.*, 129, 2739 (1982).

11. M. Lipsztajn, S. Sahami, and R. A. Osteryoung, *Inorg. Chem.*, 25, 549 (1986).

12. F. A. Uribe and R. A. Osteryoung, *J. Electrochem. Soc.*, 135, 378 (1988).

13. G. Mamantov, R. Marassi, and J. Q. Chambers, in "High Energy Cathodes for Fused Salt Batteries", Final Report, Contract DAABO7-73-7-0060 (1974), ECOM-0060-F.

14. S. Walters, Ph.D. Dissertation, University of Tennessee, Knoxville, 1983.

15. J. Hvistendahl, P. Klaeboe, E. Rytter, and H. A. Oye, *Inorg. Chem.*, 23, 706 (1984).

16. P. A. Flowers and G. Mamantov, *Anal. Chem.*, 59, 1062 (1987).

17. P. A. Flowers, Ph.D. Dissertation, University of Tennessee, Knoxville, 1988.

18. P. A. Flowers and G. Mamantov, *Anal. Chem.*, in press.

19. R. Marassi, J. Q. Chambers, and G. Mamantov, *J. Electroanal. Chem.*, 69, 345 (1976).

20. J. Andrews and P. Keefer, in "Molecular Complexes in Organic Chemistry", Plenum Press, New York (1969), p. 37.

21. Reference 15, p. 44.

22. J. Devynck, A. Hadid, P. L. Fabre, and B. Tremillon, *Anal. Chim. Acta*, 100, 343 (1978).

Table I. Major infrared features (cm^{-1}) for chloranil.

Vibration	Mode	In 63/37 Melt	In NaCl-sat'd melt	Solid*
C-O stretch	ν_{18} (B_{1u})	1698, 1630	1690	1688
C-C stretch	ν_{23} (B_{2u})	1530	1555	1572
C-Cl stretch	ν_{19} (B_{1u})	1130	1119	1111
C-Cl stretch	ν_{25} (B_{2u})	749	745	755

* from H. Yamada, M. Saheki, S. Fukushima, and T. Nagasao, *Spectrochim. Acta, Part A*, 30, 295 (1974).

Table II. Major infrared features (cm^{-1}) for chloranil (Q) and its reduction products.

Species	In 63/37 Melt	In NaCl-sat'd Melt	In DMSO*
Q	1698, 1630	1690	1693
	1530	1555	1581
	1130	1119	
	749	745	
$Q^{\cdot -}$	1486		1527
	1180		1140
	980		
Q^{2-}	1391	1435	
	880	949	

* from B. R. Clark, and D. H. Evans, *J. Electroanal. Chem.*, 69, 181 (1976).

LIST OF FIGURES

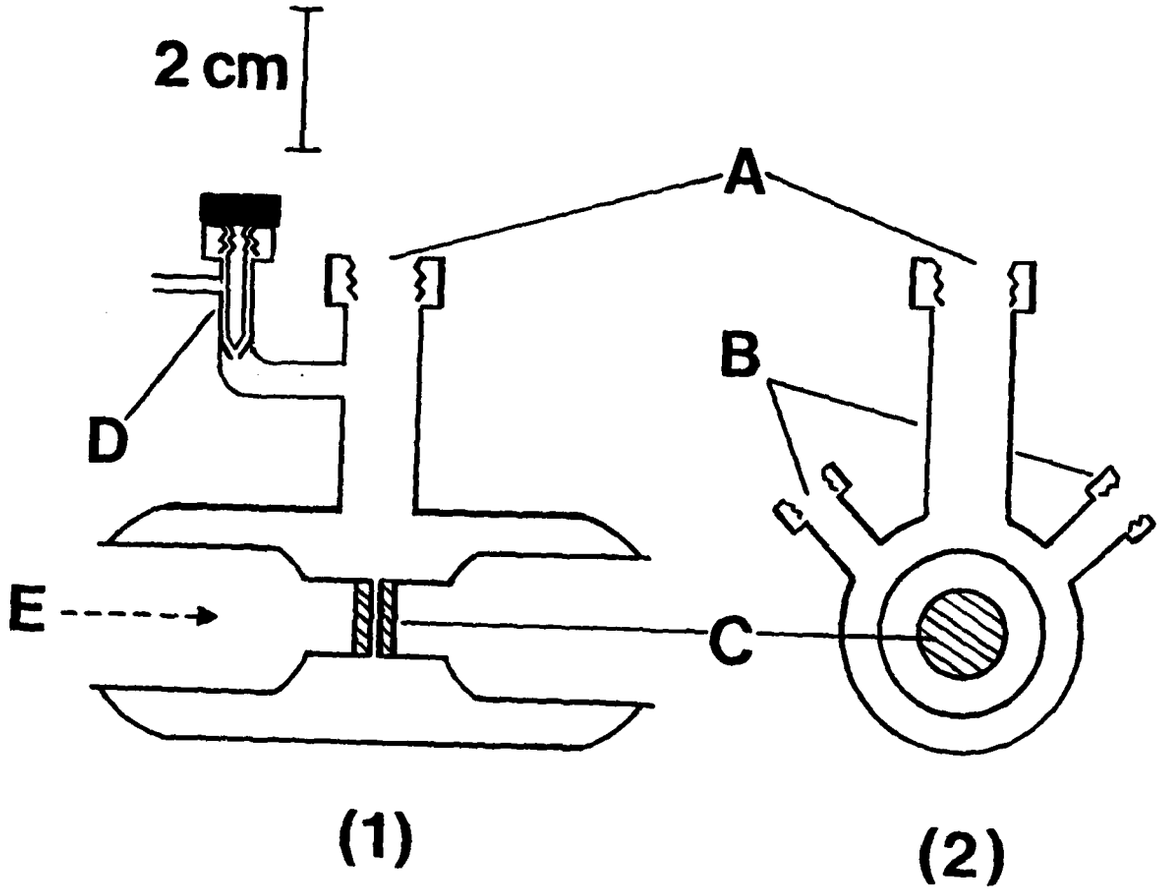
2 cm
A
B
C
D
E
(1)
(2)

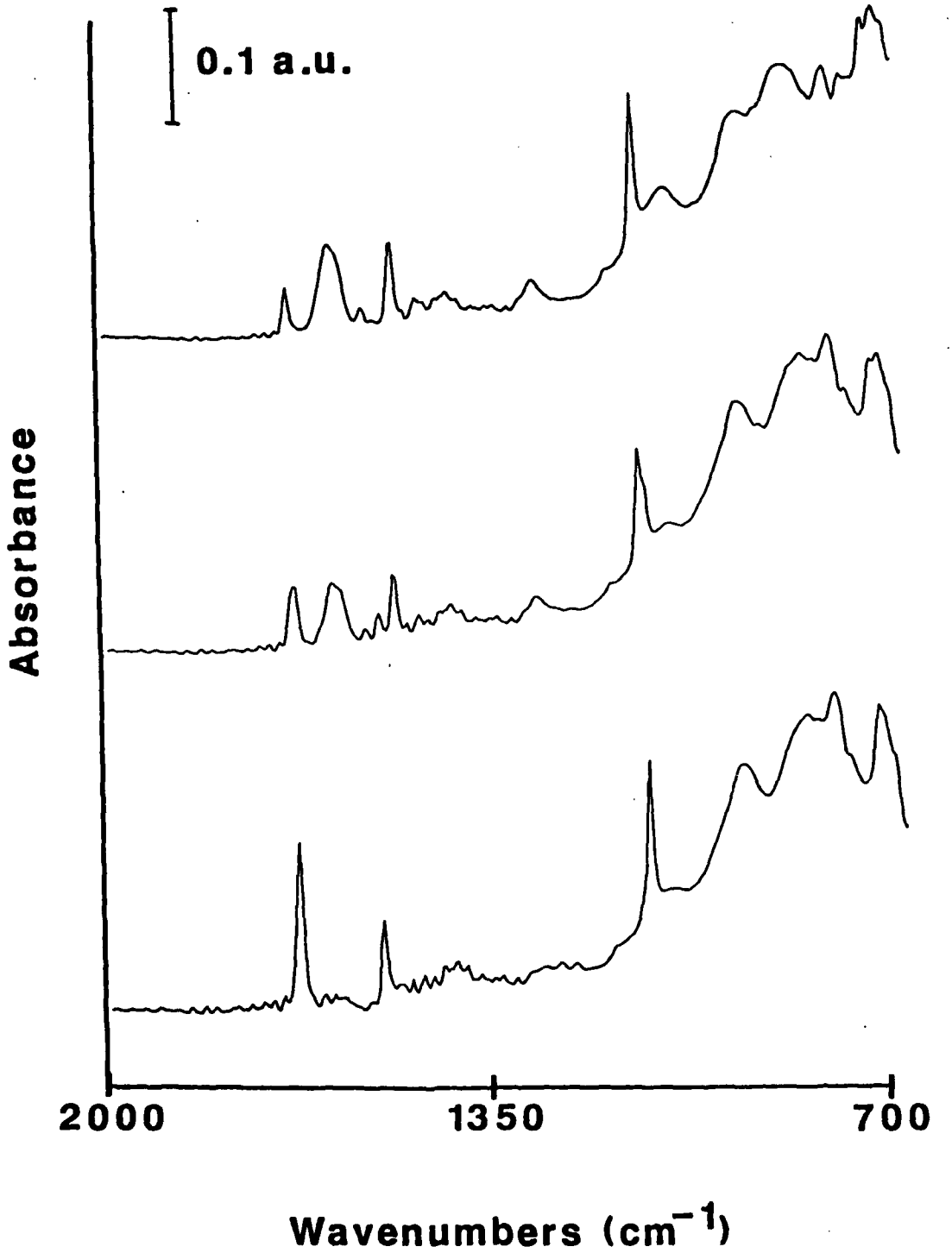
0.1 a.u.
Absorbance
2000
1350
700
Wavenumbers (cm^{-1})

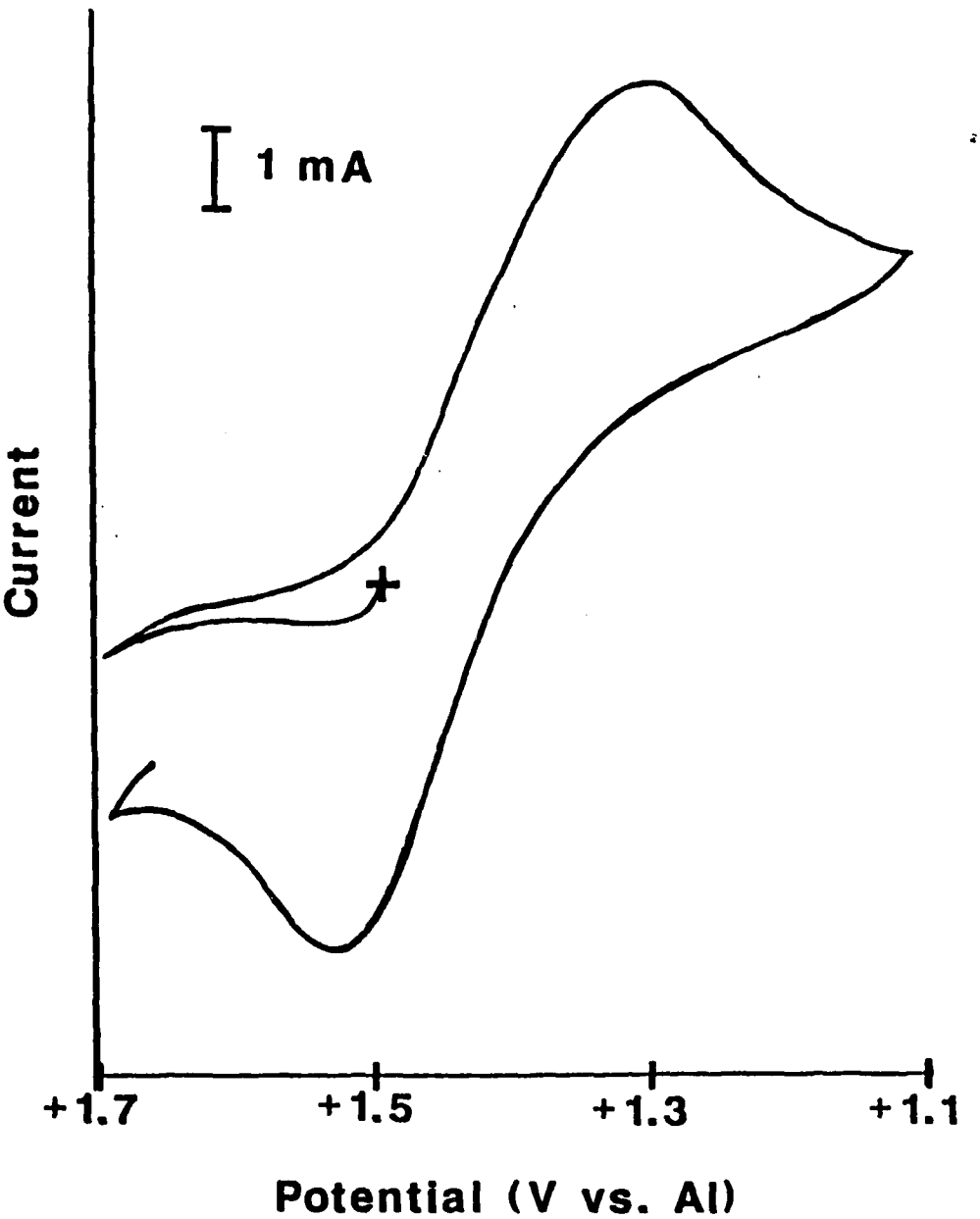
1 mA
Current
+1.7
+1.5
+1.3
+1.1
Potential (V vs. Al)

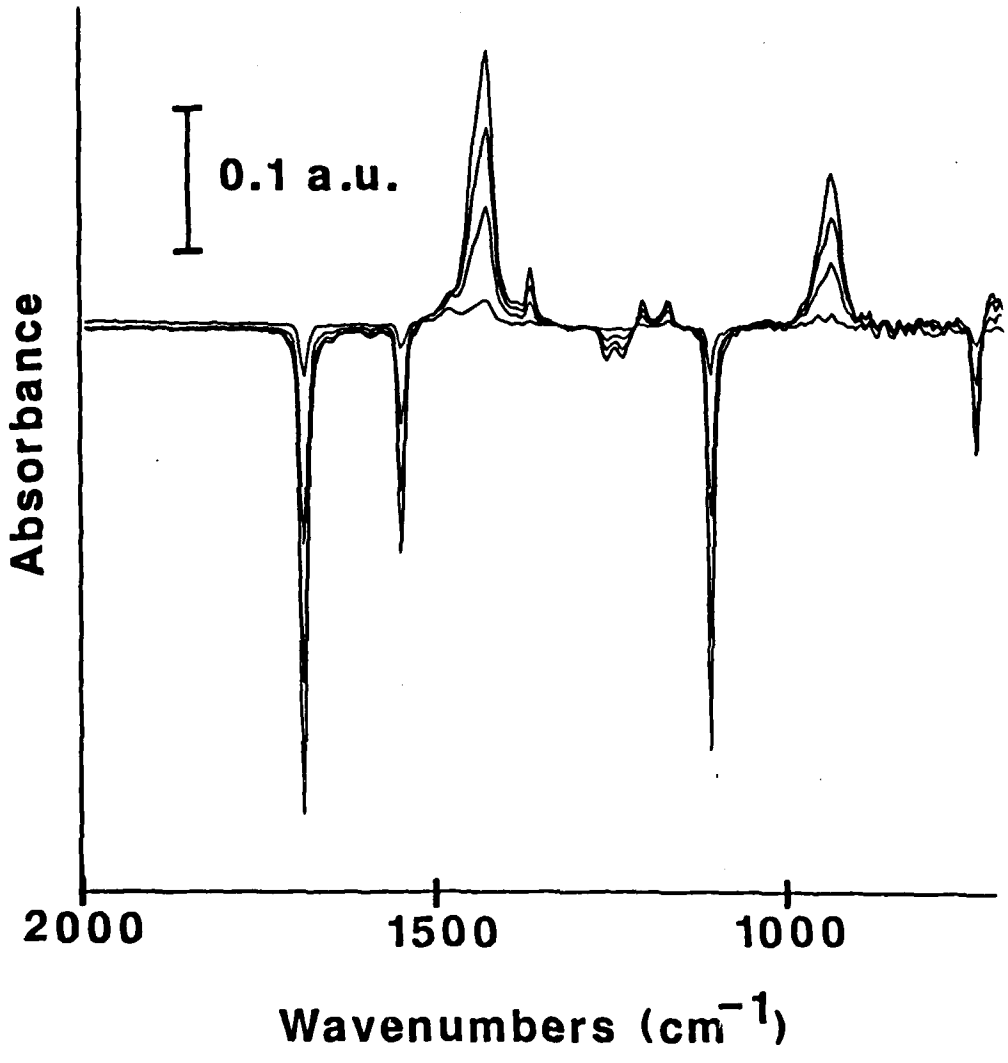
0.1 a.u.
Absorbance
2000
1500
1000
Wavenumbers (cm^{-1})

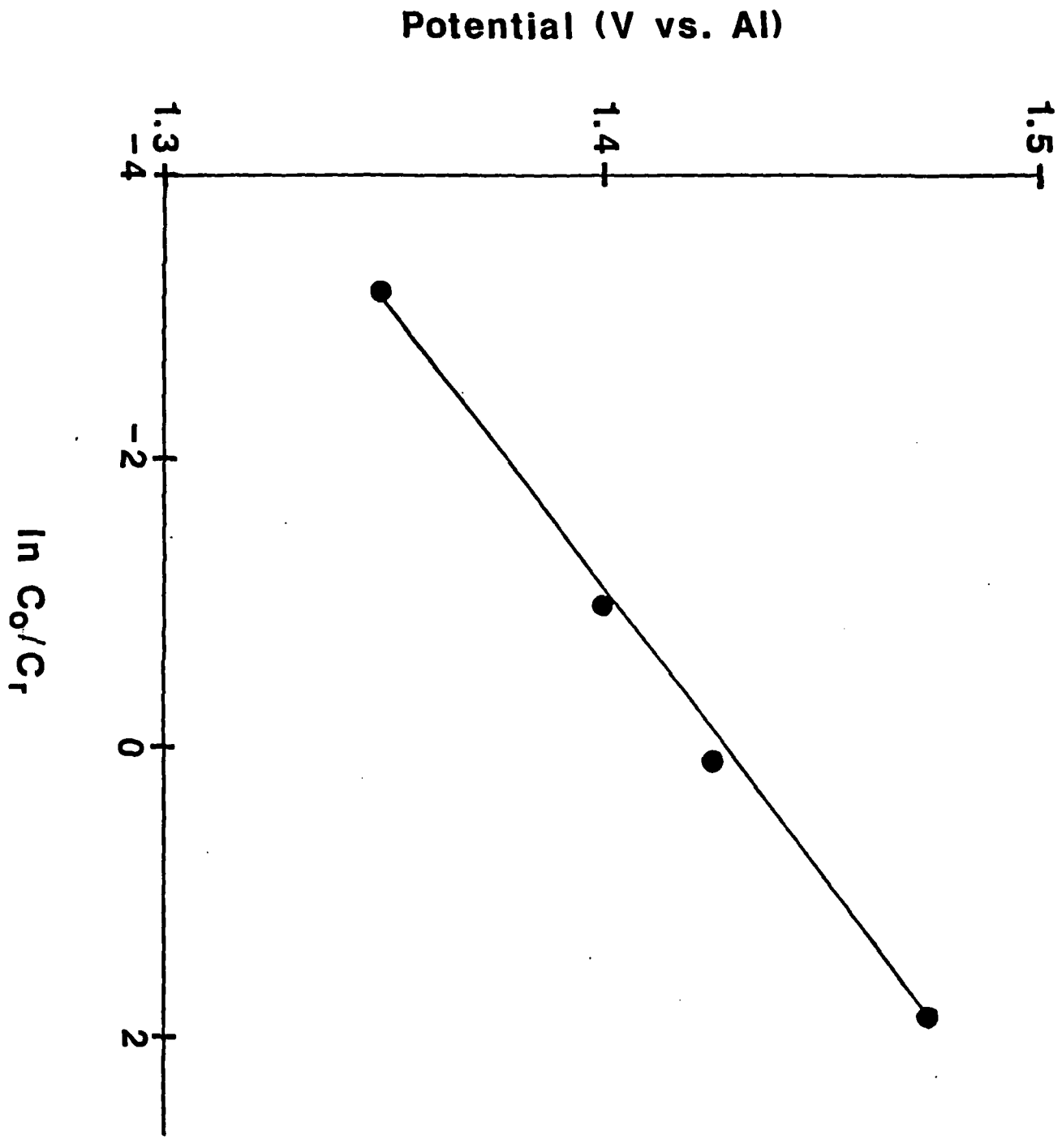
Potential (V vs. Al)
1.3
1.4
1.5
-4
-2
0
2
ln C_o/C_r

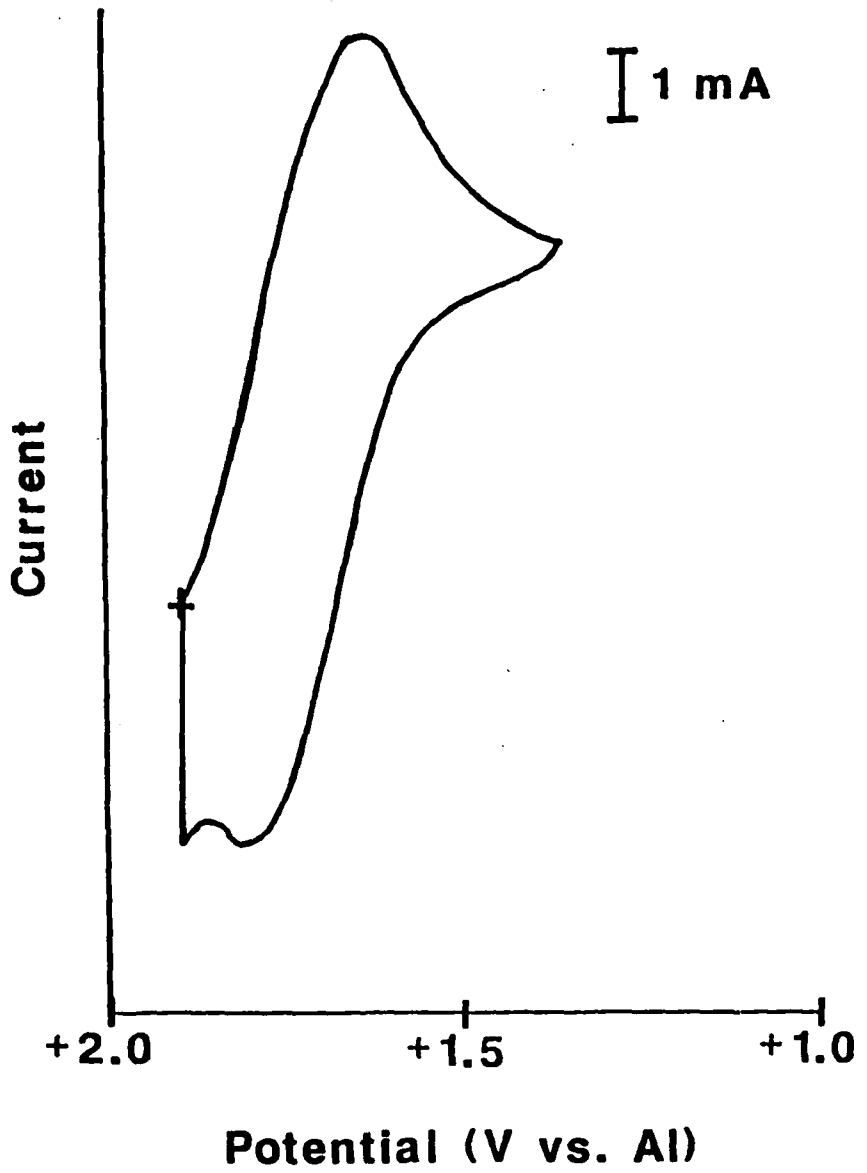
1 mA
Current
+2.0
+1.5
+1.0
Potential (V vs. Al)

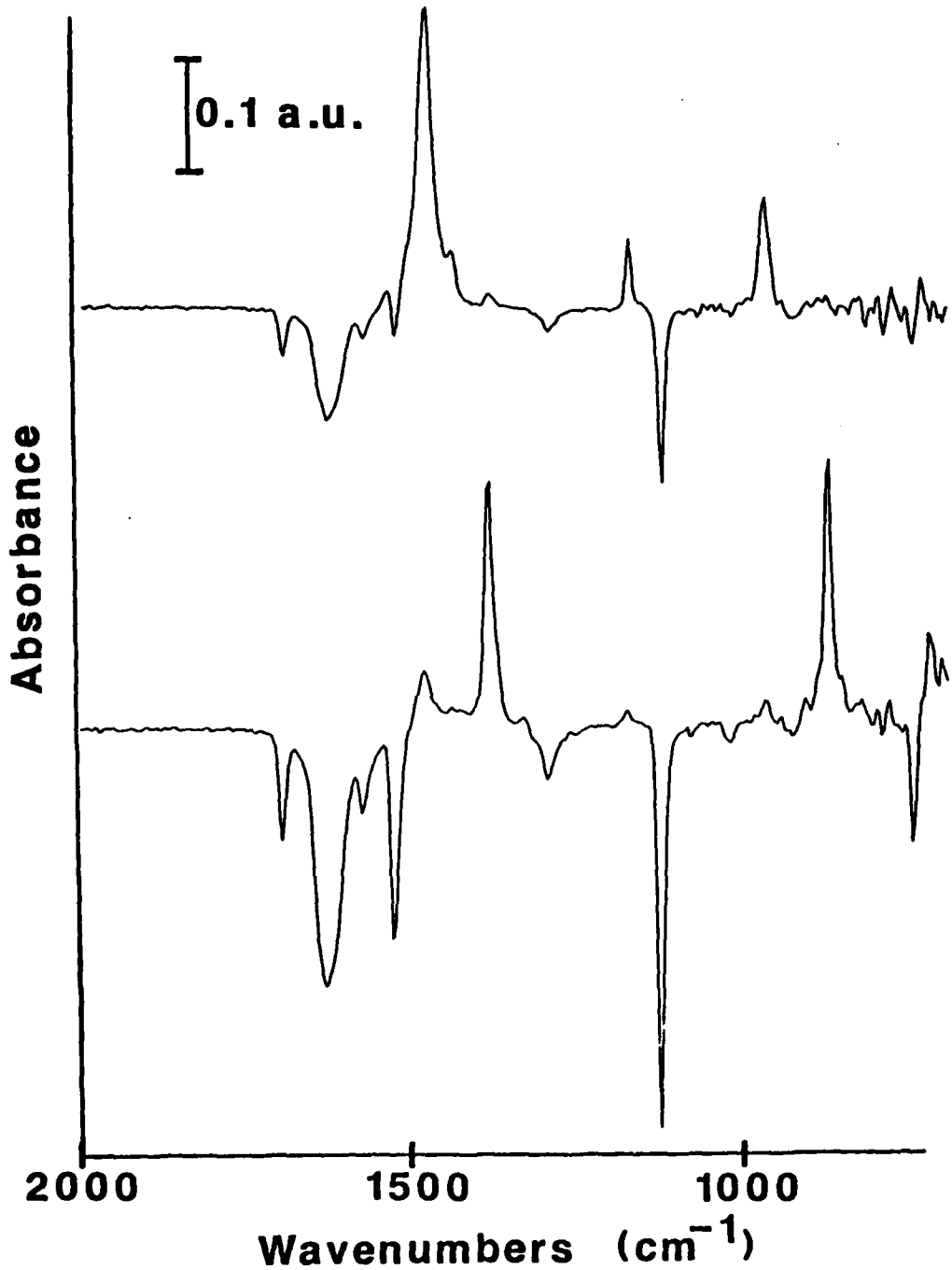
0.1 a.u.
Absorbance
2000
1500
1000
Wavenumbers (cm^{-1})

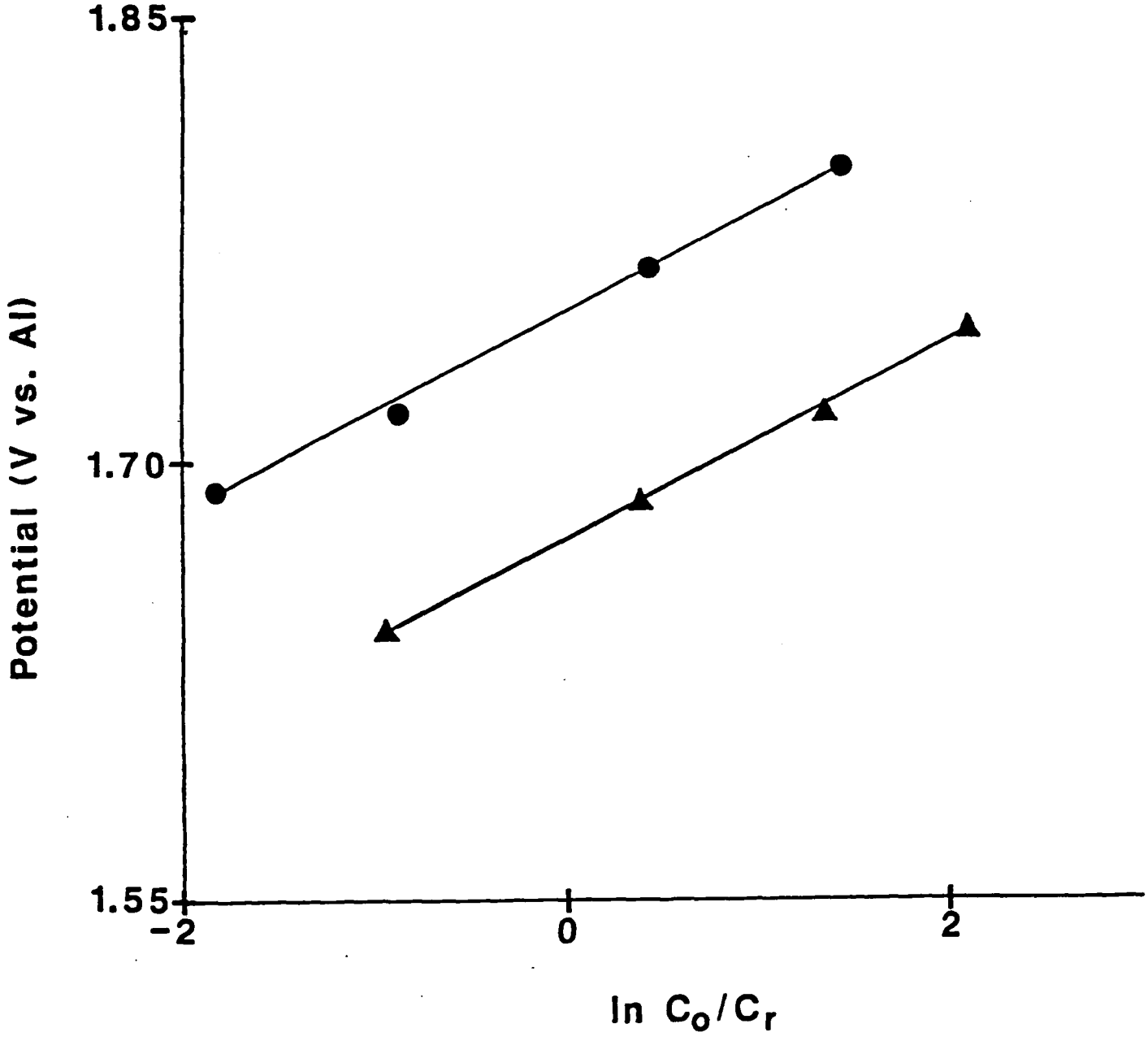
1.85
1.70
1.55
Potential (V vs. Al)
-2
0
2
ln C_o/C_r

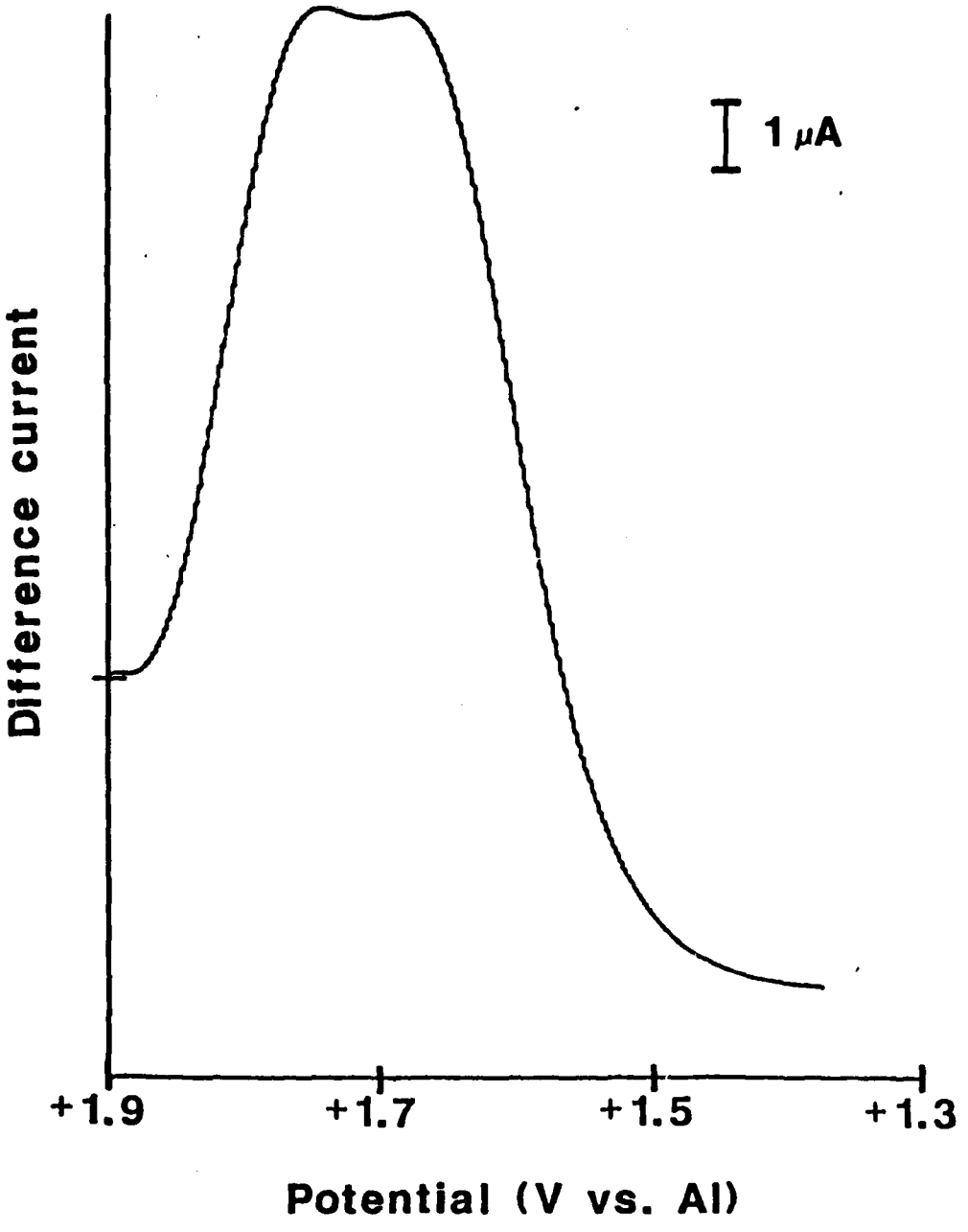
1 μA
Difference current
+1.9
+1.7
+1.5
+1.3
Potential (V vs. Al)

port by the Direction des Recherches, Etudes et Techniques (DRET, Decision n° 86186) is gratefully acknowledged.

Manuscript submitted Jan. 8, 1988; revised manuscript received April 6, 1988.

CNRS, LESCO assisted in meeting the publication costs of this article.

REFERENCES

1. P. Hagenmuller in "Non Stoichiometric Compounds, Tungsten Bronzes, Vanadium Bronzes and Related Compounds," D. J. Bevan and P. Hagenmüller, Editors, p. 569, Pergamon Press, Oxford (1973).
2. M. Pouchard, Thèse de Doctorat ès-Sciences Physiques, Bordeaux (1967).
3. A. Casalot, Thèse de Doctorat ès-Sciences Physiques, Bordeaux (1968).
4. E. V. Babenko, A. A. Fotiev, A. N. Baraboshkin, and K. A. Kaliev, *Russ. J. Inorg. Chem.*, **23**, 1241 (1978).
5. P. Strobel, *J. Solid State Chem.*, **66**, 95 (1987).
6. A. F. Reid and J. A. Watts, *J. Solid State Chem.*, **1**, 310 (1970).
7. W. G. Mumme and J. A. Watts, *J. Solid State Chem.*, **3**, 319 (1971).
8. M. S. Whittingham, *This Journal*, **123**, 315 (1976).
9. P. G. Dickens, S. J. French, A. T. Hight, and M. F. Pye, *Mat. Res. Bull.*, **14**, 1295 (1979).
10. D. W. Murphy, P. A. Christian, F. J. Disalvo, and J. V. Waszczak, *Inorg. Chem.*, **18**, 2800 (1979).
11. J. P. Pereira-Ramos, R. Messina, and J. Perichon, *J. Electroanal. Chem.*, **218**, 241 (1987).
12. W. Yu, D. Wang, B. Zhu, and G. Zhou, *Solid State Commun.*, **63**, 1043 (1987).
13. J. P. Gabano, M. Broussely, J. P. Pereira-Ramos, R. Messina, and J. Perichon, French Pat. No. 8501309 (1985).
14. J. P. Pereira-Ramos, R. Messina, and J. Perichon, *J. Appl. Electrochem.*, **16**, 379 (1986).
15. J. P. Pereira-Ramos, R. Messina, and J. Perichon, *J. Power Sources*, **16**, 193 (1985).
16. H. G. Bachmann, F. R. Ahmed, and W. H. Barnes, *Z. Kristallogr.*, **115**, 110 (1961).
17. J. Molenda, *Solid State Ionics*, **21**, 263 (1986).
18. J. J. Braconnier, C. Delmas, C. Fouassier and P. Hagenmuller, *Mat. Res. Bull.*, **15**, 1797 (1980).
19. C. Delmas, J. J. Braconnier, C. Fouassier, and P. Hagenmuller, *Solid State Ionics*, **314**, 165 (1981).
20. J. M. Tarascon and G. W. Hull, *ibid.*, **22**, 85 (1986).
21. J. P. Pereira-Ramos, R. Messina, C. Piolet, and J. Devynck, *J. Power Sources*, **20**, 221 (1987).
22. K. West, B. Zachau-Christiansen, T. Jacobsen, and S. Skaarup, 6th International Conference on Solid State Ionics, p. 372, Garmisch-Partenkirchen (1987).
23. P. G. Dickens, S. J. French, T. Hight, M. F. Pye, and G. J. Reynolds, *Solid State Ionics*, **2**, 27 (1981).
24. P. G. Dickens, M. Jewess, D. J. Neild and J. C. Rose, *J. Chem. Soc., Dalton.*, 30 (1973).
25. K. H. Cheng and M. S. Whittingham, *Solid State Ionics*, **1**, 151 (1980).
26. M. S. Whittingham, *This Journal*, **122**, 713 (1975).
27. B. Schlasche and R. Schollhorn, *Rev. Chim. Min.*, **19**, 534 (1982).
28. S. K. Joo, I. D. Raistrick, and R. A. Huggins, *Mat. Res. Bull.*, **20**, 897 (1985).
29. R. Schollhorn, R. Kuhlmann, and J. O. Besenhard, *Mat. Res. Bull.*, **11**, 83 (1976).
30. J. O. Besenhard and R. Schollhorn, *J. Power Sources*, **1**, 267 (1976/77).
31. M. Pouchard, A. Casalot, J. Galy, and P. Hagenmuller, *Bull. Soc. Chim., Fr.*, **11**, 4343 (1967).
32. Illarianov, Ozerov, and Kildisheva, *J. Inorg. Chem., Acad. Nauk S.S.S.R.*, **4**, 780 (1956).
33. K. Waltersson and B. Forslund, *Acta Crystallogr. Sect. B*, **33**, 780 (1977).
34. K. Waltersson and B. Forslund, *ibid.*, **33**, 789 (1977).
35. W. G. Mumme and J. A. Watts, *J. Solid State Chem.*, **3**, 319 (1971).
36. A. Kutoglu, *Z. Kristallogr.*, **162**, 263 (1983).
37. N. Kumagai, N. Kumagai, N. Watanabe, and T. Nakajima, 38th Meeting-ISE, p. 775, Maastricht (1987).
38. S. S. Jaswal and J. P. Sharma, *J. Phys. Chem. Solids*, **34**, 509 (1973).
39. L. Pauling, *Proc. Roy. Soc., A*, **114**, 181 (1927).
40. Briant and G. C. Farrington, *J. Solid State Chem.*, **33**, 386 (1986).
41. F. L. Lin, L. X. Xue, B. Zhu, D. Z. Wang, and W. H. Yu, 6th International Conference on Solid State Ionics, p. 629, Garmisch-Partenkirchen (1987).

Electrochemical and Spectroscopic Studies of Tungsten Hexachloride in an Acidic Sodium Chloroaluminate Melt

Determination of Dissolved Oxide

Jean-Paul Schoebrechts, Paul A. Flowers, Glen W. Hance, and Gleb Mamantov*

Department of Chemistry, University of Tennessee, Knoxville, Tennessee 37996-1600

ABSTRACT

The chemistry of tungsten hexachloride in an acidic sodium chloroaluminate melt (63 mole percent $AlCl_3$) has been investigated by electrochemical and spectroscopic techniques at temperatures of 150° and 175°C. WCl_6 undergoes several reduction steps in the melt, the first of which is sensitive to the presence of oxide impurities. UV-visible and infrared absorption measurements indicate that tungsten hexachloride reacts with oxide to produce $WOCl_4$. Comparison of spectroscopic and electrochemical data indicates that the first voltammetric wave is due to the reduction of the hexachloride to WCl_5 ($E_{1/2}$ = +1.665V *vs.* Al^{3+}/Al in the same melt) and that $WOCl_4$ is electroactive only below +1.5V. The equilibrium constant for the formation of $WOCl_4$ and the initial amount of oxide in the melt are derived from voltammetric data and compared to values obtained from infrared measurements.

The determination of oxide impurities in molten chloroaluminates has been the subject of several studies during the last decade (1-5). These impurities are very difficult to avoid in such melts (6) and may have pronounced effects on the behavior of other solute species of interest (7-9). Furthermore, understanding oxide chemistry in halide melts is of considerable importance to industrial electrolytic processes for the production of aluminum.

Most of the reported methods for quantifying oxide in chloroaluminate melts are based on electroanalytical techniques. Berg *et al.* (2) have described a method in which the oxide content is determined by comparing the weighed amount of aluminum chloride used to prepare the melt to the amount determined via potentiometric measurements. Osteryoung and coworkers (8) devised a voltammetric titration technique for determining oxide in chloride-rich (i.e., basic) aluminum chloride/N-(n-butyl)pyridinium chloride melts using Ti(IV) as a probe

*Electrochemical Society Active Member.

solute. Laher *et al.* (4) reported a similar method using Ta(V) as the probe that may be used to determine oxide in aluminum chloride-sodium chloride melts saturated with NaCl. These latter two methods are restricted to melts of basic composition where the probe metal ions are involved in an equilibrium between hexachloride and oxide tetrachloride species described by the general equation

$$MCl_6^{m-} + O^{2-} \rightleftharpoons MOCl_4^{m-} + 2Cl^- \quad [1]$$

with $m = 1$ and 2 for Ta and Ti, respectively (see the Appendix for a better description of the species containing oxide). Laher *et al.* (4) have also described a cell employing a beta-alumina membrane whose potential is sensitive to oxide concentration in $AlCl_3$-$NaCl_{sat}$ melts. More recently, Flowers and Mamantov (5) have reported a method for determining oxide in both basic and acidic sodium chloroaluminates based on infrared measurements. The authors showed the intensities of bands in the region 680-800 cm^{-1} to be linearly related to oxide concentration in $AlCl_3$-NaCl [63 mole percent (m/o) $AlCl_3$] and $AlCl_3$-$NaCl_{sat}$ melts, making direct spectroscopic determination of dissolved oxide possible.

The chemistry of tungsten in an acidic sodium chloroaluminate (63 m/o $AlCl_3$) is currently being reinvestigated in our laboratory. Results obtained several years ago (10) indicated that this element exhibits a wide variety of stable oxidation states in acidic melts (+6, +3, +2, between +2 and 0, and 0), some of which involve cluster species such as $W_6Cl_8^{4+}$. Recent results have shown that in the presence of oxide impurities, hexavalent tungsten is involved in an equilibrium between two electroactive species, the hexachloride WCl_6 and the oxide tetrachloride $WOCl_4$. In this paper, an electroanalytical method for determining oxide levels in acidic alkali chloroaluminates based on this equilibrium is proposed.

Experimental Section

Dry box system.—Because of the air- and moisture-sensitive nature of the compounds used, materials were handled and electrochemical experiments performed under nitrogen in a Vacuum Atmospheres dry box equipped with a dry train/O_2 removal column. The moisture level in the box was monitored with an Ondyne Model 1440 digital hygrometer; it was typically less than 2 ppm.

Materials.—The chloroaluminate melts were prepared from twice-sublimed $AlCl_3$ (Fluka, anhydrous) and sodium chloride (Fisher) which was dried under vacuum at 450°C for four days. Melt preparation has been described elsewhere (11). Exceptions to the cited preparative procedures were the omission of pre-electrolysis and reaction with Al metal as further purification steps.

The purification of commercially available tungsten hexachloride (Alfa) has been described previously (10). Tungsten oxide tetrachloride (Alfa) was sublimed once at 110°C prior to use. Anhydrous sodium carbonate (Fisher) was dried under a CO_2 stream at 300°C for one day prior to use. Aluminum oxide chloride was synthesized following the procedure described by Hagenmuller *et al.* (12).

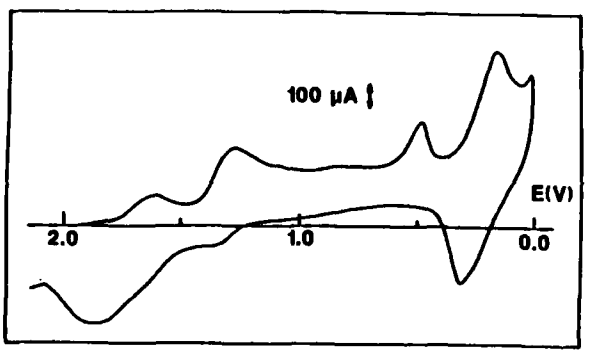

Fig. 1. Cyclic voltammogram of W(VI) at a glassy carbon electrode in $AlCl_3$-NaCl (63-37 m/o). Electrode area 0.07 cm^2; $[WCl_6] = 1.38 \times 10^{-2}$ F; scan rate = 0.1 V/s; t = 175°C.

Electrochemical measurements.—The electrochemical cell used was of the conventional three-electrode configuration and employed a glassy carbon (Tokai) working electrode, aluminum wire reference, and aluminum spiral and platinum foil counters. The working electrode was constructed by sealing a glassy carbon rod in a Pyrex tube, making electrical contact to a tungsten lead via platinum wire and silver sealing paste. The aluminum electrodes were cleaned in HNO_3-H_2SO_4-H_3PO_4 (30:30:40 by volume), rinsed with distilled water, and dried before use. The platinum electrodes were cleaned by boiling in concentrated HCl, then rinsed and dried. Reference and counter electrodes were separated from the working compartment by means of fine porosity (4.5-5.0 μm pore size) glass frits.

Electrochemical experiments were conducted using a PAR Model 174 polarographic analyzer, a PAR Model 175 universal programmer, and a Houston 2000 X-Y recorder. Potential measurements were made using a Keithley 179 TRMS digital multimeter. All potential values are given with respect to Al^{3+}/Al in a 63/37 m/o $AlCl_3$-NaCl melt.

Spectroscopic measurements.—Absorption spectra in the UV-visible region were obtained using 1.0 and 0.3 cm pathlength fused silica sealed cells (Vitro Dynamics) and a Cary 14 spectrometer in conjunction with an appropriate optical furnace and temperature controller. Fused silica spacers were used to reduce cell pathlengths when solution absorbances were too high. Neutral density filters were employed to attenuate the reference beam of the spectrometer when recording spectra with absorbances greater than 2.

Infrared spectra were obtained using a Digilab FTS-20E Fourier transform infrared spectrometer operated at 8 cm^{-1} instrumental resolution. The spectroscopic cell was equipped with silicon windows and allowed for transmittance sampling of the melts; this cell is described in detail elsewhere (13).

X-ray powder patterns were obtained using 0.5 mm diam sealed glass capillaries and a Phillips Unit, Model XR9-2600.

Results and Discussion

Electrochemical determination of oxide and calculation of the WCl_6/$WOCl_4$ equilibrium constant.—Figure 1 shows a typical cyclic voltammogram for a solution of WCl_6 in a $AlCl_3$-NaCl (63 m/o $AlCl_3$) melt. Several reduction steps are observed before the cathodic limit of the solvent, the first of which is the object of this study.

Analysis of cyclic voltammograms for the first reduction recorded at different scan rates (0.01-0.5 V/s) and for different concentrations (up to 3.0×10^{-2} F WCl_6) indicates that the reduction is a reversible one-electron diffusion-controlled step (Table I). A plot of the function $\log[(i_d - i)/i]$ *vs.* E, where i_d is the limiting reduction current measured by normal pulse voltammetry and E is the working electrode potential, is linear with a slope of 0.085V (theoretical value is 0.089V). The half-wave potential determined from this plot is +1.665V, in close agreement with the values derived from cyclic voltammetry (Table I). The reduction product obtained by controlled potential electrolysis has been identified spectroscopically as WCl_5. Additional information concerning the electrochemistry of tungsten in this melt will be publisned elsewhere.

Table I. Cyclic voltammetric data (0.007 cm^2 glassy carbon electrode) for a 2.85×10^{-2} F WCl_6 solution in $AlCl_3$/NaCl (63 m/o $AlCl_3$) at 175°C

v (V/s)	$i_{p,c}/v^{1/2}$ ($\mu A \cdot s^{1/2}/V^{1/2} \cdot cm^2$)	$E_{p,c}$ (V)	$E_{p,c} - E_{p,a}$ (V)*
0.01	9.64	1.615	0.090
0.02	9.48	1.615	0.090
0.05	9.74	1.620	0.090
0.10	9.94	1.620	0.090
0.20	10.10	1.615	0.095
0.50	9.80	1.605	0.105

*The calculated value at this temperature is 0.089V.

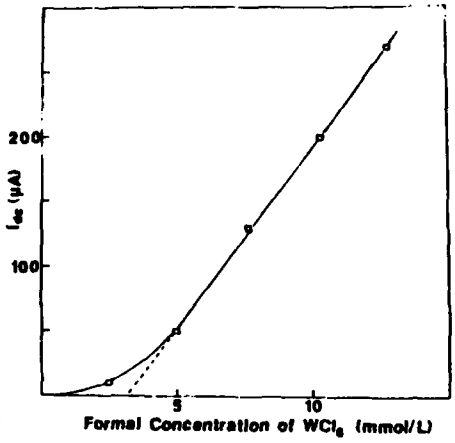

Fig. 2. Normal pulse voltammetric limiting current vs. WCl_6 concentration in 63/37 melt at 150°C.

The normal pulse voltammetric limiting current of the first wave increases with the formal concentration of tungsten hexachloride as shown in Fig. 2. For $[WCl_6] < 3.5 \times 10^{-3}$ *F*, the current is unexpectedly low, but when $[WCl_6]$ exceeds *ca.* 5.5×10^{-3} *F*, the current increases linearly with concentration. The linear portion of this curve intersects the concentration axis at a positive value, suggesting that the hexachloride is consumed by reaction with some trace constituent in the melt prior to appearance of the voltammetric wave.

Figure 3 shows the change in the UV-visible spectrum of a WCl_6 solution as the tungsten concentration is varied. For the most concentrated solution, the spectrum exhibits one intense absorption band at 333 nm. When the solution is diluted, that band disappears and two new features are observed at 355 and 230 nm, suggesting that hexavalent tungsten is involved in an equilibrium between different species. It should be noted that these spectral changes are observed in the same concentration range as the nonlinearity of the current-concentration plot (Fig. 2).

It is known that WCl_6 readily reacts with species containing oxide to produce $WOCl_4$ (14); since the melts were most likely contaminated with oxide (2, 6), it was assumed that the suspected equilibrium involved chloride and oxychloride complexes.

UV-visible absorption spectra of gaseous WCl_6 and $WOCl_4$ [known to exist as monomers (14)] are presented in Fig. 4. The wavelengths of major spectral features are summarized in Table II along with literature data from spectra obtained in carbon tetrachloride (15) and toluene (16). There is fair agreement between these sets of data, indicating that monomeric species are likely to exist in the two organic solvents. Absorbances at 355 nm ($WOCl_4$) and 330 nm (WCl_6) vary linearly with calculated vapor pressure above the solids as shown in Fig. 5. The absorptivities derived from these curves, assuming ideal gas behavior, are $\epsilon_{355}(WOCl_4) = 4.05 \times 10^3$ and $\epsilon^{328}(WCl_6) = 1.89 \times 10^4$ 1/mol · cm.

Table II. UV-visible spectral features (nm) of WCl_6 and $WOCl_4$

Compound	Vapor[a]	Solution in	
		Toluene[b]	CCl_4[c]
WCl_6	225(m), 275(sh), 330(s), 375(sh), 430(w)	328(s), 372(m), 430(w)	334, 379, 447, 514(?), 585(?), 720(?)
$WOCl_4$	220(s), 250(sh), 270(sh), 355(s), 460(w)	355(s)	

[a]This work.
[b]Ref. (15).
[c]Ref. (16).
(?) Impurities, w (weak), m (medium), s (strong), sh (shoulder).

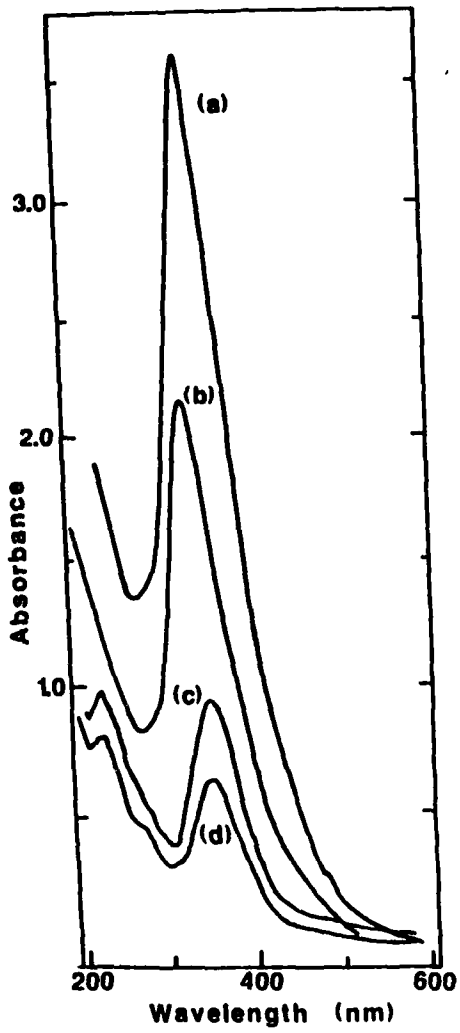

Fig. 3. UV-visible absorption spectra of (a) 0.011, (b) 0.0071, (c) 0.0035, and (d) 0.0018 *F* WCl_6 in 63 m/o $AlCl_3$ melt. Pathlength 0.025 cm; *t* = 150°C.

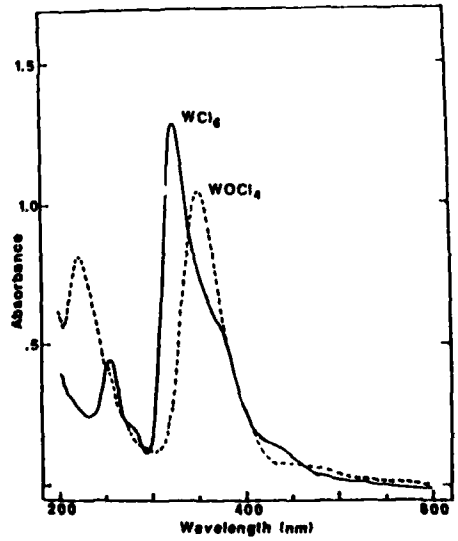

Fig. 4. UV-visible absorption spectra of $WOCl_4$(g) (broken line, *t* = 121°C, pathlength = 1.0 cm) and WCl_6(g) (solid line, *t* = 182°C, pathlength = 0.3 cm).

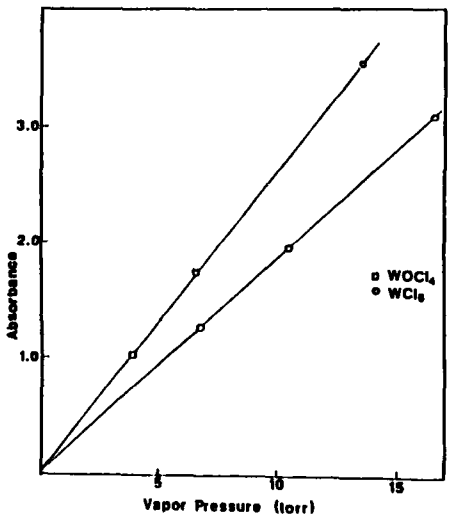

Fig. 5. Absorbance of WCl_6(g) (pathlength = 0.3 cm) and $WOCl_4$(g) (pathlength = 1.0 cm) at 328 and 355 nm, respectively, vs. vapor pressure.

Comparison of these gas-phase spectra with those of WCl_6 solutions clearly indicates that at low formal tungsten concentrations (Fig. 3c and d), the oxide tetrachloride is the only tungsten entity present in the melt. At higher concentrations, WCl_6 also exists as shown by the presence of an intense absorption at 333 nm (Fig. 3a and b). This suggests that dissolved WCl_6 reacts with oxide impurities initially present in the melt to produce $WOCl_4$ according to the equilibrium

$$WCl_6 + "O^{2-}" \rightleftharpoons WOCl_4 + 2"Cl^-" \quad [2]$$

where "O^{2-}" and "Cl^-" refer to complexed oxide and chloride, respectively, and that the electrochemical wave observed at +1.665V corresponds to reduction of WCl_6. Taking previous results into account (*vide supra*), this reduction may be written as

$$WCl_6 + \not{2}e^- \rightleftharpoons WCl_5 + \not{2}Cl^- \quad [3]$$

The observed shape of the current-concentration curve (Fig. 2) may now be understood as follows:

1. At high formal concentrations of WCl_6, the amount of added hexachloride exceeds the amount of oxide contamination present in the melt and equilibrium (2) is completely shifted to the right. The true WCl_6 concentration is then linearly related to the formal concentration and, consequently, the reduction current.

2. At low formal concentrations of WCl_6 (i.e., on the order of the melt's initial oxide concentration), W(VI) is present primarily as $WOCl_4$ and the current-concentration plot thus exhibits the observed deviation from linearity.

From the preceding developments, it is clear that an extension of the linear portion of the curve in Fig. 2 will intersect the x-axis at a value equal to the initial oxide concentration of the melt (expressed as "O^{2-}"). Data for three different samples analyzed in this manner are given in Table III. The infrared method (5) was also used to determine the oxide content of sample 3 and yielded results in reasonable agreement with the electrochemically derived value.

Table III. Oxide levels of several $AlCl_3$/NaCl (63 m/o $AlCl_3$) melt samples as determined by electrochemical and spectroscopic methods

Sample	["O^{2-}"]$_o$ (mmol/l) Voltammetric	Infrared
1	3.11	—
2	3.14	—
3	2.65	2.90

This method was evaluated further by determining the oxide levels of 63/37 m/o melt samples to which known amounts of oxide were added as Na_2CO_3. Two "spiked" samples were prepared from the same batch of melt, insuring that the ambient oxide level (determined to be 2.0 m*M*) was the same for each sample. Experimental values of 6.8 and 15.3 m*M* were obtained for samples containing 8.6 and 17.6 m*M* total oxide (ambient plus added Na_2CO_3), respectively. The differences between experimental and actual oxide levels could in part be due to a weighing error, as only milligram quantities of Na_2CO_3 were added.

Using both the linear and nonlinear portions of the plot in Fig. 2, the apparent equilibrium constant for reaction (2) was calculated to be $K = 7.2 \times 10^4$ l/mol. Details of this calculation are given in the Appendix.

Relation between vapor phase spectra and initial oxide level.—The UV-visible absorption spectra of the vapor above 63/37 melts containing WCl_6 and $WOCl_4$ are qualitatively identical to spectra of the pure gaseous compounds. Absorbance values at selected wavelengths are presented in Table IV. By combining these data with absorbance-vapor pressure data for the pure gaseous compounds (Fig. 5), the vapor pressures reported in Table IV were obtained. The oxide tetrachloride clearly exhibits an approximate ten-fold advantage in spectroscopic "detectability" at 355 nm in the vapor phase, a result of its greater volatility (ca. 20 times relative to the hexachloride) offset by a lower absorptivity at this wavelength, roughly half that of WCl_6.

Adding excess tungsten hexachloride to an oxide contaminated melt results in shifting equilibrium (2) completely to the right, quantitatively producing $WOCl_4$. Calculations employing the experimental value for the equilibrium constant of Eq. [2] (or more precisely, Eq. [A-1] of the Appendix) show that addition of a roughly threefold excess of WCl_6 to an acidic melt will reduce the concentration of dissolved aluminum oxychloride to approximately 2% of its initial value. The amount of $WOCl_4$ produced by such an addition (hence the initial concentration of oxide in the melt) could readily be determined by monitoring the vapor phase absorbance at 355 nm as illustrated in Fig. 6.

Electrochemistry of W(VI) in oxide-rich melts.—In order to study the effect of oxide impurities on the first reduction process of tungsten hexachloride, successive additions of oxide in the form of Na_2CO_3 were made to a concentrated solution of WCl_6 in a $AlCl_3$-NaCl (63 m/o $AlCl_3$) melt. The voltammetric wave at +1.665V decreased in intensity after the first addition (Fig. 7b), then disappeared completely when oxide was added in excess of the tungsten hexachloride (Fig. 7c). The observed relation between the magnitude of the decrease and the amount of

Table IV. Vapor phase absorbance of several W(VI) containing melts at 175°C

Solute	Concentration (*F*)	Absorbance[a] 330 nm	Absorbance[a] 355 nm	Vapor pressure[b] (torr)
WCl_6	0.1475	1.13	0.82	1.7
$WOCl_4$	0.044	—	2.63	10.0
	0.032	—	1.76	6.66
	0.007	—	0.40	1.40

[a]10 mm pathlength cell.
[b]Calculated from absorbance data in Fig. 5.

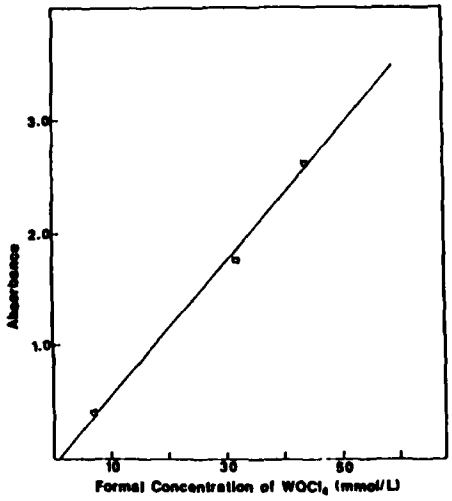

Fig. 6. Absorbance at 355 nm of the vapor above a solution of $WOCl_4$ in 63 m/o $AlCl_3$ melt vs. [$WOCl_4$] (pathlength = 1.0 cm, t = 175°C).

added oxide supports a one-to-one reaction between WCl_6 and "O^{2-}". Finally, Fig. 7d shows an increase in the wave below +1.5V that results from addition of $WOCl_4$, suggesting that this species is more difficult to reduce than WCl_6.

Solid-state reaction between WCl_6 and AlOCl.—The indication that W(VI) is a stronger oxoacid than Al(III) was confirmed by reacting tungsten hexachloride with aluminum oxide chloride at 180°C. The reaction quantitatively produced $WOCl_4$ and $AlCl_3$ as determined by x-ray diffraction analysis of the product mixture.

Infrared measurements.—Figure 8 shows infrared difference spectra for a 63/37 $AlCl_3$-NaCl melt after additions of oxide (upper spectrum) and subsequently WCl_6 (lower spectrum). After obtaining a background spectrum of the melt, water was added to make the solution 13.3 m*M* in O^2; the spectral change thus induced was the appearance of a band characteristic of solvated oxide (5) at 791 cm^{-1}. Adding WCl_6 to the same melt [making the formal concentration of W(VI) 8.93 m*M*] resulted in a decrease in the intensity of this band and the appearance of two overlapping features attributed to $WOCl_4$ at 1026 and 1011 cm^{-1} [literature values for the tungsten-oxygen stretch in thionyl chloride (14) and carbon disulfide (15) solutions of tungsten oxide tetrachloride are 1019 and 1030 cm^{-1}, respectively]. Strong solvent absorptions prevented observation of features in the region below *ca.* 700 cm^{-1} where WCl_6 bands are expected (17). From these data the equilibrium constant for Eq. [2] was calculated to be 1.6×10^5 l/mol, in fair agreement with the electrochemically derived value. Details of this calculation are given in the Appendix.

Acknowledgments

We gratefully acknowledge the support of this research by grants from the U.S. Air Force Office of Scientific Research and Martin-Marietta Laboratories.

Manuscript submitted Nov. 16, 1987; revised manuscript received April 25, 1988. This was Paper 1497 presented at the Honolulu, HI, Meeting of The Society, Oct. 18-23, 1987.

The University of Tennessee assisted in meeting the publication costs of this article.

APPENDIX

Calculation of the $WCl_6/WOCl_4$ Equilibrium Constant from Electrochemical Data

According to a recent paper by Zachariassen *et al.* (18), reaction [2] is more accurately written as

$$2WCl_6 + (AlO^+)_2(AlCl_4^-)_2 + 4AlCl_4^- \rightleftharpoons 2WOCl_4 + 4Al_2Cl_7^- \quad [A\text{-}1]$$

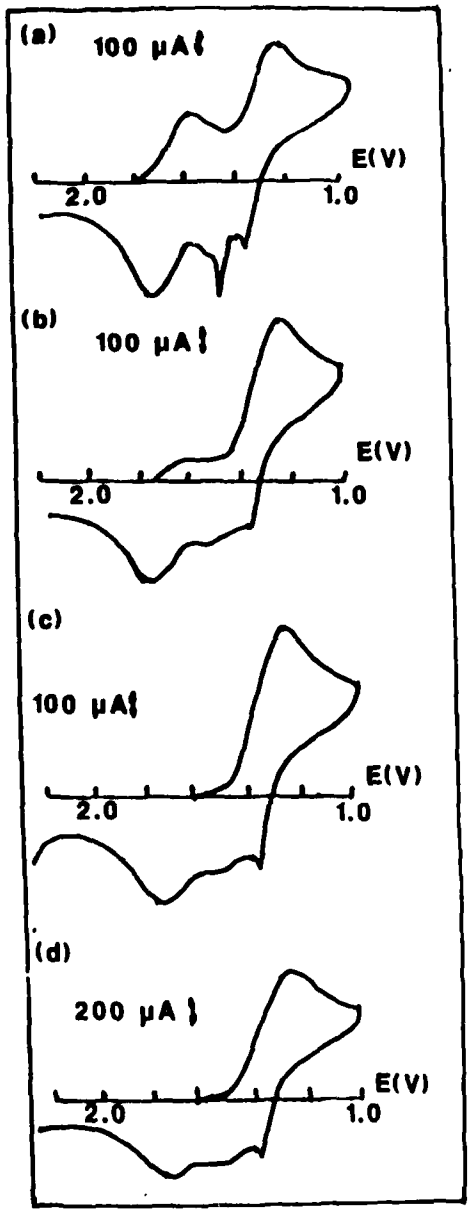

Fig. 7. Cyclic voltammograms of W(VI) solutions ([WCl_6] = 7.41×10^{-3} *F*) in 63 m/o $AlCl_3$ melt at a glassy carbon electrode after additions of (b) 4.47 m*M* Na_2CO_3, (c) 7.93 m*M* Na_2CO_3, and (d) 4.61 m*M* $WOCl_4$. *No oxide source was added in (a). Electrode area* 0.07 cm^2, *scan rate* = 0.1 V/s, t = 175°C.

For a dilute solution of V(VI) in a 63 m/o melt, the concentrations of the tetra- and heptachloroaluminate ions may be considered constant. The apparent equilibrium constant may therefore be expressed as follows

$$K = [WOCl_4]^2/[WCl_6]^2[(AlO^+)_2(AlCl_4^-)_2] \quad [A\text{-}2]$$

Employing data from an experiment at 150°C, the above constant was calculated as described below.

In the absence of oxide impurities, the calibration curve in Fig. 2 would be linear and pass through the origin, i.e.

$$i_d = kF(WCl_6) \quad [A\text{-}3]$$

where the proportionality constant k is given by the slope of the linear segment of the curve in Fig. 2 (k = 46.93 μA/m*M*). The concentration of WCl_6 at equilibrium may thus be obtained from the current value for $F(WCl_6)$ = 2.52 m*M* (first data point, equilibrium applies) and Eq. [A-3]. The value for [WCl_6] determined in this manner was 0.36 m*M*. The $WOCl_4$ produced in order to account for the dif-

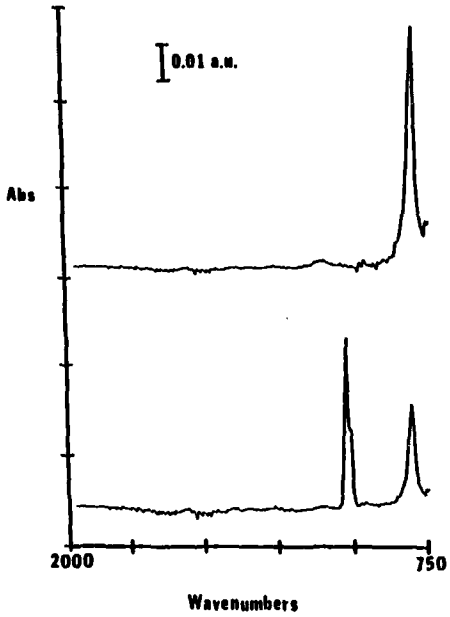

Fig. 8. Infrared difference spectra of 63 m/o $AlCl_3$ melt (solvent subtracted) after additions of (upper) 13.3 mM oxide and (lower) 8.93 mM WCl_6. Transmittance sampling, 8 cm^{-1} resolution, 50 scans, 175°C.

ference in formal and true hexachloride concentrations is then

$$[WOCl_4] = [WCl_6]_f - [WCl_6] = 2.52 - 0.36 = 2.16\ mM \quad [A\text{-}4]$$

Finally, using the value for initial oxide concentration obtained by extrapolation of Fig. 2, the equilibrium oxide concentration is

$$[(AlO')_2(AlCl_4^-)_2]_o - (1/2)[WOCl_4]$$
$$= 1.58 - (1/2)2.16 = 0.50\ mM \quad [A\text{-}5]$$

where $[(AlO')_2(AlCl_4^-)_2]_o$ is the initial oxide concentration. The apparent equilibrium constant is then

$$K = (0.00216)^2/(0.00036)^2(0.00050) = 7.2 \times 10^4 \quad [A\text{-}6]$$

Calculation of the $WCl_6/WOCl_4$ equilibrium constant from infrared data

Employing the difference spectra shown in Fig. 8 (and a previously obtained calibration curve for aluminum oxychloride in a 63 m/o melt), the equilibrium constant for Eq. [A-1] was calculated as follows.

From the stoichiometry of Eq. [A-1], the concentration of tungsten oxychloride may be defined as

$$[WOCl_4] = 2\{[(AlO')_2(AlCl_4^-)_2]_o - [(AlO')_2(AlCl_4^-)_2]\} \quad [A\text{-}7]$$

This quantity is obtained from the difference in band intensities at 791 cm^{-1} in Fig. 8, yielding $[WOCl_4] = 8.58\ mM$. Substituting this value and the known value for $F(WCl_6)$ into Eq. [A-4] gives $[WCl_6] = 0.35\ mM$. Finally, the equilibrium concentration of $[(AlO')_2(AlCl_4^-)_2]$ was obtained directly from the absolute oxide band intensity of the lower spectrum in Fig. 8 (i.e., prior to solvent subtraction), giving a value of 3.81 mM. Using these concentration values the apparent equilibrium constant for Eq. [A-1] was calculated to be

$$K = (0.00858)^2/(0.00035)^2(0.00381) = 1.6 \times 10^5\ l/mol \quad [A\text{-}8]$$

REFERENCES

1. B. Tremillon, A. Bermond, and R. Molina, *J. Electroanal. Chem.*, **74**, 53 (1976).
2. R. W. Berg, H. A. Hjuler, and N. J. Bjerrum, *Inorg. Chem.*, **23**, 557 (1984).
3. Z. Stojek, H. Linga, and R. A. Osteryoung, *J. Electroanal. Chem.*, **119**, 365 (1984).
4. T. M. Laher, L. E. McCurry, and G. Mamantov, *Anal. Chem.*, **57**, 500 (1985).
5. P. A. Flowers and G. Mamantov, *ibid.*, **59**, 1062 (1987).
6. G. Mamantov and R. A. Osteryoung, in "Characterization of Solutes in Nonaqueous Solvents," G. Mamantov, Editor, pp. 223-249, Plenum Press, New York (1978).
7. G. Ting, Ph.D. Dissertation, University of Tennessee, Knoxville, TN (1973).
8. H. Linga, Z. Stojek, and R. A. Osteryoung, *J. Am. Chem. Soc.*, **103**, 3754 (1981).
9. J. B. Scheffler, C. L. Hussey, K. R. Seddon, C. M. Kear, and P. D. Armitage, *Inorg. Chem.*, **22**, 2089 (1983).
10. D. L. Brotherton, Ph.D. Dissertation, University of Tennessee, Knoxville, TN (1974).
11. R. Marassi, J. Q. Chambers, and G. Mamantov, *J. Electroanal. Chem.*, **69**, 345 (1976).
12. P. Hagenmuller, J. Rouxel, J. David, A. Colin, and B. LeNeindre, *Z. Anorg. Allg. Chemie*, **323**, 1 (1963).
13. P. A. Flowers, Ph.D. Dissertation, University of Tennessee, Knoxville, TN (1988).
14. J. R. Canterford and R. Colton, "Halides of the Third Row Transition Metals," pp. 220-221, John Wiley & Sons, Inc., New York (1968).
15. E. Thorn-Csanyi and H. Timm, *J. Mol. Cat.*, **28**, 37 (1985).
16. C. K. Jorgensen, *Mol. Phys.*, **2**, 309 (1959).
17. K. Nakamoto, "Infrared and Raman Spectra of Inorganic and Coordination Compounds," 4th ed., p. 151, John Wiley & Sons, Inc., New York (1986).
18. K. Zachariassen, R. W. Berg, N. J. Bjerrum, and J. H. Von Barner, *This Journal*, **134**, 1153 (1987).

63

RAMAN SPECTROELECTROCHEMISTRY OF MOLTEN SALTS UTILIZING A PHOTODIODE ARRAY DETECTOR SYSTEM

DAVID S. TRIMBLE and GLEB MAMANTOV, Department of Chemistry, University of Tennessee, Knoxville, TN 37996-1600

Raman spectroscopy has been used previously to characterize electrochemically generated species. The structural information available from Raman spectroscopy makes it an especially valuable spectroelectrochemical probe. Although intensified photodiode arrays have been used previously as detectors for Raman scattered light, their application to studies of molten salt solutions has not been previously reported.

This paper presents a comparison of Raman spectra of molten salts obtained using two spectrometer and detector combinations. 'Conventionally' scanned spectra were obtained using an additive dispersion double spectrometer in conjunction with a cooled photomultiplier. An intensified linear photodiode array was used with a 'triple' spectrograph (Czerny-Turner spectrograph with a subtractive dispersion double prefilter) for much faster spectral acquisition. Samples can be probed by either continuous wave (argon ion, rhodamine dyes, frequency doubled argon ion) or pulsed (Nd:YAG and associated dye and optical system) laser sources. Criteria for comparison include instrument sensitivity, optimum sample geometry and concentration, and overall performance for static or dynamic Raman measurements.

A Raman spectroelectrochemical cell will be described which is suitable for use with molten salt systems. Optical electrodes of various dimensions and composition can be employed. The angle of the incident laser beam can be adjusted such that the Raman scatter is collected 90 degrees to the beam, or in the other extreme, a backscattering geometry is used. The aqueous ferricyanide/ferrocyanide system was used to characterize this cell.

The Raman spectroelectrochemical reduction of 25 mM ferricyanide in 0.5 M KCl is presented in Figure 1. The ferricyanide complex exhibits two overlapping vibrational frequencies at 2132 and 2126 cm^{-1}. After the potential of the working electrode is stepped past the E^{o} of the couple, bands associated with the ferrocyanide complex appear at 2080 and 2062 cm^{-1}. The 496.5 nm argon ion line (350 mW) was used and the spectra were recorded using the diode array based instrument.

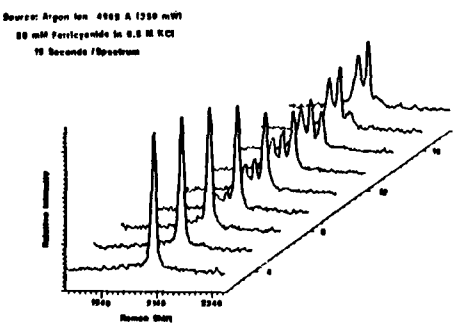

Figure 1. Raman Spectroelectrochemistry of Ferricyanide/ Ferrocyanide

Efforts are presently focused on determining which instrument configuration is best suited to studies of molten salt systems. The resonance Raman spectroelectrochemistry of I_2/I_2^+ in an acidic chloroaluminate mixture will be presented.

This work was supported by the Air Force Office of Scientific Research.

APPENDIX VI J. Electrochem. Soc.
(in press).

VOLTAMMETRY OF Ag(I) IN SOLID $NaAlCl_4$

Thomas R. Blackburn† and Gleb Mamantov*

Department of Chemistry, University of Tennessee, Knoxville, TN 37996

We have observed cyclic voltammograms for the AgCl/Ag couple in polycrystalline $NaAlCl_4$ using a tungsten ultramicroelectrode. Cathodic and anodic peaks are observed symmetrically about the potential of a Ag(I)/Ag reference electrode in the same medium, with overpotentials and peak currents that are strongly temperature-dependent. On the assumption of Fickian diffusion in the polycrystalline solid we have calculated approximate diffusion coefficients and an activation energy for diffusion of Ag(I) in the solid electrolyte.

The working electrode was a 25μm diameter tungsten wire, sealed in Pyrex to present a circular disk of area 4.9×10^{-6} cm^2. The reference electrode was a Pt wire electrolytically coated with Ag, and the counter electrode was a Pt wire. All three electrodes were immersed in the same compartment. Temperatures were measured with a standardized type K thermocouple in a thin-walled thermocouple well immersed in the electrolyte. Fluka anhydrous reagent grade $AlCl_3$ was purified by double distillation in vacuo; sodium chloride and silver chloride were oven-dried before use. All reagents were handled in a dry box under dry (<1 ppm H_2O) N_2, and the cell contents were maintained under a nitrogen or an argon atmosphere. Cyclic voltammetry was performed with the aid of Princeton Applied Research Model 174A potentiostat and Model 175 signal generator. A slightly basic (mol% $AlCl_3$<50) solvent composition was chosen for this preliminary work since the basic eutectic at 49.8 mol% $AlCl_3$ has a melting point only about two degrees lower (154° vs 156.5°) than the melting point of pure $NaAlCl_4$ (1); thus temperatures nearer the latter can be investigated without the presence of a liquid phase due to partial melting above the eutectic temperature. In contrast, the acid ($AlCl_3$-rich) eutectic temperature of 113°C would prevent completely solid phases above this temperature in melts with mol% $AlCl_3$>50. The melting point of our solvent ($AlCl_3$-NaCl, 49.96-50.04 mol%) was measured as 156 ± 0.5°C, in agreement with the data of Berg, et al. (1) for this melt composition.

Fig. 1 shows cyclic voltammograms of 0.03 M AgCl in this solvent, in both liquid and solid states. The liquid-phase CV is similar to that reported by Boxall, et al. (2) except that limiting current plateaus characteristic of ultramicroelectrodes (3), are observed for the diffusion-controlled $Ag(I) + e^- \rightarrow Ag$ step, with an increasing diffusion current reflecting the growth of the electrode area through silver deposition. The solid-phase CV exhibits a current maximum similar to that characteristic of linear diffusion (4). Cyclic voltammograms for the solid and liquid solvents without AgCl are shown in Fig. 2. It is apparent that these are essentially featureless in the region of interest, namely ± 0.5 V vs. Ag(I)/Ag. The background CV in the solid state is simply an Ohm's-law plot, reflecting a cell resistance of 2×10^7 ohm.

The small cathodic peak currents and their strong temperature dependence suggest that diffusion of Ag^+ in solid $NaAlCl_4$ is not the low-energy, structure-facilitated process that takes place in Ag_2S and in complex silver halosulfides such as Ag_3SI, for which activation energies of 10 to 30 kJ/mol are observed (5). Diffusion coefficients for the present system calculated from the Randles-Sevcik equation (4) range from 1.0×10^{-8} cm^2 sec^{-1} at 114.5° to 1.8×10^{-7} cm^2 sec^{-1} at 151°C. A linear regression of 15 experimental values of ($\ln i_p + 0.5 \ln T$) vs. T^{-1} yields an activation energy of 120 kJ mol^{-1}. This

*Electrochemical Society Member
†Permanent Address: Department of Chemistry and Physics, St. Andrews Presbyterian College, Laurinburg, NC 28352

rather large value is comparable to that for the formation of Frenkel defects in silver halides (6) and suggests that diffusion of silver ions in solid $NaAlCl_4$ may involve a similar process. The diffusion coefficients reported here are about two orders of magnitude smaller than those measured for Ag^+ in liquid $NaAlCl_4$ by Boxall, et al. (2), namely 3.0×10^{-6} cm^2 sec^{-1} at 175°C.

Acknowledgement: This work was supported by a grant from the Air Force Office of Scientific Research. We would like to acknowledge useful discussions with S. W. Orchard, P. A. Flowers, C. Woods, and J. Q. Chambers.

References

1. R.W. Berg, H.A. Hjuler, and N.J. Bjerrum, Inorg. Chem., 23, 557 (1984).
2. L.G. Boxall, H.L. Jones, and R.A. Osteryoung, J. Electrochem. Soc., 121, 212 (1974).
3. S. Pons, and M. Fleischmann, Anal. Chem., 59, 1391A (1987).
4. A.J. Bard, and L. Faulkner, Electrochemical Methods, Wiley, New York, 1980.
5. S. Geller, in Solid Electrolytes, S. Geller, ed., New York, Springer Verlag, 1977.
6. P.W.M. Jacobs, J. Corish, B.A. Devlin, and C.R.A. Catlow, in Fast Ion Transport in Solids, P. Vashishta, J.N. Mundy, and G.K. Shenoy, eds., New York, North-Holland, 1979.

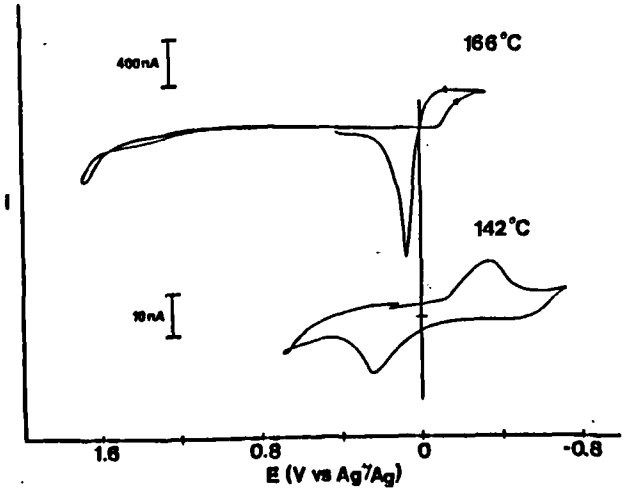

ig. 1. Cyclic voltammograms for 0.03 M AgCl in liquid (upper curve) and solid (lower curve) $NaAlCl_4$. Solvent composition: 49.96 mol% $AlCl_3$, 50.04 mol% NaCl. Scan rate 100 mV sec^{-1}.

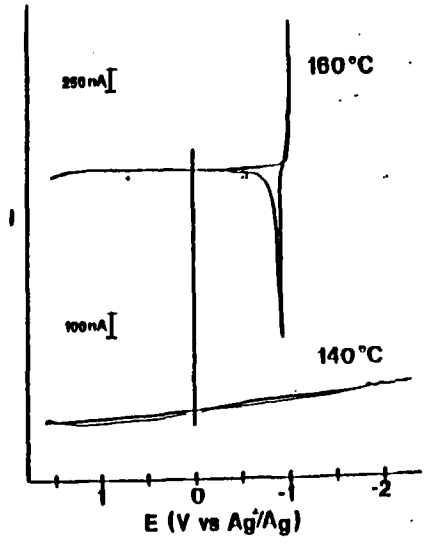

Fig. 2. Background cyclic voltammograms in the same solvent as in Fig. 1, before addition of AgCl. Upper curve: liquid 160°C. Lower curve: solid, 144°C. Scan rate 100 mV sec^{-1}.

Abstract No. 298

THE SPECTROELECTROCHEMICAL INVESTIGATION OF TUNGSTEN CHLORIDES IN ACIDIC SODIUM CHLOROALUMINATES

G. Mamantov, C. W. Hance, and J.P. Schoebrechts
Department of Chemistry, University of Tennessee, Knoxville, TN 37996

Several tungsten chloride species exist in acidic sodium chloroaluminates, such as $AlCl_3$-NaCl (63-37 mole %). Cyclic voltammetry (Figure 1) points to complex redox chemistry of tungsten in these media. This paper deals with the UV-visible absorption spectroelectrochemistry of tungsten species in this melt.

The spectroelectrochemical cell is shown in Figure 2. The optically transparent electrode was a Pt minigrid. The solution layer thickness (optical pathlength) was 0.025 cm which allowed for complete conversion from one oxidation state to another in ca. 5 minutes. Optical data were collected with a Tracor Northern 6500 diode array detector. Assignment of the specific tungsten chloride species to the appropriate electrochemical waves in Figure 1 was possible by comparing the spectra obtained in spectroelectrochemical experiments with those of known tungsten chloride spectra. The formation of WCl_6, WCl_5, $WOCl_4$, and W_6Cl_{12} at appropriate controlled potentials has been confirmed.

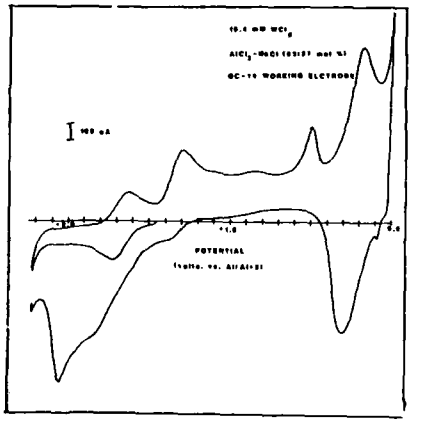

Figure 1

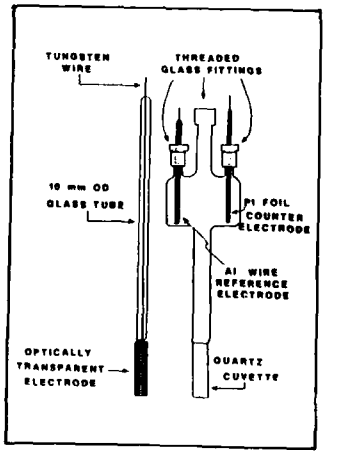

Figure 2

Reprinted from Inorganic Chemistry, 1988, 27, 2359

Contribution from the Department of Chemistry,
University of Tennessee, Knoxville, Tennessee 37996-1600

Raman Spectroscopy of Fluoride-Containing Chloroaluminate Melts

B. Gilbert,† Stephen D. Williams,‡ and G. Mamantov*

Received December 23, 1987

The effect of adding fluoride ions to chloroaluminate melts has been studied by Raman spectroscopy. In acidic (AlX_3/MX mole ratio greater than 1, where M^+ is an alkali-metal ion) melts at 200 °C, the fluoride ion acts as a dibase and the new species $Al_2Cl_6F^-$ is formed, as indicated by comparison of observed and calculated frequencies. The polarization of the Raman bands indicates that a fluoride replaces a terminal chloride. Measurements have also been made on several basic melts (AlX_3/MX mole ratio <1) at much higher temperatures (between 580 and 850 °C). The best results were obtained at 820 °C for mixtures of $NaAlCl_4$ with increasing amounts of NaF. It was found that fluoride replaces chloride progressively, depending on the molar ratio of NaF to $NaAlCl_4$. The new species $AlCl_3F^-$, $AlCl_2F_2^-$, and $AlClF_3^-$, together with the previously observed AlF_4^-, are clearly identified. Intensity measurements made on the characteristic bands allow a quantitative study of the distribution of each species as a function of melt composition. The calculated equilibrium constants follow the same trend as was found for similar chloro bromo species.

Introduction

Aluminum halide containing molten salt systems are of major importance to aluminum production; they are also of interest for high-energy batteries. Unusual redox and coordination chemistry has been observed in these melts.[1,2] The haloaluminate ions present in these melts are usually formed by the reaction between the alkali-metal halide and an aluminum halide, although lower melting point systems formed with organic halides have also been studied.[3] Mixed-halide melts have received some attention: for example, chlorobromoaluminate and chloroiodoaluminate systems have been studied by spectroscopic methods,[4-7] while electrochemical methods have been used to probe the behavior of F^- ion in acidic chloroaluminate melts.[8]

Tetrachloroaluminate ion has been shown to undergo fast exchange with a higher mass halogen (Br, I), in the liquid state (in CH_3CN solutions or in the molten state).[4-7] Vibrational spectroscopy and ^{27}Al NMR measurements provide evidence that when $AlCl_4^-$ is mixed with $AlBr_4^-$ or AlI_4^- the various mixed ions $AlCl_nX_{4-n}^-$ (X = Br, I) are formed, with n depending only on the mole ratio of the respective halides.[4-7]

Mixtures of $AlCl_4^-$ and fluoride ion should also exhibit similar behavior; however, no spectroscopic studies of such species have been reported, except for the Raman spectroscopic characterization of simple fluoro complexes, AlF_4^- and AlF_6^{3-}, in fluoride melts.[9,10]

In this paper we describe Raman spectroscopic studies of several new species formed by the exchange of fluoride for chloride in chloroaluminate melts.

Experimental Section

All chemicals were purified by the usual methods for chloroaluminate melt preparation.[11,12] The alkali-metal chlorides were melted in quartz tubes, treated with HCl and nitrogen, and crystallized from the melt. $AlCl_3$ (from Fluka) was distilled twice. NaF was melted in a nickel crucible and recrystallized twice by slow cooling. Clear crystals of each starting material were used to make the mixtures. Chemicals were handled in a drybox (water level <1 ppm) or under vacuum.

Because of the much lower viscosity of the present melts compared to that of pure fluoride melts, a windowless cell such as that used previously[13] was found to be impractical. With the size of the main holes

† Permanent address: Department of Chemistry, University of Liege, Liege, Belgium.
‡ Permanent address: Department of Chemistry, Appalachian State University, Boone, NC 28608.

(1) Mamantov, G.; Osteryoung, R. A. In *Characterization of Solutes in Non-Aqueous Solvents*; Mamantov, G., Ed.; Plenum: New York, 1978; pp 223–249.
(2) Boston, C. R. In *Advances in Molten Salt Chemistry*; Braunstein, J., Mamantov, G., Smith, G. P., Eds.; Plenum: New York, 1971; Vol. 1, pp 129–163.
(3) Hussey, C. L. In *Advances in Molten Salt Chemistry*; Mamantov, G., Ed.; Elsevier: New York, 1983; Vol. 5, pp 185–230.
(4) Bradley, B. H.; Brier, N. P.; Jones, D. E. H. *J. Chem. Soc. A* **1971**, 1397.
(5) Jones, D. E. H. *J. Chem. Soc., Dalton Trans.* **1972**, 567.
(6) Berg, R. W.; Kemnitz, E.; Hjuler, H. A.; Fehrmann, R.; Bjerrum, N. J. *Polyhedron* **1985**, *4*, 457.
(7) Kidd, R. G.; Truax, D. R. *J. Am. Chem. Soc.* **1968**, *90*, 6867.
(8) Tremillon, B.; Duchange, J. P. *J. Electroanal. Chem. Interfacial Electrochem.* **1973**, *44*, 389.
(9) Gilbert, B.; Mamantov, G.; Begun, G. M. *Inorg. Nucl. Chem. Lett.* **1974**, *10*, 1123.
(10) Gilbert, B.; Mamantov, G.; Begun, G. M. *J. Chem. Phys.* **1975**, *62*, 950.
(11) Torsi, G.; Fung, K. W.; Begun, G. M.; Mamantov, G. *Inorg. Chem.* **1971**, *10*, 2285.
(12) Marassi, R.; Chambers, J. Q.; Mamantov, G. *J. Electroanal. Chem. Interfacial Electrochem.* **1976**, *69*, 345.
(13) Gilbert, B.; Mamantov, G.; Begun, G. M. *Appl. Spectrosc.* **1975**, *29*, 276.

0020-1669/88/1327-2359$01.50/0

about 3 mm, it was not possible to hold a drop of reasonable size (filling most of the sample compartment). Reducing the size of the hole to 1 mm allowed to drop to be stabilized occasionally, but the spectral intensities were frequently weak and not very reproducible. Fortunately, the acidic melts (those with $AlCl_3$ present in excess) could be studied in glass or quartz cells, since for these systems the fluoride ion was strongly complexed, and the temperature of the melt was quite low (near 200 °C).

In basic melts, reasonable solubility of the fluoride ion is achieved only at very high temperatures. Provided that the following sequence in the preparation of the solutions is followed, for the composition ranges studied here, quartz cells can still be used, and fluoride ion does not attack the cell. No changes in the Raman spectra were found even after repeated meltings at 820 °C for 3 h (the time period for the melt to reach its equilibrium temperature and for the recording of a spectrum).

The procedure used is as follows. The starting solvents LiCl/NaF (80/20 mol %) and NaCl/NaF (60/40 mol %) were first prepared by premelting the required amounts in a glassy-carbon crucible under an argon atmosphere. After the solids were melted, the liquids were frozen and the resulting pellet was broken into several chunks. A chunk of the required weight was then added to the quartz Raman cell (a simple round tube, 6 mm i.d.) together with the necessary amount of $NaAlCl_4$ (also previously prepared, but in glass ampules). The cell was sealed under vacuum and placed in the Raman furnace. When the mixture was heated, the $NaAlCl_4$ melted first and totally surrounded the still solid chunk containing the fluoride. When the temperature reached 400–600 °C, depending on the mixture, the $NaAlCl_4$ reacted rapidly with the fluoride-containing material. Using this procedure and keeping the F/Al molar ratio below 4 ensures that no free fluoride is present and no attack of the quartz cell occurs, even at 850 °C.

The furnace used is similar in design to the one previously described.[13] The only difference is that the inside of the main quartz tube contained a nickel block with the required openings for the laser and Raman light, to ensure a better temperature homogeneity in the sample.

A Ramanor HG2000 spectrometer (Jobin-Yvon) equipped with concave, aberration-corrected, holographic gratings was used to record the Raman spectra. A Coherent Radiation Model 52B Ar ion laser operating at 514.5 nm with power ranging from 40 to 200 mW was used as the excitation source. Spectra could be accumulated or subtracted through the use of an LSI 11/23 computer. For accurate measurements used in quantitative calculations, the slit length was kept much smaller than the projected mage of the laser beam, resulting in much better reproducibility of the intensities. The slit widths used were between 3 and 4 cm^{-1}, and the time constants were between 0.5 and 1 s, depending on the sample.

Results and Discussion

Because the results obtained depend on the modified Lewis acidity of the mixture, the results for basic and acidic melts will be presented and discussed separately.

Mixtures of Alkali-Metal Halides with $NaAlCl_4$. As explained in the Experimental Section, quartz cells were required for these samples; this fact severely restricts the type of mixture and composition range that could be studied. While it is possible that mixtures of $NaAlCl_4$ with Na_3AlF_6 where the amount of the latter is low may be relatively inert, they were not investigated.

Initial measurements were made with the lowest melting temperature alkali-metal chloride/alkali-metal fluoride mixtures in order to keep the attack on the container as low as possible. The first mixture chosen as solvent contained 80 mol % LiCl and 20 mol % NaF. This is a eutectic mixture that melts at 490 °C.[14] $NaAlCl_4$ is quite soluble in this mixture; Raman spectra of such solutions at 580 °C are shown in Figure 1. All of the observed bands, except the one at 490 cm^{-1}, are strongly polarized (the polarized spectra are not shown for the sake of clarity for this and several other figures). The spectrum at the top of the figure is that of a mixture containing an amount of $NaAlCl_4$ slightly lower than the amount of NaF. This spectrum shows a large background in the low-frequency region, which is characteristic of all LiCl-based melts and which precludes the observation of low-frequency bands. Despite this large background, an intense doublet located at 349 and 375 cm^{-1} and two weak bands at 416 and 490 cm^{-1} are observed. The 349-cm^{-1} band is the ν_1 band of $AlCl_4^-$ slightly shifted toward higher frequencies because of the presence of the Li cation.[15] The broad depolarized band at 490 cm^{-1} is the ν_3 band of $AlCl_4^-$. The other two bands are new and are believed to be due to the ν_1 mode of mixed chloro–fluoro aluminum tetrahalides, located between the ν_1 band of $AlCl_4^-$ at 349 cm^{-1} and the ν_1 band of AlF_4^- at 622 cm^{-1}.[9]

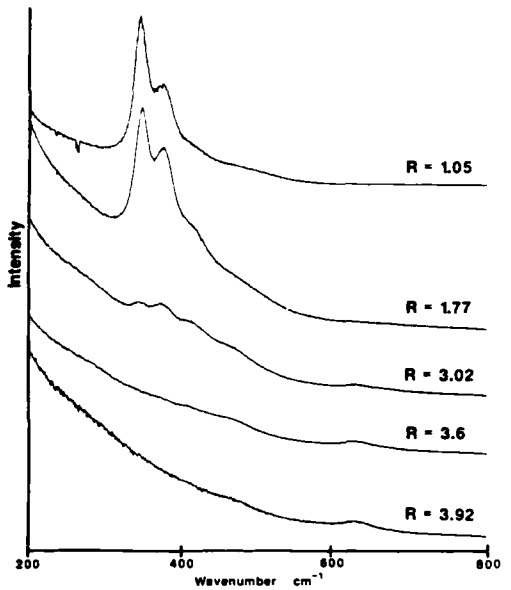

Figure 1. Raman spectra of several solutions of $NaAlCl_4$ in LiCl/NaF (80/20 mol %) mixtures (temperature 580 °C). The symbol R represents the formal ratio of NaF to $NaAlCl_4$.

If this is correct, the 375-cm^{-1} band should correspond to the species most likely to be present when the amounts of NaF and $NaAlCl_4$ are nearly equal, i.e. $AlCl_3F^-$, and the 416-cm^{-1} band to a species with more chloride exchanged for fluoride, i.e. $AlCl_2F_2^-$. In order to check this hypothesis, various mixtures were made by further diluting $NaAlCl_4$ with the solvent, thus increasing the ratio R. The resulting spectra, presented in Figure 1, exhibit other new, albeit very weak, bands found at 470 and 632 cm^{-1}. The 632-cm^{-1} band is almost certainly the ν_1 band of AlF_4^- (again shifted due to the effect of Li^+), and the 470-cm^{-1} band is probably due to the same vibration of the ion $AlClF_3^-$. The variation of the ν_1 band intensities as a function of R is consistent with a progressive replacement of Cl^- in $AlCl_4^-$ with F^- and a strong decrease in the molar scattering efficiency of each $AlCl_{4-n}F_n^-$ species as n increases.

Since the presence of Li^+ ion produces a large background and distorts the bandwidth and frequency of ν_1 bands,[16] solutions of $NaAlCl_4$ were made by using melts containing only Na^+ as the cation. For the system NaCl–NaF, a eutectic exists at 66 mole % of NaCl, which melts as 675 °C.[14] A solvent with the composition NaCl–NaF (60/40 mol %) was chosen for the following reasons. First, it allows a ratio $R = 1$ with a higher content of $NaAlCl_4$, thus increasing the intensity of the spectra. Second, the following exchange reaction is expected to produce a large amount of NaCl so that the resulting solution is far different from the initial solvent:

$$NaAlCl_4 + nNaF \rightleftharpoons NaAlCl_{4-n}F_n + nNaCl \qquad (1)$$

Despite the higher melting temperature of such solutions (820 °C, which is above the melting point of NaCl), much better spectra were obtained (Figure 2). The bands are sharper and are better defined; however, a similar variation of the band intensities as a function of the composition was observed as for mixtures with LiCl/NaF. Even better spectra were obtained by simply using mixtures of pure $NaAlCl_4$ with increasing amounts of NaF (Figure 3). In this case the spectra are more intense and the background in the low-frequency range is much lower, allowing the observation

(14) Bergman, A. G.; Kozachenko, E. L.; Berezina, S. I. *Russ. J. Inorg. Chem.* (*Engl. Transl.*) **1964**, *9*, 663.
(15) Rytter, E.; Oye, H. A. *J. Inorg. Nucl. Chem.* **1973**, *35*, 4311.
(16) Gilbert, B. In *Molten Salt Chemistry*; Mamantov, G., Marassi, R., Eds.; NATO ASI Series C; Kluwer: Boston, MA, 1987; pp 201–216.

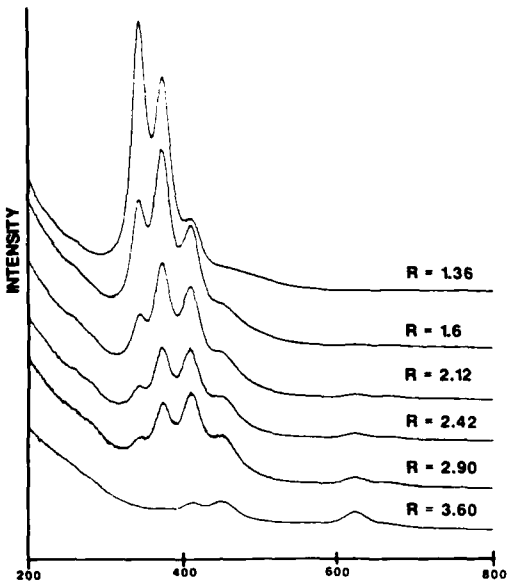

Figure 2. Raman spectra of several solutions of $NaAlCl_4$ in NaCl/NaF (60/40 mol %) mixtures (temperature 820 °C).

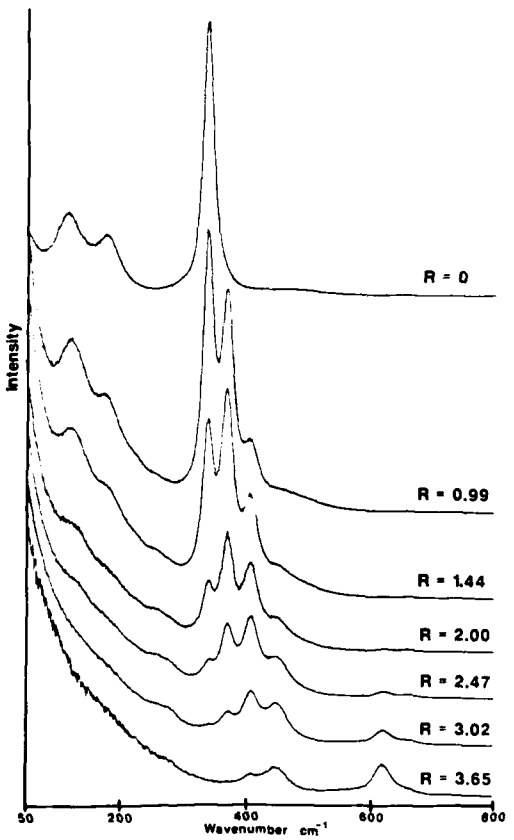

Figure 3. Raman spectra of several molten mixtures of $NaAlCl_4$ with NaF (temperature 820 °C). For the spectrum of pure $NaAlCl_4$ the laser power was 40 mW; for the other spectra the power was 200 mW. All other experimental conditions were kept identical.

of several new low-frequency bands.

Digital subtraction of the Raman spectra was used to enhance the presentation of the spectra of the new species. The spectrum of pure $NaAlCl_4$ was recorded under conditions identical with those used for the spectra presented in Figure 3. This $NaAlCl_4$ reference spectrum was then scaled and subtracted from the spectra of Figure 3 in such a way that the ν_1 band of $AlCl_4^-$

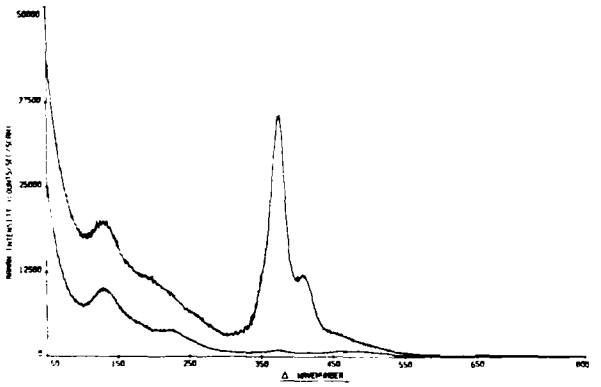

Figure 4. Raman spectra of the mixture of $NaAlCl_4$ with NaF (R = 0.99) from which the spectrum of $AlCl_4^-$ has been quantitatively subtracted: (upper curve) polarization parallel; (lower curve) polarization perpendicular.

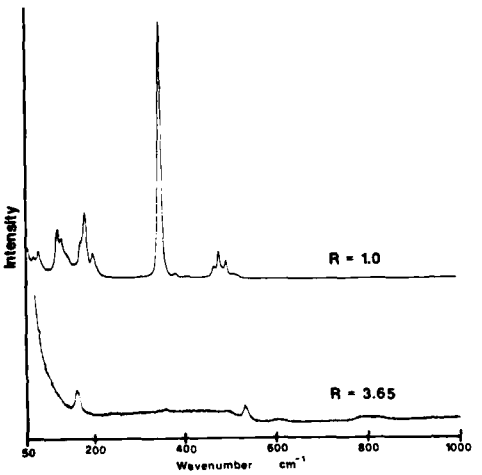

Figure 5. Raman spectra of frozen solutions of $NaAlCl_4$ with NaF. This slit width is 0.33 mm, and the laser power is 200 mW.

Table I. Observed Frequencies for $AlCl_nF_{4-n}^-$

species	freq, cm^{-1}	ref
$AlCl_4^-$	490, 351, 186, 121	9
$AlCl_3F^-$	372, 216, 195, 132	this work
$AlCl_2F_2^-$	665, 404, 260	this work
$AlClF_3^-$	453, 279	this work
AlF_4^-	760, 622, 322, 210	9

vanished without any distortion of the background. This allowed several features in the spectra of the new species to be clearly observed. Figure 4 presents the results of such a subtraction where the major features of $AlCl_3F^-$ (with a small amount of $AlCl_2F_2^-$) can be identified. Table I presents all of the new frequencies found and their assignment to each of the species. This assignment was made by considering the variation of intensity with R and the results of the subtraction technique.

After spectra of the molten solutions were recorded, the solutions were cooled to room temperature and spectra of the frozen solutions were recorded. Examples of such spectra are shown in Figure 5. The sample whose spectrum is presented in the top of the figure contained equimolar amounts of NaF and $NaAlCl_4$, yet the spectrum corresponds very closely to the spectrum of $NaAlCl_4$ at room temperature obtained by Wallart et al.[17] When R is increased, the intensity of the spectrum of $NaAlCl_4$ decreases; it is replaced by two very weak bands at 156 and 531 cm^{-1}. These bands belong to AlF_6^{3-},[18] indicating that neither the mixed

(17) Wallart, F.; Lorriaux-Rubbens, A.; Mairesse, G.; Barbier, P.; Wignacourt, J. *J. Raman Spectrosc.* **1980**, *9*, 55.

90

Table II. Calculated Mole Fractions for $AlCl_nF_{4-n}^-$

ratio	$X(AlCl_4^-)$	$X(AlCl_3F^-)$	$X(AlCl_2F_2^-)$	$X(AlClF_3^-)$	$X(AlF_4^-)$
0.99	0.3	0.4	0.3		
1.44	0.14	0.3	0.39	0.17	
2.0	0.05	0.18	0.39	0.32	0.06
2.5	0.02	0.1	0.36	0.44	0.08
3.0		0.04	0.23	0.5	0.22

chloro–fluoro species nor AlF_4^- exists in the solid state.

Halogen Distribution Equilibria. In order to compare the intensities of the spectra of the various mixed-tetrahalide species, the spectra of the whole series of $NaAlCl_4$ + NaF mixtures were recorded with all experimental conditions kept as constant as possible, pure $NaAlCl_4$ at 820 °C being used as a standard of intensity. A quantitative evaluation of the equilibria relating the various species was performed on the basis of the following two assumptions: (1) The fluoride exchanges with chloride in a fashion similar to the exchange of bromide and iodide with chloride. The general reaction scheme follows reaction 1. (2) In each reaction mixture no free fluoride is present, which implies that reaction 1 is essentially quantitative. This assumption is based on the fact that mixtures with R greater than 4 very quickly attack the quartz container, whereas mixtures with R less than 4 do not.

Under these conditions the equilibria among the tetrahaloaluminates can be written as three disproportionation reactions:[5]

$$2AlCl_{4-n}F_n^- \rightleftharpoons AlCl_{3-n}F_{n+1}^- + AlCl_{5-n}F_{n-1}^- \qquad (2)$$

For these reactions n = 1, 2, 3, and K_1, K_2, and K_3 are the corresponding equilibrium constants.

The analysis of these equilibria has been carried out in a stepwise fashion. Consideration of the first mixture of Figure 3 (R = 0.99) shows that there is apparently no $AlClF_3^-$ present. This implies that only the equilibrium where n = 1 should be considered for this mixture. From the relative intensity of the ν_1 band of $AlCl_4^-$ in the mixture, compared to that of pure $NaAlCl_4$, the mole fraction X of $AlCl_4^-$ in the mixture can be deduced, if the mole fractions are expressed in terms of 1 mol of total aluminum halide. Since there is apparently no $AlClF_3^-$, $X(AlCl_4^-) = X(AlCl_2F_2^-)$. Finally, $X(AlCl_3F^-)$ was deduced from mass balance. These calculations give the mole fractions of the species present in this mixture; these mole fractions, together with the intensities of the bands for the various species, were used to calculate the relative Raman scattering coefficients for the various species.[10] These relative scattering coefficients were then used to calculate the mole fractions of $AlCl_4^-$, $AlCl_3F^-$, and $AlCl_2F_2^-$ in the next mixture. A similar procedure was applied to the other mixtures, allowing the compositions of all the mixtures to be calculated. The results of this analysis are presented in Table II.

The averaged values for the equilibrium constants K_n were found to be $K_1 = 0.59 \pm 0.02$, $K_2 = 0.35 \pm 0.02$, and $K_3 = 0.19 \pm 0.04$. The relative scattering coefficients were found to be 135.4 (n = 0), 79.8 (n = 1), 25.8 (n = 2), 10 (n = 3), and 8 (n = 4).

It can be observed that the trend in the equilibrium constants observed here follows nearly the trend observed in the case of mixed chlorobromoaluminates. It does not correspond exactly to a purely random distribution, indicating stronger bonding between aluminum and fluoride. Fluoride ion exchanges very readily with chloride to form more stable fluoroaluminate complexes. Also, the trend observed in the scattering coefficients when n increases is expected, considering the much lower polarizability of an Al–F bond versus that of an Al–Cl bond.

As a general conclusion it is interesting to recall that the investigated mixtures do not attack quartz sample cells, provided that the ratio of total fluoride to aluminum does not exceed 4. This also means that the activity of the fluoride ion (which cannot be calculated from our Raman data) must be very low in these composition ranges and rises sharply when the ratio exceeds 4. In addition, by carefully choosing the composition range, it should be possible to study the behavior of various solutes in the presence of aluminum fluoride with much less experimental difficulty than with pure fluoride melts.

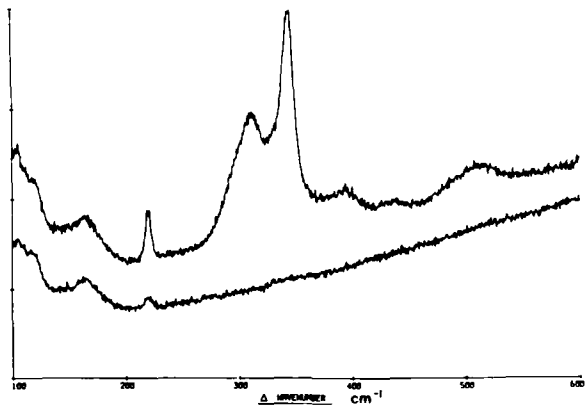

Figure 6. Raman spectra of molten Al_2Cl_6 saturated with NaF (temperature 205 °C): (upper curve) polarization parallel; (lower curve) polarization perpendicular.

Acidic Chloroaluminates. The influence of NaF on the Raman spectra of acidic chloroaluminates (that is, melts where the molar ratio of $AlCl_3$/NaCl is greater than 1) has also been studied. Tremillon and Duchange[8] have shown from electrochemical measurements that F^- ion added to acidic chloroaluminate melts acts as a dibase. The proposed reaction is

$$2Al_2Cl_7^- + F^- \rightarrow Al_2Cl_6F^- + 2AlCl_4^- \qquad (3)$$

If indeed $Al_2Cl_6F^-$ is formed, it should exhibit a characteristic Raman spectrum that, in a favorable case, should show if the F atom is occupying a terminal or bridging position. Since the Raman spectrum of 63/37 mole % $AlCl_3$/NaCl mixture is already quite complex (it contains bands due to $Al_2Cl_7^-$, $AlCl_4^-$, and Al_2Cl_6[19]), NaF was simply added to pure Al_2Cl_6. Figure 6 shows the Raman spectrum of a saturated solution of NaF in Al_2Cl_6 at 200 °C. In addition to Al_2Cl_6 bands at 102, 118, 166, 218, 341, and 512 cm^{-1}, four new bands are observed, at 312, 395, 437, and 489 cm^{-1}, all of which are totally polarized. These four new bands are located at frequencies nearly equal to several of the bands of $Al_2Cl_7^-$, but the respective intensities and bandwidths are not the same. For example, the 389-cm^{-1} band of $Al_2Cl_7^-$ is clearly depolarized[20] whereas the 395-cm^{-1} band shown here is polarized.

The nature of the products of the reaction between aluminum chloride and sodium fluoride that are responsible for these new bands will now be discussed. The two most likely candidates for the products are $Al_2Cl_6F^-$ or a mixture of $Al_2Cl_7^-$ and Al_2Cl_5F. These species could be formed by the reaction

$$Al_2Cl_6 + NaF \rightarrow Al_2Cl_6F^- + Na^+ \qquad (4)$$

or

$$Al_2Cl_6 + NaF \rightarrow Al_2Cl_5F + NaCl \qquad (5)$$

and

$$Al_2Cl_6 + NaCl \rightarrow Al_2Cl_7^- + Na^+ \qquad (6)$$

In the former case the product would be similar to $Al_2Cl_7^-$ with one of the chlorines replaced with a fluorine, while in the latter the product would be similar to Al_2Cl_6 with one of the chlorines replaced with a fluorine. While it is unlikely for a species like Al_2Cl_5F to exist in the presence of excess Cl^- (a basic melt), its possible existence in the acidic systems discussed here is not so easily dismissed. In either case it seems that the replacement occurs at a terminal chlorine, not a bridging one. There are two arguments in favor of this assumption: The spectrum of this mixture is very similar to that of acidic chloroaluminate melts,

(18) Reisfeld, M. J. *Spectrochim. Acta, Part A* **1973**, *29A*, 1923.

(19) Torsi, G.; Mamantov, G.; Begun, G. M. *Inorg. Nucl. Chem. Lett.* **1970**, *6*, 553.

(20) Gilbert, B., to be submitted for publication.

71

Table III. Force Field for $AlCl_nF_{4-n}^-$

force const	interpretation	value
F_1	Al–F str	3.393 mdyn/Å
F_2	Al–Cl str	1.658 mdyn/Å
F_3	Cl–Al–Cl bend	0.7081 mdyn Å/rad^2
F_4	Cl–Al–F bend	0.6124 mdyn Å/rad^2
F_5	F–Al–F bend	0.6784 mdyn Å/rad^2
F_6	Al–F:Al–F str–str	0.3437 mdyn/Å
F_7	Al–Cl:Al–Cl str–str	0.2912 mdyn/Å
F_8	Al–Cl:Al–F str–str	0.8076 mdyn/Å
F_9	X–Al–X:X–Al–X bend–bend[a]	−0.2311 mdyn Å/rad^2

[a] X = F or Cl.

indicating that the species present in the two melt systems must have similar structures; much larger differences would be expected for a bridged substitution. Also, it is important to note that *all* of the new bands are polarized; this implies a rather low symmetry for the reaction product. If the product were $Al_2Cl_6F^-$ with the fluorine as the bridge, the relatively small size of fluorine would favor a linear Al–F–Al structure, giving rise to D_{3h} or D_{3d} symmetry for the product.[21] It is unlikely that all of the observed bands would be polarized in such a case. A similar argument applies for the Al_2Cl_5F case: bridge substitution would give rise to a species with C_{2v} symmetry, and again it is unlikely that all of the observed bands would be polarized. For these reasons only F terminal species will be considered further. Hence, the question to be answered here is as follows: Is $Al_2Cl_6F^-$ or Al_2Cl_5F, both with terminal fluorines, present in the aluminum chloride/sodium fluoride mixtures?

Normal-coordinate calculations were made to determine approximate valence force fields for $Al_2Cl_7^-$ and Al_2Cl_6 with use of vibrational data from Manteghetti and Potier[22] and Tomita et al.[23] Similar calculations were carried out for $AlCl_4^-$, $AlCl_3F^-$, $AlCl_2F_2^-$, $AlClF_3^-$, and AlF_4^-, with use of data from this work and from Gilbert et al.[9] In addition to these calculations, a similar force field for AlF_3 was developed with use of the IR data of Snelson.[24] Appropriate valence force constants for Al–F and Cl–Al–F motions were then used together with the force fields for $Al_2Cl_7^-$ and Al_2Cl_6 to calculate frequencies for $Al_2Cl_6F^-$ and Al_2Cl_5F. The normal-coordinate calculations were carried out on an IBM XT personal computer, using a modified version[25] of the QCPE program No. 342. For the species whose structures were not known ($Al_2Cl_6F^-$ and Al_2Cl_5F), geometric parameters needed for the normal-coordinate calculations were obtained from semiempirical (MNDO Hamiltonian) molecular orbital calculations.[26] It should be emphasized that the results of the normal-coordinate calculations described should not be considered an accurate description of the potential energy of the species involved; they are quite approximate. The force field calculated for $Al_2Cl_7^-$ was able to reproduce 12 known frequencies with an rms error of 15.6 cm^{-1}; the calculation for Al_2Cl_6 was able to reproduce 16 known frequencies with an rms error of 9.1 cm^{-1}. Since the purpose of the calculations was to transfer force constants from the $AlCl_nF_{4-n}^-$ ions to either of the dialuminum species, the force fields used for the latter contained only bond-stretching and bond-angle-bending diagonal force constants, since these are the types calculated for the mononuclear ions. The force fields in ref 22 and 23 are more accurate since they include torsion and ring-puckering coordinates as well.

Table IV. Calculated Frequencies for Al_2Cl_xF

	$Al_2Cl_6F^-$		Al_2Cl_5F	
obsd	calcd	error	calcd	error
489	509.9	20.9	506.7	17.7
437	449.3	12.3	412.0	−25.0
393	364.4	−28.6	338.4	−54.9
311	290.8	−20.2	318.0	8.0
rms error		21.3		31.3, 31.9[a]

[a] The calculation giving this result used the Al–F stretching force constant derived from the fit of AlF_3 IR data.

A 9-parameter force field (5 diagonal and 4 interaction force constants) was developed that could fit the 17 known frequencies for the $AlCl_nF_{4-n}^-$ ions with an average rms error of 13.8 cm^{-1} for all five ions. Either of the two possible dialuminum species contains a single F atom; this implies that force constants from $AlCl_4^-$ and $AlCl_3F^-$ will be more important for this calculation than constants from other species. The force field for the tetrahaloaluminates gave less than 4 cm^{-1} error for $AlCl_4^-$ and $AlCl_3F^-$. The force constants are presented in Table III. In Table IV the results of transferring the appropriate force constants from Table III into the force fields for $Al_2Cl_7^-$ and Al_2Cl_6 to calculate the frequencies for $Al_2Cl_6F^-$ and Al_2Cl_5F are presented. It can be seen that the frequencies associated with the product of the reaction between Al_2Cl_6 and NaF are more closely matched with the frequencies calculated for $Al_2Cl_6F^-$. It may be argued that it is not appropriate to transfer force constants for an anion into the calculation of frequencies for a neutral species, such as Al_2Cl_5F. To address this point, the frequencies for Al_2Cl_5F were also calculated with use of the Al–F stretching force constant derived from the treatment of AlF_3; the error for this calculation is also presented in Table IV. Even when this possible source of error is included, it still seems that the predominant species is likely to be $Al_2Cl_6F^-$. While this does not constitute definite proof of the existence of $Al_2Cl_6F^-$ in this system, the vibrational data favor its existence.

This is also consistent with the chemistry observed for the chloroaluminate systems: the reaction to form $Al_2Cl_6F^-$ is an acid–base reaction very much like the one that results in the formation of $Al_2Cl_7^-$. The reaction that forms Al_2Cl_5F is a ligand-exchange reaction similar to the ones that result in the formation of $AlCl_nF_{4-n}^-$; such reactions are expected in these systems, but only at rather high temperatures. For these reasons it is the opinion of the authors that $Al_2Cl_6F^-$ ion is formed by the reaction between aluminum chloride and sodium fluoride in the 200 °C temperature range.

Conclusions

Quartz sample tubes may be used for Raman studies of fluoride-containing chloroaluminate melts, at temperatures up to 850 °C, provided that the molar ratio of fluorine to aluminum does not exceed 4. In basic melts of this type the new species $AlCl_3F^-$, $AlCl_2F_2^-$, and $AlClF_3^-$ were observed; halide ion distribution equilibrium constants indicate that aluminum–fluoride bonding is somewhat stronger than bonding between aluminum and other halogens. Acidic fluoride-containing chloroaluminate melts show spectroscopic evidence for the presence of the previously proposed species $Al_2Cl_6F^-$.

Acknowledgment. Support from the Air Force Office of Scientific Research (Grant 85-0321) and from the UTK Science Alliance Program is gratefully acknowledged. The support of the Appalachian State University Research Committee for the purchase of some of the computer software is appreciated.

(21) Curtis, L. A. In *Proceedings of the Joint International Symposium on Molten Salts*; Mamantov, G., Hussey, C., Saboungi, M. L., Blander, M., Mamantov, C., Wilkes, J., Eds.; Electrochemical Society: Pennington, NJ, 1987; Vol. 87-7.

(22) Manteghetti, A.; Potier, A. *Spectrochim. Acta, Part A* **1982**, *38A*, 141.

(23) Tomita, T.; Sjogren, C. E.; Klaeboe, P.; Papatheodorou, G. N.; Rytter, E. *J. Raman Spectrosc.* **1983**, *14*, 415.

(24) Snelson, A. *J. Phys. Chem.* **1967**, *71*, 3202.

(25) McIntosh, D. F.; Peterson, M. R. *QCPE* **1977**, *11*, 342. O'Leary, T. J. *QCPE Bull.* **1985**, *5*, 145 (QCMP012).

(26) Dewar, M. J. S.; Stewart, J. J. P. *QCPE Bull.* **1986**, *6*, 24 (AMPAC). Dewar, M. J. S.; Thiel, W. *J. Am. Chem. Soc.* **1977**, *99*, 4899. Dewar, M. J. S.; Rzepa, H. S. *J. Am. Chem. Soc.* **1978**, *100*, 60. Dewar, M. J. S.; Rzepa, H. S. *J. Comput. Chem.* **1983**, *4*, 158. Davis, L. P.; Guidry, R. M.; Williams, J. R.; Dewar, M. J. S.; Rzepa, H. S. *J. Comput. Chem.* **1981**, *2*, 433.

12

Reprinted from the Journal of the American Chemical Society, 1987, *109*, 2218.

A New Room Temperature Molten Salt Solvent System: Organic Cation Tetrachloroborates

Stephen D. Williams,† J. P. Schoebrechts, J. C. Selkirk, and G. Mamantov*

Department of Chemistry, The University of Tennessee Knoxville, Tennessee 37996-1600

Received January 12, 1987

In the past decade there has been considerable interest in $AlCl_3$-containing molten salts. These melts provide novel media for fundamental studies and are also of interest in high-energy batteries and for catalytic applications.[1] Relatively few molten salt systems are liquid at or below room temperature. The properties of these systems, mainly organic chloroaluminates, have been reviewed by Hussey;[2] several other room temperature molten salts have been described recently.[3] This paper describes tetrachloroborate salts that are stable liquids at room temperature; they are products of the reaction between *n*-butylpyridinium chloride or methylethylimidazolium chloride and boron trichloride.

N-Butylpyridinium chloride (BPC) and 1-methyl-3-ethylimidazolium chloride (MEIC) were prepared as described in ref 4–6. Melts were prepared by distillation of a measured volume of BCl_3 onto a weighed amount of BPC or MEIC in a glass tube cooled with liquid nitrogen. The tube was then sealed and warmed to room temperature. The composition of such melts is uncertain by about 15%.

Conductivity cells were calibrated with standard KCl; a YSI conductivity bridge was used for specific conductance measurements. PAR equipment was used for electrochemical measurements. Raman spectra were obtained with an ISA Ramanor 2000 spectrometer, an argon ion laser, and a photon-counting system.

Both solid chlorides react exothermically with gaseous BCl_3 to form droplets of colorless, viscous melt at room temperature. The reaction with MEIC is more exothermic. When the mole ratio of BCl_3 to the organic chloride is approximately 1:1, a single phase is formed; when the ratio is 2:1, two immiscible liquid phases

† Present address: Department of Chemistry, Appalachian State University, Boone, North Carolina 28608.

(1) Mamantov, G.; Osteryoung, R. A. In *Characterization of Solutes in Non-Aqueous Solvents*; Mamantov, G., Ed.; Plenum: New York, 1978; pp 223–249.

(2) Hussey, C. L. In *Advances in Molten Salt Chemistry*; Vol. 5, Mamantov, G., Ed.; Elsevier: New York, 1983; Vol. 5, pp 185–230.

(3) Poole, C. F.; Kersten, B. R.; Ho, S. S. J.; Coddens, M. E.; Furton, K. G. J. *Chromatography* **1986**, *352*, 407.

(4) Robinson, J.; Osteryoung, R. A. *J. Am. Chem. Soc.* **1979**, *101*, 323.

(5) Zingg, S. P.; Pagni, R. M.; Smith, G. P., submitted for publication in *J. Org. Chem.*

(6) Wilkes, J. S.; Levisky, J. A.; Wilson, R. A.; Hussey, C. L. *Inorg. Chem.* **1982**, *21*, 1263.

0002-7863/87/1509-2218$01.50/0

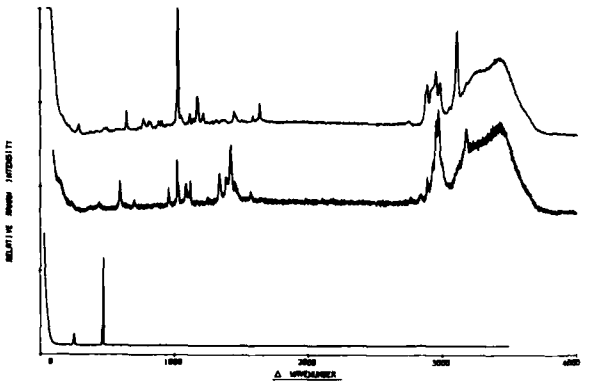

Figure 1. Raman spectra of BPC, (top), MEIC, (center) as aqueous solutions, and liquid BCl_3 (bottom).

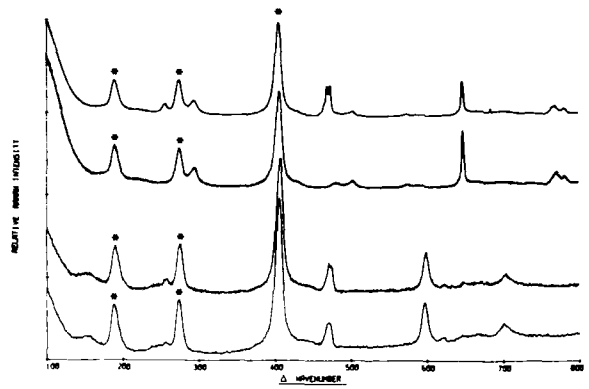

Figure 2. Raman spectra of room temperature tetrachloroborate melts: acidic BPC melt (molar ratio BCl_3:BPC = 2:1) (top); neutral BPC melt (BCl_3:BPC = 1:1) (second from top); acidic MEIC melt (BCl_3:MEIC = 2:1) (second from bottom); neutral MEIC melt (BCl_3:MEIC = 1:1) (bottom). Bands assigned to BCl_4^- are indicated by an asterisk. The composition of the neutral melt sample was nominally 1:1; however, some BCl_3 was present (peak near 470 cm^{-1}).

are formed at ~0 °C, one of which is BCl_3.

Raman spectra of aqueous solutions of BPC, MEIC and liquid BCl_3 are presented in Figure 1. Raman spectra of neutral (mole ratio BCl_3:organic chloride is approximately 1:1) and acidic (mole ratio approximately 2:1) melts prepared from BCl_3 and BPC or MEIC are presented in Figure 2. Three of the four modes of the tetrachloroborate anion are clearly seen for both the neutral and acidic melts; their positions are noted with an asterisk. The fourth mode (ν_3) is very weak and is obscured by a cation mode in the MEIC melt. The frequencies for BCl_4^- in the melts agree quite well with the tetrachloroborate frequencies reported by Bullock et al.[7] The melt frequencies and assignments are (with Bullock's frequency in parentheses) ν_1 405 (396), ν_2 188 (196), ν_3 696 (696), and ν_4 273 (275). No significant composition dependence was observed for the peak positions. In acidic melts, the spectra show the presence of dissolved BCl_3 in the melt phase; since these are saturated solutions, the intensity of the BCl_3 ν_1 peak, when compared to that of neat BCl_3, indicates that the solubility of BCl_3 in both BPC and MEIC melts is about 1 M.

Table I. Properties of Tetrachloroborate Melts

composition[a]	phases[b]	liquid temp[c]	density[d]	conductivity[e]	EC window[f] Pt	EC window[f] GC
1:1 BCl_3:BPC	1	+16.5	1.28	1.6×10^{-2}	1200	3300
2:1 BCl_3:BPC	2	−18	1.26	6.1×10^{-3}	900	
1:1 BCl_3:MEIC	1	+16.5	1.29	1.6×10^{-2}	1000	3300
2:1 BCl_3:MEIC	2	−12	1.23	1.6×10^{-2}	1000	

[a] Approximate mole ratio BCl_3:organic chloride. [b] Number of liquid phases present. [c] °C (±0.5 °C). [d] g/mL (±0.05 g/mL). [e] Ω^{-1} cm^{-1} (±10%). All measured near room temperature, except for the 1:1 BPC melt which was measured at 110 °C. [f] Electrochemical window width, mV. Pt refers to platinum working electrode; GC refers to glassy carbon working electrode.

Chloroaluminate melts with an excess of $AlCl_3$ are known to contain the $Al_2Cl_7^-$ ion.[8] All of the peaks in the spectra of acidic BCl_3 melts can be attributed to either the cation modes, BCl_3 modes, or BCl_4^- modes. There is no evidence for the presence of $B_2Cl_7^-$ ion in these systems, even when the melts are cooled to about 77 K.

Electrochemical and physical properties of the neutral and acidic melts are collected in Table I. The electrochemical measurements were made with a quasi-reference electrode;[9] hence only the width of the electrochemical window is reported. At the anodic limit a gaseous product, probably Cl_2, is formed; the cathodic limit corresponds to cation reduction, as suggested by the intense blue for BPC,[10] or orange for MEIC,[11] color formed at both platinum and glassy carbon (GC) electrodes. There is no evidence for boron deposition from these melts.

Acknowledgment. Support of the National Science Foundation, Grant CHE-8605166, and of the Air Force Office of Scientific Research, Grant 85-0321, is gratefully acknowledged. We wish to express sincere thanks to S. P. Zingg for her generous donation of a sample of MEIC.

(7) Bullock, J. I.; Taylor, N. J.; Parrett, F. W. *J. Chem. Soc., Dalton Trans.* **1972**, 1843.

(8) Torsi, G.; Mamantov, G. *Inorg. Chem.* **1972**, *11*, 1439. Brooker, M. H.; Papatheodorou, G. N. In *Advances in Molten Salt Chemistry*; Mamantov, G., Ed.; Elsevier: New York, 1983; Vol. 5, pp 26–184.

(9) Fung, K. W.; Mamantov, G. In *Wilson & Wilson's Comprehensive Analytical Chemistry*; Volume III, Svehla, G., Ed.; Elsevier: New York, 1975; Vol. III, pp 305–370.

(10) Gale, R. J.; Osteryoung, R. A. *J. Electrochem. Soc.* **1980**, *127*, 2167.

(11) Hussey, C. L.; Sanders, R. J.; Oye, H. A. *J. Electrochem. Soc.* **1985**, *132*, 2156.